CHALMERS

Ringhals Diagnostics and Monitoring:
An overview of 30 years of collaboration
1993 - 2023

I. PÁZSIT

Nuclear Engineering Group
Division of Subatomic, High Energy and Plasma Physics
CHALMERS UNIVERSITY OF TECHNOLOGY
Gothenburg, Sweden, 2023
CTH-NT-350/RR-27 June 2023

CTH-NT-350/RR-27 June 2023

Ringhals Diagnostics and Monitoring: An overview of 30 years of collaboration 1993 - 2023

I. Pázsit

Nuclear Engineering Group
Division of Subatomic, High Energy and Plasma Physics
Chalmers University of Technology
SE-412 96 Göteborg, Sweden
ISSN 0281-9775

Ringhals Diagnostics and Monitoring: An overview of 30 years of collaboration 1993 - 2023

I. Pázsit

Nuclear Engineering Group
Division of Subatomic, High Energy and Plasma Physics
Chalmers University of Technology
SE-412 96 Göteborg, Sweden

Abstract

A joint research project between Chalmers University of Technology and the Ringhals power plant was conducted regarding development of noise analysis methods and their application to reactor diagnostics between 1995 - 2023. The project was financially supported by Ringhals. The actual contacts and collaboration started actually in 1993, although at the beginning with support from SKI. This report gives a historic overview of the project; its origins, start-up, the problems tackled, and the results obtained. The emphasis is more on providing a full descriptive inventory of the methods and results with explaining their significance, without going in deeply into technical details. For these latter, references will be made to the project reports and other publications. In addition to the research items, the report also includes lists of papers published and conference talks presented from the results of the collaboration, as well as the list of persons contributing to the results, the list of PhD and Licentiate exams, and finally a list of various prizes obtained by the Chalmers participants of the project.

This report constitutes the closing part of the above mentioned long-term collaboration, and is supported financially by with Ringhals, Vattenfall AB, contract No. 4501756928-062. The work in the contract was performed between 1 July 2022 and 30 June 2023.

The work was performed by Imre Pázsit, who was the Principal Investigator for the whole long-term project. Contact person from Ringhals was Henrik Nylén.

CONTENTS

PROLOGUE **1**

1 INTRODUCTION **2**

2 BWR RESEARCH (R1) **7**

2.1 In-phase and out-of-phase instability in R1, 1990 7

2.2 Further study of the separation of the global and local components and its application for the R1 stability measurements made in 1991, 1993 and 1994 9

2.3 Search for unseated fuel elements from in-core noise 11

2.4 Detection of BWR instrument tube impacting with wavelet techniques 14

2.5 Determination of the void fraction and its axial dependence 18

2.6 Determination of the axial dependence of the void velocity 21

3 PWR RESEARCH (R2 - R4) **25**

3.1 Determination of the axial elevation of control rods from the axial flux profile with ANNs 25

3.2 Core-barrel vibration analysis 28

3.2.1 Introduction 28

3.2.2 Elaborating a more general analysis tool 31

3.2.3 Diagnostics of shell-mode vibrations 34

3.2.4 Diagnostics of beam mode vibrations - long-term and short-term trends 36

3.2.5 Quantification of the peak amplitudes with curve fitting and the double peak at 8 Hz 38

3.2.6 Calculation of the evolution of the conversion factor between the vibration modes and noise amplitude during the cycle . . . 41

3.2.7 Evidence of tilting mode vibrations 43

3.2.8 Long-time trend analysis 44

3.3 Determination of the MTC by noise methods 47

3.3.1 Introduction 48

3.3.2 The principles of the solution of the problem 49
3.3.3 Experimental verification with gamma-thermometers 50
3.4 Thimble tube vibrations 53

4 MISCELLANEOUS 55

4.1 Investigation of the ultra-low frequency oscillations in PWRs 55
4.2 Determination of the response time and health test of gamma-thermometers 56
4.3 Estimation of water flow velocity with gamma-thermometers 56
4.4 Determination of subcritical reactivity through the source modulation technique 56
4.5 Axial dependence of the in-core noise for determining fuel vibration modes 56
4.6 Basic study of the power reactor noise in non-multiplying systems . . 57
4.7 Study of the possibility of using fission chambers in the current mode for zero power reactor measurements 57
4.8 Investigation of baffle jetting 57
4.9 Study of detection of subcooled boiling in PRWs 58
4.10 Eigenvalue separation for BWR stability 58
4.11 Conceptual study of a neutron flux gradient detector 59
4.12 Water flow with measurement of N-16 activity 59

5 PROJECT CONTRIBUTORS 60

5.1 Chalmers staff 60
5.2 External staff/visitors 60

6 THESIS WORK 62

6.1 PhD theses 62
6.2 Licentiate theses 62

7 PUBLICATIONS ARISING FROM THE PROJECT 64

7.1 Journal publications 64
7.2 Conference papers/talks 67

8 ACKNOWLEDGEMENT 72

PROLOGUE

On a sunny day in the early summer of 1991, while driving from Nyköping to Göteborg on motorway No 40, I stopped at a parking lot for a rest. The trip was part of my regular visits to Chalmers before I started as successor of Nils Göran Sjöstrand as professor and head of the Department of Reactor Physics (which was at that time an autonomous Department within the School of Physics in Chalmers). Then the driver of another car, who I might have seen before but could not directly identify, came to talk with me. He knew who I was, because we were essentially in the same trade and have already seen each other on some occasion. The driver, Magnus Johansson (later changed his name to Magnus Kruners) was a reactor physicist and nuclear engineer, working at Ringhals. He knew very well what position I would soon take up in Chalmers, and he had a message to me. He expressed the expectation, primarily on behalf of Ringhals, but to some extent also on behalf of the Swedish nuclear industry, that the new holder of that state-endowed chair at Chalmers in Reactor Physics would tighten the contacts and collaboration with the industry, and would conduct more research in applied reactor physics and nuclear engineering than the Department did until then.

The fact that the Swedish nuclear industry had already a message to, and an expectation from a newly appointed, but hitherto unknown professor struck me with surprise. On the other hand, although before coming to Sweden and Studsvik in 1983 from Hungary, I was a pure theoretician (not to mention that our first power plant in Hungary was started up just in 1983), my 8 years of more pragmatic experience in the noise group in Studsvik and later at the R2 reactor made it easy for me to welcome such a message. Actually, my original invitation to Studsvik as a guest researcher in 1983 concerned participation in a collaboration project between Studsvik and Forsmark (the FOLNAS project), and apart from Forsmark, we also had some less concrete contacts with Ringhals. To apply theoretically developed methods to real world problems in collaboration with the nuclear industry was a very promising possibility.

Although it took a couple of years before the collaboration with industry and in particular with Ringhals de facto started, this expression of trust and expectation even before I started my new role in Chalmers, was a very significant first step. There were several further decisive moments on the way which were essential in the process of starting the collaboration, which will be mentioned below, but I count that unplanned meeting at a parking lot on motorway 40 in the summer of 1991 when "it all started".

1. INTRODUCTION

The first contact with Ringhals after my inauguration in Chalmers came about by coincidence. IMORN-23, the 23rd International Meeting on Reactor Noise was held in 1992 in Nyköping, organised by my previous colleagues in the Studsvik Noise Group, by that time detached from Studsvik and belonging to the Vattenfall-owned subsidiary Eurosim AB.

Figure 1.1: The Studsvik Noise Group in 1985. From left to right: the author, Joachim Lorenzen, Fredrik Åkerhielm†, Ritsuo Oguma and Bengt-Göran Bergdahl.

.

The only PhD student who I advised in Hungary before coming to Sweden, Oszvald Glöckler, attended the IMORN meeting. At that time he worked as the chief noise expert at Ontario Hydro, Canada, where he built up noise analysis activities from scratch. He was accompanied to the meeting by his department boss, Armando Lopez. They came to Göteborg after the meeting, and Lopez wanted to visit a nuclear power plant in Sweden and meet people to discuss current issues in operation, maintenance and surveillance. Although their visit fell to the week of Easter holiday, Tell Andersson, whom I knew through his licentiate studies with Nils Göran where I took over the advisorship, was kind enough to organise a visit for us.

During an interesting and informative meeting Tell mentioned to the guests a question which had concerned him since some time, namely to find an alternative method to determine the position of the tip of a partially inserted control rod cluster in a PWR. I did not have a suggestion for a solution at that time, but several years later we found an interesting method, which will be described later. At that point I only appreciated the openness of the power plant staff in mentioning current problems, which could serve as research topics for applied research in academia.

The next step which did lead to a concrete joint project, although still singular,

came in early 1993. Bengt Melkersson, who was then Head of research at Ringhals, contacted me with a suggestion of a study. It concerned an unusual event during the start-up the Ringhals-1 BWR in 1990. Stability measurements were made in various points of the power-flow map. These showed that when moving from a certain point of the power-flow map to another but close point, the decay ratio (DR) increased from 0.6 (very stable operation) to 1 (unstable operation) in one single step. This was alarming, since it showed that the DR was not a good indicator of the closeness to instability. Bengt arranged financing from SKI for a joint project, and this became our first commercial project during my time. As it happened, we had Tim van der Hagen from the Technical University of Delft as a visiting post-doc at our department, who became the driving force of this project. We managed to understand and to explain the mechanism behind this phenomenon as the interplay of global and regional BWR instability, and could suggest a method to separate the stability properties of these modes, thereby lending a method which can be used to efficiently predict instability even in such cases. The report on the work was submitted to Ringhals in December 1993 [1], and the paper we published in 1994 in Nuclear Technology is one of our highest cited publications.

The Canadian connection had some further influence and catalyser effect on the development of our contacts with Ringhals. In the fall of 1992, on the suggestion of Oszvald, I wrote a proposal to Ontario Hydro (OH) for a noise diagnostic development program for CANDU reactors, which would be performed in collaboration between Chalmers and OH. The proposal was not focussed on diagnostic methods for specific cases, rather suggested a systematic study of the noise transfer properties as functions of frequency and system size; the space dependence of the response and the relative weight and spatial range of the local component etc. Such a knowledge did exist for LWRs, but not for CANDU reactors, and it was expected that due to the very different neutronic and geometric properties of HWRs, it was worth performing such a systematic study. The gain would be an increased understanding on how to optimise specific noise measurements for maximum sensitivity and accuracy.

The proposal was not granted at OH, but it had a domestic effect. I got a new call from Bengt Melkersson, who told me that he and Tell Andersson had read this proposal and were quite enthusiastic about it. They both thought that a similar program could be discussed also for Ringhals.

This is the way it went. We had a meeting at Ringhals on 1993-08-23 to discuss the possibility to start a joint project for reactor diagnostics, with the goal of developing specific methods to tackle problems of interest for Ringhals, and to test and apply them. Since for practically all applications we needed measured data, a data handling confidentiality agreement was signed (Appendix A). A first contract, which was to become the first stage of a long project, was signed and the project was executed between 1 October 1995 and 30 June 1996. It consisted of two parts. One part concerned the analysis of a large number of signals, from measusrements in 1993-94 in Ringhals-3, in order to get acquainted with the data structure of the measurements, and to get familiarity with the main characteristics of the measured signals and the system characteristics they reflected on, such as the 8 Hz peak of the beam mode and the 20 Hz peak of the shell mode core barrel vibrations in the

ex-core detector signals. The report on these measurements ("Stage 0"), written in Swedish, was submitted in May 1996 [2]. The second report, in English, designated as Stage 1 and constituting the formal start of the project, had the same structure as all the consecutive reports, namely consisted of a few selected concrete problems that were treated during the project, and it was submitted in September 1996 [3].

To give a flavour of what type of problems were tackled at the start of the project and how the project was defined, we cite here the Abstract of the report of Stage 1:

ABSTRACT

This report gives an account of the work performed by the Department of Reactor Physics in the frame of a research contract with Ringhals, Vattenfall AB, contract No. R53060-YVDI. The contract constitutes the first stage of a long-term co-operative research work concerning diagnostics and monitoring of the PWR units. The work in Stage 1 has been performed between 1 October 1995 and 30 June 1996 and it consisted of the following items:

- a general analysis of noise measurements made by Ringhals personnel in the unit R3 during 1993 and 1994;
- signal transmission path analysis of the low frequency oscillations in cold leg temperature, ex-core detectors and core outlet temperatures;
- detailed analysis of core-barrel vibrations from the ex-core detector signals;
- a feasibility study of the determination of axial control rod elevation from the axial flux profile by using neural networks.

This work was performed at Chalmers by Imre Pázsit (principal investigator), Ninos S. Garis, Joakim Karlsson, Ola Thomson, and Lennart Norberg. Several visiting scientists have also contributed: Drs. Oszvald Glöckler (Ontario Hydro), and Emese Temesvári and A. Rácz (KFKI Budapest). Contact persons at Ringhals were Tell Andersson (project leader) and Anders Johansson.

A proposal for the continuation of the work in Stage 2 is also given.

From that point on, the collaborative project was continued with annual contracts, labelled as Stages, numbered with running numbers. A total of 23 further Stages followed until 2023, and a final summary report (the present one) in 2023. All projects were published as Chalmers internal reports [3, 4, 5, 6, 7, 8, 9, 10, 11, 12, 13, 14, 15, 16, 17, 18, 19, 20, 21, 22, 23, 24, 25], and are available on-line from the web page of the Department (now reduced to a group within the Division of Subatomic, High Energy and Plasma Physics):

http://www.nephy.chalmers.se/research/Ringhals/projects.html

After Stage 14 (completed in 2011), the labelling of the Stages was changed from

the serial running number to the year number (the year number in which the project was started). That is, instead of Stage 15, the next project after Stage 14 was called "Stage 2012". Actually, in Stage 2012, a three-year contract was signed, with annual reports in 2012 and 2013, and a 3-year summary report was written for 2012-2014. Thereafter the project returned to the previous annual contract system.

The contact person from Ringhals from the start (Stage 1) until Stage 12 was Tell Andersson. From Stage 13 to the end, Stage 2022, the contact person was Henrik Nylén. To strengthen the contacts and the collaboration, in 2011 Henrik Nylén was appointed as adjunct professor at the then Division of Nuclear Engineering (a successor of the Department of Reactor Physics). Henrik was adjunct professor from 2011-01-01 to 2016-12-31.

During the years, many present and past members of the Department, as well as PhD students and visitors contributed to the project. A list of these is given in Chapter 5. Some external people were also formally attached to the project. Assoc. Prof. Tatiana Tambouratzis from the University of Pireus was a visiting guest scientist with a part-time employment (5%) between 2009-01-01 and 2011-12-31. Cristina Montalvo, from the Technical Univerity of Madrid (UPM) was visiting guest scientist with a part-time employment (10%) between 2014-06-01 and 2016-05-31. She had also a visiting research position in the frame of a contract between UPM and Chalmers.

In the next Sections, all research subjects pursued will be described and discussed. This description will not be a summary of each report sequentially; for this, we refer to the actual annual reports. Instead, these subjects will be grouped thematically. This is much more practical and gives a better overview, not the least since several of the topics were developed and followed up during a long time, covering several Stages, and sometimes they were returned on after a temporary break. The research projects will be grouped in three chapters: BWR research (Chapter 2); PWR research (Chapter 3); and Miscellaneous smaller problems (Chapter 4). By this thematic grouping, the present report will also serve as a manual to the reports of the individual Stages. If a reader is interested in a specific topics, he/she can look up the corresponding section in the present report, find a summary, and a list of the Stage reports in which some aspect of the topics was investigated.

A word on terminology is in order here what regards the reference to the Chalmers staff and the corresponding affiliations. At the beginning of the collaboration, 1993, we were the Department of Reactor Physics ("Institutionen för Reaktorfysik" in Swedish), a self-standing Department in the School of Physics (Sektionen för fysik) of our own. In June 2005, a substantial reorganisation of Chalmers took place: the former Schools disappeared by being divided into two (or some of them three) large Departments, which basically replaced the former departments, which ceased. Reactor Physics ended up in the Department of Applied Physics as a division, and also changed name, becoming the Division of Nuclear Engineering ("Avdelningen för Nukleär teknik" in Swedish). In connection with the reorganisation, we had to give up our previous building at Gibraltargatan, by moving to a corridor of the Origo building of Physics. On this move we lost our excellent experimental facilities, most notably our stationary 14 MeV neutron generator.

After that, two more reorganisations happened in Chalmers. First the Department of Physics was merged with the Department of Fundamental Physics. Nuclear Engineering was merged with parts of Fundamental Physics, and was re-named "Division of Subatomic and Plasma Physics". After yet another reorganisation, being in force from 1 January 2020, when some groups from Theoretical Physics joined our division, the name was changed again to "Division of Subatomic, High Energy and Plasma Physics". (SHP)

As a consequence, the staff of the former Department of Reactor Physics, and its successor, the Division of Nuclear Engineering, is now a small minority group within the SHP Division, referred to as "Reactor Physics, Modelling and Safety", and the noise diagnostics is only a part of this terminology. This makes it difficult to refer to ourselves, since one should use either of the words Department, Division or Group, depending on which year the reference is made to. Hence the words "Department", "Division", or just "nuclear engineering" will be used interchangeably when referring to ourselves.

2. BWR RESEARCH (R1)

2.1 In-phase and out-of-phase instability in R1, 1990

As mentioned in the Introduction, this project was the first joint work between the Department of Reactor Physics and Ringhals. Although it was not part of the long-term collaborative project, it counts as its pre-decessor, and the significance of the topics tackled in this first singular project, and the experience and insight we gained from it, was very useful in our later work. In fact, related problems occurred later on, and we had good use of the understanding and insight gained from this project. Therefore it will be described into this report.

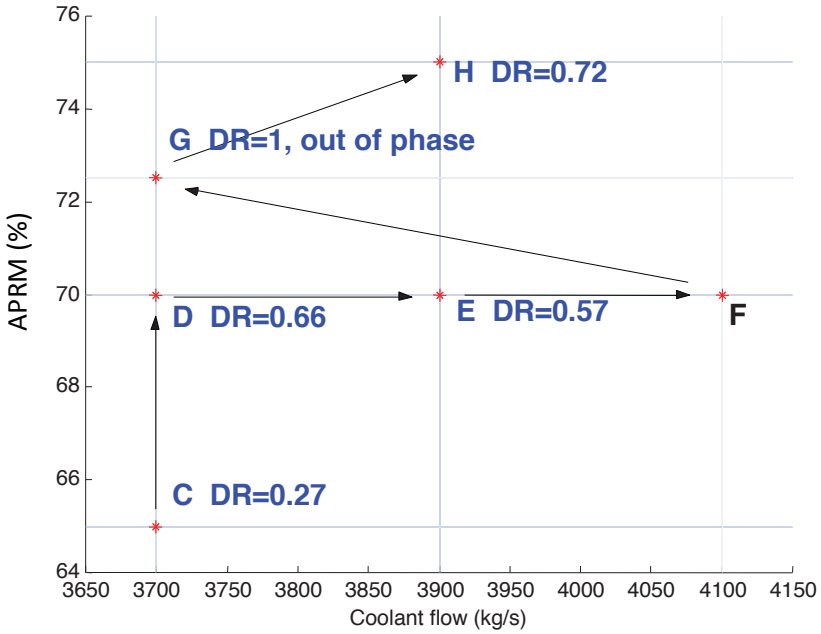

Figure 2.1: A schematic description of the 1990 Ringhals-1 instability event by showing the measurement points on the power-flow map

.

The BWR instability event took place in the Ringhals-1 BWR in 1990 [26]. In this event, a number of measurements were made in various operational points of the power-flow map, as shown in Fig. 2.1. Details of the measurement are found in [27]. The figure shows the measurement with its chronological sequence indicated by the arrows, and the corresponding decay ratios, extracted from each measurement. In point G, the core became unstable, and got into the state of limit cycle oscillations.

The remarkable in this event is that based on the measurement in point D, relatively close to point G on the power flow map, the core appeared to be rather stable. Although point G was approached from F, which is far to the right on the power-flow map and hence a large change in the DR between point F and G is not surprising, if the measurement had a different sequence and one progressed from

point D to G, the change would have been interpreted as "discontinuous", or at least highly non-linear (as function of the control parameters). This suggested that there are cases when the traditional decay ratio (DR) is not a suitable indicator of the closeness of instability.

Our analysis, summarised in [1] and later in [26], showed that the main reason of the unusual behaviour of the DR was that there were two oscillating modes co-existing: a global (in-phase) and a regional (radially out-of-phase) oscillation. As it was shown in [28], in case when two oscillation modes are present, whose effects add up linearly in a single detector (LPRM), the DR extracted from the detector signal is a linear combination (a weighted average) of the DRs of the two modes, the weighing factors being the amplitudes of the corresponding oscillations. In the instability event in Ringhals-1 in 1990, the global mode was stable (low DR), whereas the regional mode had a higher DR in all of the measurement points. However, in most of the measurement points, the amplitude of the global oscillations was (much) higher than those of the regional ones, and hence the measured DR was low (close to that of the global mode). In the unstable point G, the DR of the regional mode reached unity, i.e. it became unstable, and hence its amplitude then largely exceeded that of the global component. This is why in point G, the DR "jumped" to unity from a significantly lower value.

It became also clear that if the effect of the two oscillations could be separated in the detector signal, and hence the DRs of the global and regional modes could be determined separately, then the DR of the more unstable mode could be used as an indicator of the closeness to instability. We managed to find such a separation method for extracting the regional (out-of-phase oscillations) from the total signal, by taking the difference of the signals of detector pairs placed diagonally opposite to each other in the same horisontal plane, and taking the average of several such signal differences. This made it possible to determine the DR of the regional mode. It was shown, that the DR of the regional mode was already much closer to unity in the measurement points D and H than the DR extracted from the pure detector signal. Hence the DR of the regional mode proved to be a reliable instability indicator.

Although it was not part of the project, the interesting question remained what is the reason of the sudden increase of the amplitude of the regional component. This was explained later by the fact that if one treats the two oscillation types as damped linear oscillations driven by a white noise source, then their amplitudes are inversely proportional to their respective damping factor. If any of the modes approaches instability, its damping factor tends to zero, and its amplitude tends to infinity. Due to this, the measured DR changes from the low value of the global mode to unity in a highly non-linear (abrupt) manner [28].

As a curiosity, much later an alternative hypothesis was formulated for sudden increase of the DR in terms of catastrophe theory [29]. In this hypothesis, based on the non-linear character of the BWR instability problem, it is suggested that the behaviour of the DR shows a cusp catastrophe. This hypothesis is purely based on some generic properties of non-linear systems, and it does not require the presence of two simultaneous oscillations. Since in the Ringhals case, the simultaneous presence of two oscillations with different stability properties was proven, the model based

on catastrophe theory does not apply to the Ringhals case; it only states that the seemingly discontinuous behaviour of the DR can happen also for other reasons than two simultaneous oscillations.

2.2 Further study of the separation of the global and local components and its application for the R1 stability measurements made in 1991, 1993 and 1994

As described in the previous Section, the explanation of the abrupt change of the DR with smooth changes of the operational point on the power-flow map was found in the co-existence of a global and a regional oscillation, with different stability properties. In order to obtain a reliable indicator of the closeness to instability was found to determine the DRs of the two oscillations separately, by separating the two modes in the detector signals. As is also described in the foregoing, this mode separation was achieved by taking differences of two detector signal placed diagonally opposite to each other, and taking the average of several such differences for different detector pairs. This eliminated the global oscillations, and left only the effect of the regional (out of phase) oscillations in the differences in the detector signals.

Actually, during the course of the work, a more fundamental mode separation was attempted, which was based on orthogonality properties of the two oscillation modes. Splitting the flux fluctuation $\delta\phi(\boldsymbol{r},t)$ into a global (point kinetic) component $\delta P(t)\phi_0(\boldsymbol{r})$ and a space-dependent component $\delta\psi(\boldsymbol{r},t)$in the usual way, i.e.

$$\delta\phi(\boldsymbol{r},t) = \delta P(t)\phi_0(\boldsymbol{r}) + \delta\psi(\boldsymbol{r},t) \tag{2.1}$$

by assuming orthogonality between $\delta\psi(\boldsymbol{r},t)$ and $\phi_0(\boldsymbol{r})$, the amplitude factor $\delta P(t)$ of the point kinetic component can extracted from $\delta\phi(\boldsymbol{r},t)$ by a projection to the static flux as

$$\delta P(t) = \frac{\displaystyle\int_V \phi_0(\boldsymbol{r})\,\delta\phi(\boldsymbol{r},t)\,\mathrm{d}\boldsymbol{r}}{\displaystyle\int_V \phi_0^2(\boldsymbol{r})\,\mathrm{d}\boldsymbol{r}} \tag{2.2}$$

Having obtained the point kinetic term, the space dependent term, assumed to represent the regional (out-of-phase) oscillations as

$$\delta\psi(\boldsymbol{r},t) = \delta R(t)\,\phi_1(\boldsymbol{r}) \tag{2.3}$$

where $\phi_1(\boldsymbol{r})$ stands for the first azimuthal mode, can be obtained by subtracting the point kinetic term (the first term on the r.h.s. of (2.1)) from the total noise (the l.h.s.). Since the noise $\delta\psi(\boldsymbol{r},t)$ is only measured in a number of discrete spatial points (2 axial positions in 36 radial positions), in practice the integrals in (2.2) have to be approximated by a summation as

$$\delta P(t) \approx \frac{\displaystyle\sum_{i=1}^{M} \phi_0(\boldsymbol{r}_i)\,\delta\phi(\boldsymbol{r}_i,t)}{\displaystyle\sum_{i=1}^{M} \phi_0^2(\boldsymbol{r}_i)} \tag{2.4}$$

where M isthe number of detectors used in the sum (a maximum of 72 detectors). By this procedure the regional component

$$\delta\psi(\boldsymbol{r}_i, t) = \delta R(t)\, \phi_1(\boldsymbol{r}_i) \tag{2.5}$$

for each detector could be obtained, from which the amplitude factor $R(t)$ of the regional term can be extracted, and the corresponding DR determined.

However, using $M = 72$ in (2.4), the procedure failed. According to (2.5), from the regional component $\delta\psi(\boldsymbol{r}_i, t)$ of each detector signal, the same regional DR should be obtained, and moreover the signals $\delta\psi(\boldsymbol{r}_i, t)$ of diagonally opposite detectors should show out-of-phase behaviour. However, none of these assumptions were found in the regional detector signals generated by the above procedure. The individual regional decay ratios were strongly space dependent, and the signals of diagonally opposite detectors did not show out-of-phase behaviour.

The explanation was found in later work, and its details are analysed in detail in [30], and were summarised also in Stage 2 [4]. Very briefly, the failure can be found in the interplay of two circumstances. One is the fact that the detector signals in a BWR, through the existence of the local component, always contain the effect of the propagating two-phase flow even in the case of instability. This component was neglected before in all work concerning BWR stability. For detectors in the same radial position but different axial height, the propagating character of the two-phase flow generates a strong correlation. If the mode separation was perfect, i.e. one could calculate $\delta P(t)$ by (2.2), the correct point kinetic component could be determined, and both the regional and local components eliminated. However, since the separation is only approximative through (2.4), after the separation the regional and local parts are still present, although with small amplitudes. In calculating the auto-correlation function, this would be still no problem if the point kinetic, regional and local components were statistically independent from each other in each spatial point. However, the strong correlation between the two detectors in the same detector string adds a component with an appreciable weight, which does fulfil the assumptions of the separation method, thereby introducing a substantial error.

As can be expected from the explanation of the reason of the failure, the remedy is to use detectors only at the same axial level simultaneously, i.e. using $M = 36$ (representing the radial positions) either for detectors at axial level 2 or 4 at a time. By this procedure, called the "partial factorisation method", consistent results were obtained. The R1 measurements from 1990 were re-evaluated with this method, and it was seen that the DRs of the global and the regional oscillations were determined properly [4].

Having obtained a robust method for the separation of the global and regional oscillations in the form of the partial factorisation method, it became interesting to evaluate the measurements made during a few consecutive years after 1990, with the goal to see whether the phenomenon of dual unstable regional oscillations occurred again. As was seen in the previous Section, the potential problem with dual oscillations is if there is an unstable component but initially with low amplitude, hence it goes unnoticed without the mode separation method. In the case of the 1990 mea-

surements, it was the regional mode which became unstable, hence the motivation was to see if there were unstable regional oscillations in the new measurements.

We received data from measurements made in 1991, 93 and 94, corresponding to fuel cycles 15, 16 and 17, for beginning of cycle (BOC) and middle of cycle (MOC). The data were not complete in the sense that in some measurements not all detector signals were accessible, hence the evaluation is not perfectly complete either. These data were analysed with the partial factorisation method during Stage 4, and the result are reported in [6]. In the analysis the results from the 1990 measurements (cycle 14) were also included. An overview of the analysis results is shown in graphical form in Fig. 2.2 It is seen that in the measurements made

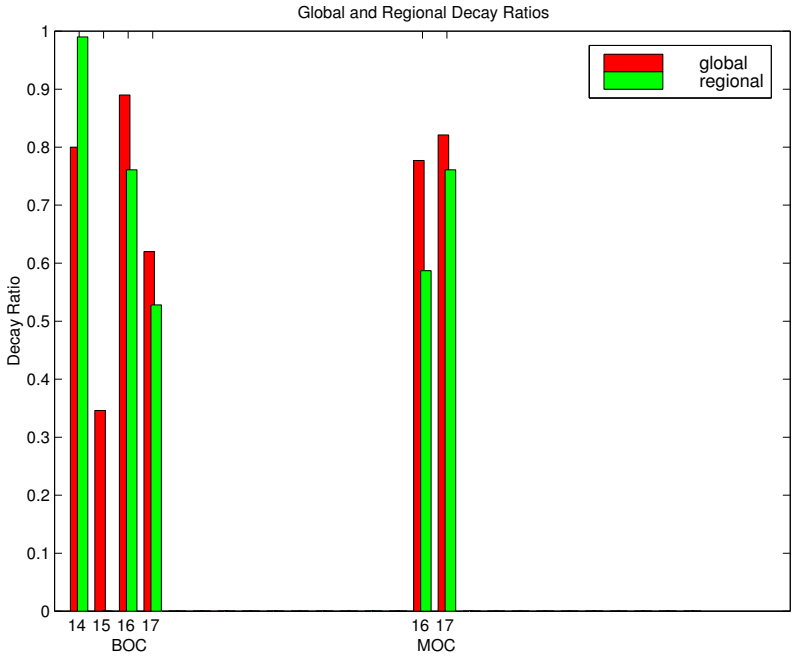

Figure 2.2: Maximum global and regional decay ratios sorted by cycles, for both the BOC and MOC measurements

.

after 1990, the DR of the regional oscillations was consistently lower than that of the global oscillations. In cycle 15, no regional mode was detected at all. This shows that the case in 1990 was a special one, due to a particular control rod pattern, leading to loose coupling between different quadrants of the core. Avoiding such a type of control rod pattern eliminated the possibility of unstable regional oscillations.

2.3 Search for unseated fuel elements from in-core noise

Regarding BWR stability and the special cases of dual oscillations, in Chalmers we performed several related studies, which nevertheless were not part of the Ringhals project. A notable topic was the interpretation of the local instability which occurred during start-up after the outage in 1997 in Forsmark-1, and the elaboration of a method for localising a local (channel-type) instability [31]. As it was understood soon after the event, such channel-type instabilities (density wave oscillations) arise as a consequence of so-called unseated fuel elements. The local instability was

induced by the thermal-hydraulic instability due to the unseated fuel assembly.

It was also in connection with this work that we recognised the possibility of a strongly space dependent DR when calculating it from the individual detector signals. [32]. This can be understood in the terms of the decay ratio in the case of dual oscillations, where the DR will be determined by that of the oscillation with the highest amplitude. This means that in the neighbourhood of a local instability, the DR deducted from the signal of any LPRM will be that of the local instability (i.e. close to unity). Farther away, which in the Forsmark case meant about half of the core, the DR was much smaller, corresponding to the stable oscillations of the global mode. This is in some contrast to the case of the simultaneous global-regional oscillations which, due to the spatially smooth dependence of the two oscillations types, no such strong spatial dependence of the DR (basically, having two different DRs in the two halves of the core) was observed.

From the above it also follows that the presence of an unseated fuel assembly can be detected by observing a local instability in the core, either by the high DR of the local instability (where the local component of the noise is separated with the same methods as described in the previous chapter), or by the strong space dependence of the DR as calculated from the individual detector signals. To test the method, and at the same time investigate whether unseated fuel elements can occur in Ringhals-1, a dedicated series of measurements were made in September 2002, which were analysed and reported in Stage 8 [10]. A total of four measurements were made (labelled as a, b, c and d), out of which the first three at reduced flow and power level, and the fourth at full power and full core flow.

The measurements were analysed both in the time domain and the frequency domain. In the time domain, one method was to plot a 2-D movie of the space dependence of the radial oscillations, to see if there are any local oscillations. This was achieved by showing the temporal variation of the flux in the 36 radial detector positions, by interpolating linearly between the detector positions to obtain an oscillating surface. An example, showing a snapshot of the videos for the total signal (top), the global (point kinetic part, middle) and the space-dependent part (bottom), for the LPRMs at levelt 2 (left columnt) and level 4 (right column) is shown in Fig. 2.3.

To amplify the visibility of a possible local oscillation, the point kinetic component was eliminated from the signals with the factorisation method mentioned in the previous Section, and further a band-pass filter around the expected frequency of 0.5 Hz of the oscillations was applied.

By eliminating the point kinetic component, what remains is the space dependent part $\delta\psi(\boldsymbol{r}, t)$ of the noise (see Eq. (2.1)), which can consist of either the regional, or the local component, or both. A visual inspection showed that in the first three measurement, a slight regional component could be observed, but no local oscillations. In the fourth measurement, taken at full power, neither local, no regional oscillations were noted. The lack of local oscillations, together with the presence of regional (out-of-phase) oscillations, is clearly visible in bottom plots of Fig. 2.3, which also illustrates the presentation of the videos, generated from the band-filtered

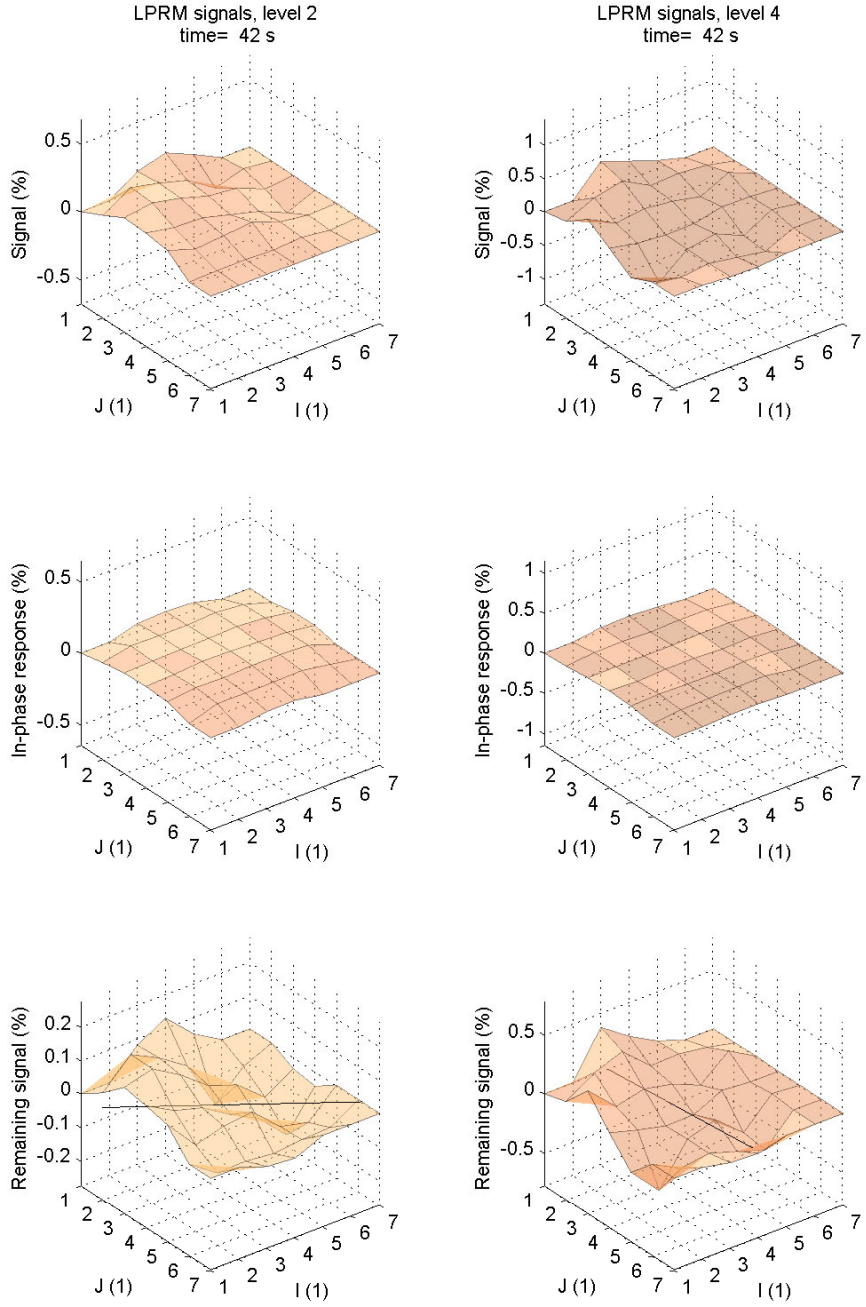

Figure 2.3: Snapshot of the movie displaying the response of the LPRMs in the time-domain, for the first measurements. Top figures: full (band-filtered) signals; middle: the global oscillations; bottom: the space-dependent part. Left column: level 2 detectors, right column: level 4 detectors.

LPRM signals. These findings indicate that there are no unseated fuel elements in this core loading.

The frequency analysis showed also consistent results. Small peaks in the LPRM auto power spectra were found in measurements $a-c$, corresponding to the regional oscillations, and no peaks in measurement d which was taken at full power. The DR was also calculated for all LPRMs, and no strong space dependence, which would be an indication of a local instability, was found. The phase relations between detectors

at different radial position have not given an indication of a local instability either.

Sumarising the results of the investigation, it was found that no suspected unseated fuel assemblies were found in the measurements. Since no indication of a local instability was found in R1 earlier either, such a study was not repeated in the continuation of the project.

2.4 Detection of BWR instrument tube impacting with wavelet techniques

It has long been known that instrument tubes in BWRs, housing the stationary LPRM detectors can execute vibrations, which can lead to impacting against the fuel box walls [33]. We have encountered such a situation already with the Studsvik Noise Group in 1986, when we analysed the signals of in-core detectors in the now shut down Barsebäck-1 reactor. Based on spectral and correlation analysis of the detector signals, we came to the conclusion that several detector strings executed vibrations, and in case of string 03, the vibrations were so strong, that impacting very likely occurred [34]. Inspections during refuelling after the cycle showed impacting wear on the fuel boxes around LPRM 03, and it was also observed that the signal of the LPRMs in detector position 03 showed some irregularities (spikes and shift of the DC value at random time points). This proved that detector tube impacting indeed occurred.

As is described in Ref. [35], the basis of the analysis of the vibrations and possible impacting was based on spectral and coherence analysis of the signals, which only supplies information about the vibrations and their severity, but does not give a direct evidence of impacting. The presence of the detector tube vibrations manifests itself by the occurrence of a peak in the frequency range 3 - 5 Hz, and by the fact that the phase of the CPDS between pairs of detectors in the same instrument tube starts to deviate from linear. Without vibrations, the phase is linear, it crosses zero (or a multiple of 360°) and the coherence has maxima at frequencies n/τ where τ is the transit time of the bubbles in the core, and the phase crosses $\pm\pi$ and the coherence has minima at frequencies $(n + 1/2)/\tau$. In case of strong vibrations, the linear phase is distorted - it tends to be zero within the frequency range of the vibrations, and the sink-peak structure of the coherence is also distorted.

However, these indicators, similarly to others (such as the widening of the vibration peak in the power spectra) only indicate the presence of strong vibrations, but not the fact or severity of impacting. Moreover, widening of the vibration peak requires knowledge of a reference, i.e. how the peak looked before the impacting occurred. One definite sign of impacting could be, as suggested by J. Thie [36], the distortion of the amplitude probability density (APD) of the signal. In the case without impacting, the APD due to the vibrations would have a Gaussian shape; impacting means that the amplitude of the vibrations is limited by the impacting surface, hence the tails of the APD would be cut off. However, this indicator only works if the detector signal is solely due to the detector tube vibrations; however, in a BWR core, there is a higher amplitude broad-band noise with Gaussian APD present, which masks the distortion of the APD which would only be seen without this large background. Attempts to eliminate the effect of the background noise

with a band-pass filter, centred on the vibration peak failed; the filtering eliminated the low-frequency backgrund, but distorted the APD "back" to become Gaussian.

However, another suggestion by J. Thie seemed to be more promising [36]. Thie suggested the hypothesis that the impacting of the detector tube on the fuel channel box should induce short, damped oscillations of the fuel box itself, presumably with a higher frequency as the eigenfrequency of the detector tube vibrations, which would manifest itself as a 'spike" in the detector signal. Hence detection of impacting could be performed by finding such spikes, and their intermittent frequency would indicate the severity of impacting. The problem here again is that such spikes should be extracted from a noisy signal, where they are not visually visible.

Wavelet analysis, via wavelet filtering, lends a possibility to find such spikes in a noise signal. The essence is to perform a discrete wavelet transform, which generates the signal as a sum of scaled and shifted versions of the mother wavelet, then setting the components whose coefficient is below a given threshold, to zero, and perform an inverse wavelet transform back to time domain. With a proper choice of the threshold for the filtering, the wavelet filtered time signal contains only the spikes.

This method was first tried with Haar wavelets, and was tested on the old Barsebäck measurements, were one had access to signals both with and without impacting. The test was successful, i.e. the wavelet filtering showed a manifold time more spikes for an impacting detector than for a non-impacting detector [37]. Later on this method was developed further, such as using different thresholds for the different levels of the transformed signal, and a wavelet-based coherence method was also used. In the discrete wavelet transform, the so-called impacting rate (IR) was introduced, which expresses the number of spikes per unit time. The continuous wavelet-transform based coherence was taken between detector 2 and 4 of the same string.

This development, and the applications to R1 data, took place from Stage 8 to Stage 12. For the details, we refer to the corresponding reports (Refs [10] - [14]). Here we only show some sample results of both the wavelet filtering and the wavelet coherence method, in Figs. 2.4 and 2.5, respectively.

The wavelet based impacting analysis was performed during several years. The analysis indicated low probability of impacting, and at the same time no visible damage on the detector tubes and/or the fuel channel boxes were observed. Therefore, this activity was discontinued after Stage 12. However, the problem re-occurred, although in a different form, relatively recently. It concerned the thimble tube vibrations in PWRs, and also the possibility of impacting of the thimble tubes to the fuel assemblies. This topics will be described in Section 3.4.

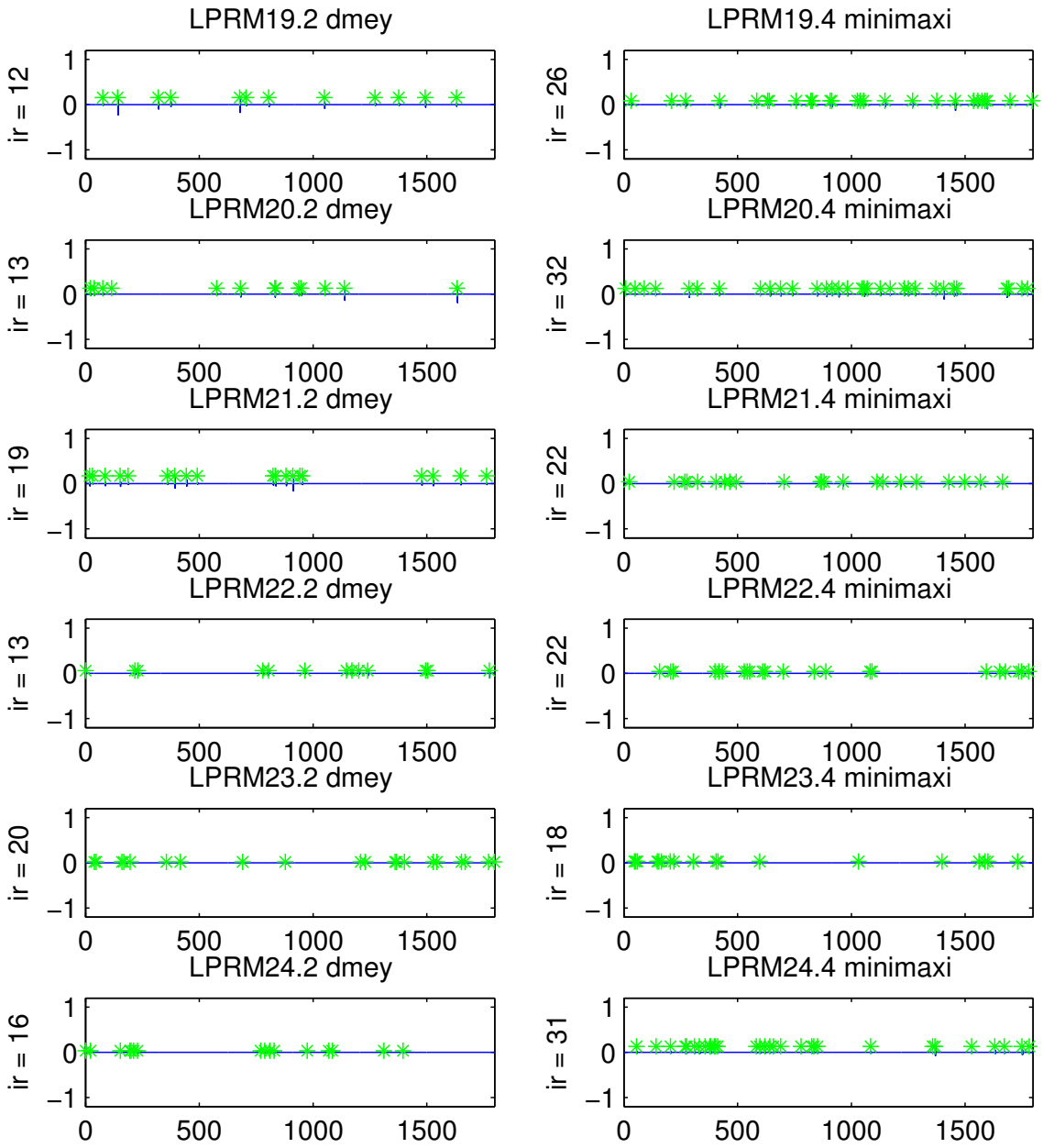

Figure 2.4: Results of the discrete wavelet analysis (wavelet filtering) for the detector strings 19 - 24, with two different wavelets and at two different axial levels.

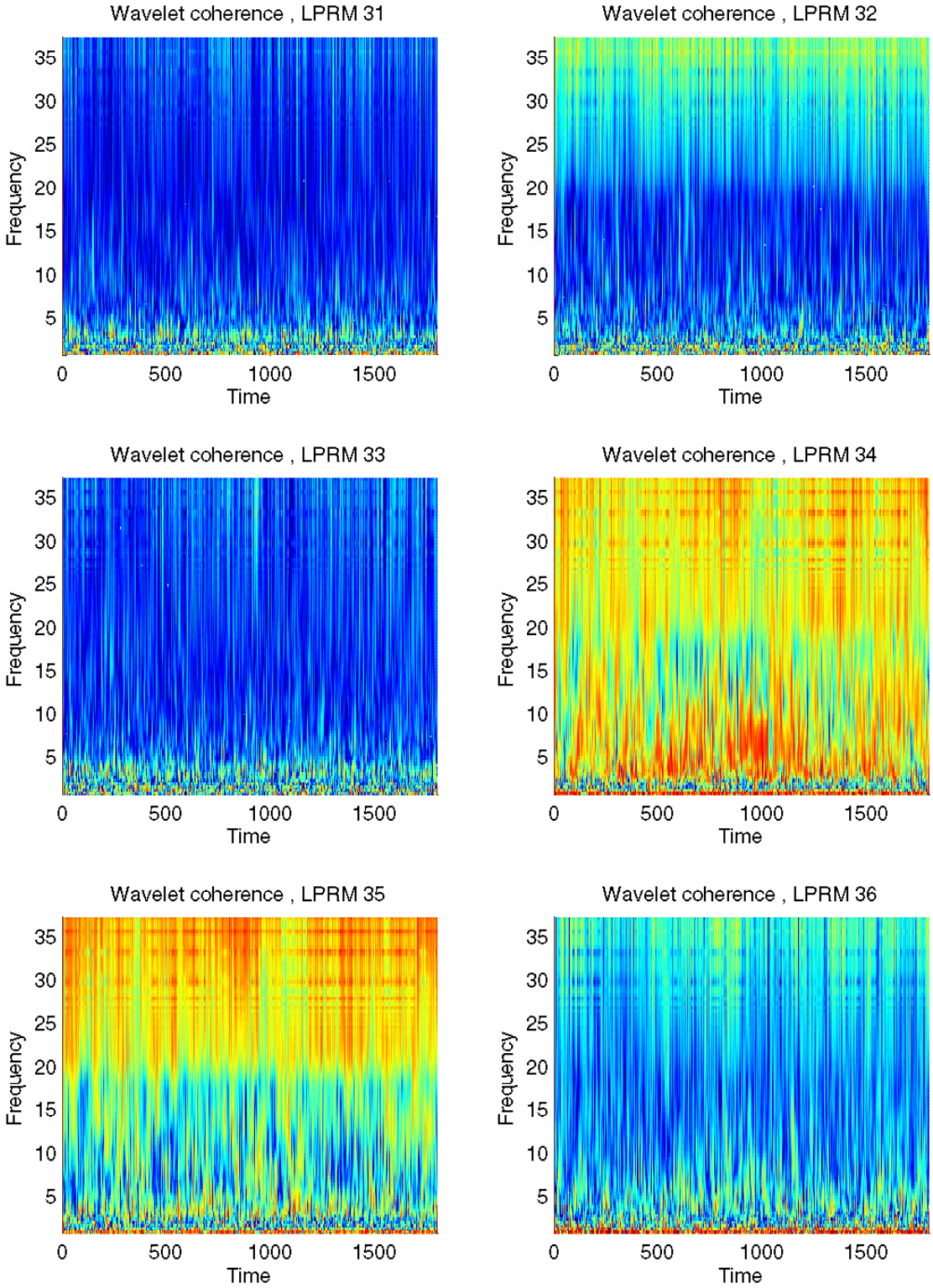

Figure 2.5: Results of the continuous wavelet analysis for detectors 31 - 36. Detectors 34 and 35 show a high coherence at the higher frequencies, i.e. at and above 15 Hz, and are therefore classified as impacting with a high probability.

2.5 Determination of the void fraction and its axial dependence

Determination of the local void fraction in BWRs through measurements has been a matter of interest since long. It became clear in the early and mid 79's that in-core neutron detectors can supply information on the local fluctuation of the void fraction through the existence of the so-called local component of the neutron noise. Among others, it was shown that it is possible to extract the transit time of the void between two axially displaced detectors in the same detector string from the cross-correlation or cross-spectra between the two detectors [38]. It was also seen that there was a correlation between some statistical properties of the neutron noise, most notably the normalised root mean square (NMRS) of a detector signal between 1-10 Hz, and the upper break frequency of the auto power spectral density, and the axially dependent void content [33].

However, these correlations are rather implicit, and they could only be used in an empirical way, which also requires calibrations which are specific for the given case. Early on, some attempts were made to elaborate more involved methods by a stochastic theory of bubble generation and transport to find a relationship between the neutron noise and the average void content [39]. However, the method in the latter publication used too many simplifications and assumptions that were not met in practice, which made in unsuitable for practical applications. There was no follow up of the work, probably due to lack of interest.

A renewed interest from the industry in Sweden was noted in the early 2010's [40], and we also took up the subject within the project. This subject was taken up at Stage 13 [15] and was followed up until Stage 2014 [16, 17, 18, 19]. We revisited the two possibilities mentioned above: the band-limited NMRS, and the upper break frequency of the APSD of the detector signals.

In Stage 13 we started by evaluating measurements taken in R1 in February 2009. The NRMS between 1-10 Hz from APSD was evaluated for a number of detectors in four adjacent detector strings, in all four axial detector positions. Due to a low sampling rate, the break frequency method could not be tested. On the other hand, tt was found that there was a monotonic, but non-linear relationship beween the axial dependence of the NRMS and the average of the calculated void fraction in the four adjacent fuel elements. Since this non-linear relationship cannot be derived from theory, use of such method has a very limited interest in real applications, and hence was not followed-up more.

Thus in the continuation we concentrated on the method of using the break frequency of the APSD for the determination of the void fraction $\alpha(z)$ at an axial elevation z. Assuming that in the signal of an in-core detector the noise due to the local component of the neutronic transfer function dominates, one find that the upper break frequency f_b [Hz] of the APSD is given as

$$f_b = \frac{1}{2\,\pi} v(z)\,\lambda(z) \tag{2.6}$$

Here, $v(z)$ is the velocity of the void fluctuations (or rather, the velocity of the density perturbation, which for low void fraction is that of the void, and at very high void fraction it is the velocity of the water droplets), and $\lambda(z)$ is the spatial

decay constant of the local component of the neutron noise at elevation z. this latter is clearly a function of the void fraction, and this is the key how the void fraction can be determined from the break frequency. As (2.6) shows, in possession of the void velocity $v(z)$ at the detector position, as well as knowing the dependence of the decay constant $\lambda(z)$ of the local component at elevation z, the local void fraction can be determined. The dependence of the spatial decay of the local component as a function of the void fraction can be determined by core calculational methods, or dedicated Monte-Carlo codes, which we have not dealt with within the project. The void velocity at the detector position, on the other hand, has to be determined from experiment. Although, as mentioned, the transit time between the detectors in the same string can be determined from the cross-correlation or from the phase of the coherence between two detectors, the extraction of the void velocity in a given point from the transit times is far more more involved, and therefore it will be dealt with separately in the next Section.

We also mention by passing that if the void velocity can be determined at the detector position, there exists a simpler, but rather rough way of estimating the local void fraction. Assuming a slip ratio equal to unity (void and fluid velocities being equal), the void fraction can be determined from the simple relationship

$$v(z) \approx \frac{v_0}{1-\alpha(z)} \tag{2.7}$$

where v_0 is the velocity of the liquid phase at the channel inlet. This is of course only a rough estimate, which can be improved by using empirical correlations between the slip ratio and the void fraction.

For a pilot test and a proof of principle of the method from Stage 13 and on, we developed a simulation tool for bubbly two-phase flow. Such a method, in a much simpler form, has been used a long time ago for testing the so-called "crossed beam correlation method" [41]. In this project we developed a 2-D model of bubbly flow (one axial and one radial position), with generating bubbles in a random manner along the axial lengtt of the core in the whole radial extension, having them propagating upwards, wich an increasing speed which is calculated from the mass conservation laws. The axial profile of bubble generation intensity was taken from the power profile, and bubble overlapping (when occurred at higher void fractions) were handled properly. Different boiling intensities and hence void fractions were used to generate several different scenarios. When the bubble flow reached a stationary state, the flow was taken as the noise source input to a neutronic transfer model, and the induced normalised neutron noise was calculated through the spatial convolution between the void fraction signals and the local component of the transfer function as

$$\frac{\delta\phi(z,t)}{\phi_0(z)} \int_0^H e^{-\lambda(z)|z-z'|}\,\delta\alpha(z',t)\phi_0(z')\mathrm{d}z' \tag{2.8}$$

where $\phi_0(z)$ is the static flux, and the void fluctuation is taken from the simulation. In later work, this formula was extended to take into account also the radial coordinate, and hence the full spatial dependence of the two-phase flow.

An illustration of the simulation results is shown in Fig. 2.6 for four different times after the start of the simulation. It is seen how the asymptotically stationary

flow is formed after a few seconds time. For better visibility, the bubble size is not correct, rather it is enlarged. Hence, it looks as if the bubbles overlapped, which is not the case with the proper bubble size.

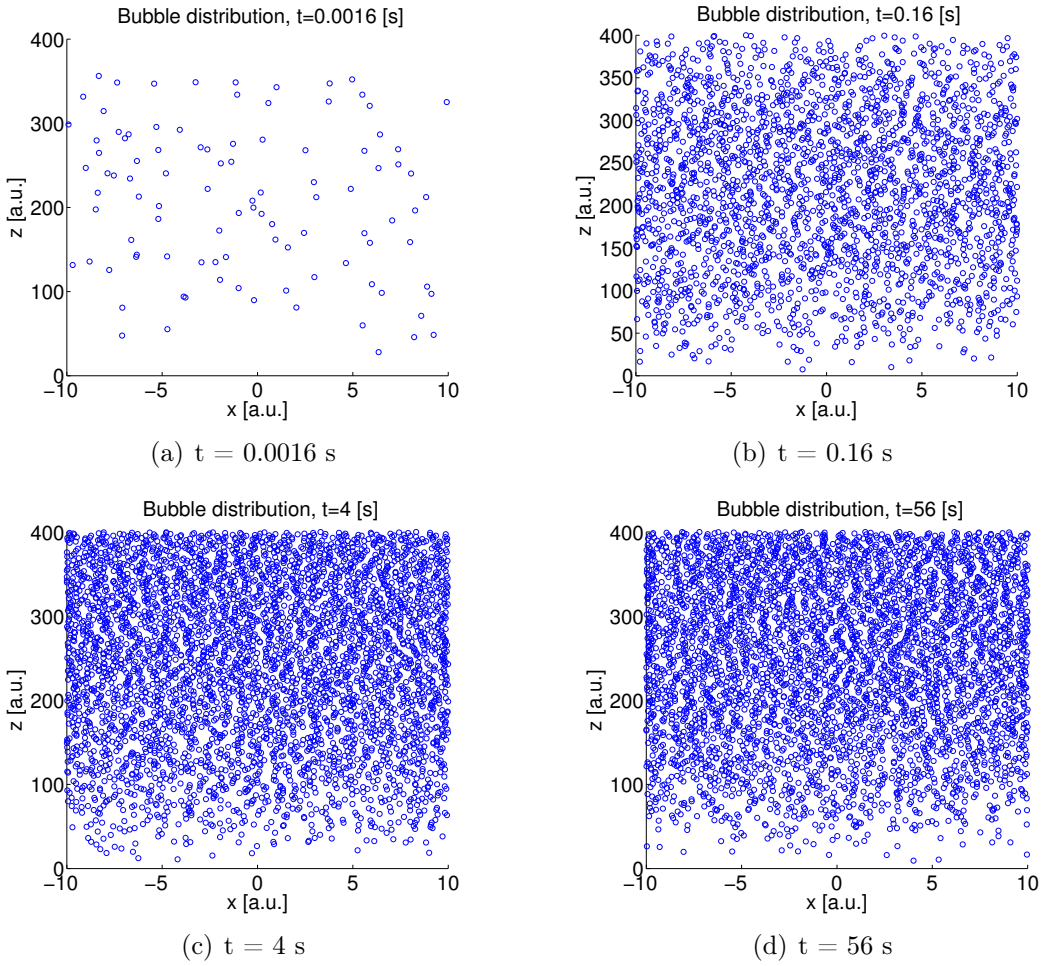

(a) t = 0.0016 s (b) t = 0.16 s

(c) t = 4 s (d) t = 56 s

Figure 2.6: Illustration of the generated bubbly flow from the Monte Carlo simulations for four different time instants after the start of the bubble generation.

At the same time, a simple analytical model of the dependence of the spatial decay constant $\lambda(z) = \lambda(z(\alpha))$ on the void fraction was assumed in the calculations of the induced neutron noise, which made it possible to investigate the feasibility and correctness of the procedure of the unfolding the void fraction from the simulated measurement using (2.6). The advantage of this model is that from the simulations, the true void fraction, as well as the true void velocity, is known, hence the accuracy of the method can be estimated. For the application of the break frequency method, Eq. (2.6), the void velocity has to be determined from the simulated neutron noise signals. Neutron detectors were assumed to be placed at 6 to 8 different axial positions, and the axial void velocity profile, in form of a third order polynomial, was reconstructed from the 5 to 7 transit times, thereby supplying the void veloicities at the detector positions. More details on the determination of the velocity profile are found in the next Section.

This way a complete measurement could be simulated, and the suggested void

profile reconstruction from the simulated numerical data, representing a measurement, could be made, and the obtained data could be compared to the true data. Regarding the accuracy of the reconstruction procedure, one case is shown in Fig. 2.7. The result from the simulated data is shown with a continuous line marked with circles. For comparison, the "true" void profile, from Monte Carlo simulation calculated by time averaging over the corresponding set of void fraction signals is given by a dashed line.

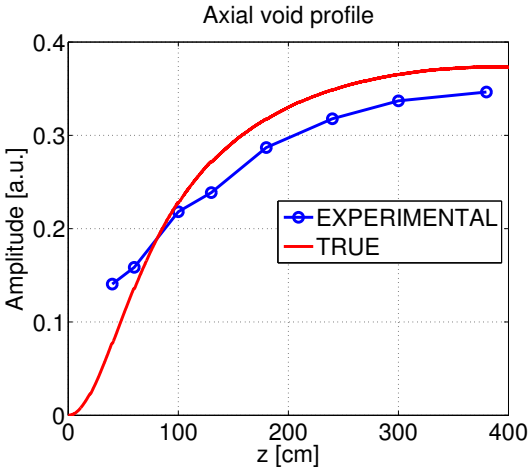

Figure 2.7: The true axial void profile (the output from the Monte Carlo model, red line) and "reconstructed" (blue line) axial void profile, as calculated by the break frequency method.

More details of the simulations and the assumptions of the model, as well as the unfolding procedure can be found, in addition to the Ringhals reports for Stages 13 - 2014, also in the journal publication [42]. The work was even noticed and invited as a feature article in Nuclear Engineering International [43].

2.6 Determination of the axial dependence of the void velocity

As mentioned in the previous section, the determination of the axial void velocity from the detector signals represents a special difficulty. Although there is ample experience what regards the determination of the transit time of the void between two detectors spaced along the propagation at different axial heights by spectral or correlation methods, the transit time does not bear a direct information on the local velocity, unless the velocity is constant (independent of the axial elevation). However, if the velocity $v(z)$ is a function of the axial position z, which is the case in a BWR, then the transit time τ_{12} between two detectors placed at z_1 and z_2, $z_1 < z_2$, is given as an integral of the inverse of the velocity as

$$\tau_{12} = \int_{z_1}^{z_2} \frac{\mathrm{d}z}{v(z)} \tag{2.9}$$

If an analytical formula for the shape of the velocity profile is assumed which contains a few unknown parameters, such as a polynomial with unknown coefficients, then substituting it into (2.9), a relationship between the unknown parameters is obtained in analytic form if $v^{-1}(z)$ is analytically integrable; otherwise the relationship will

be numerical. If there are as many different and independent τ_{ij} values available as the number of unknowns, then an algebraic equation system can be obtained for the parameters/coefficients which can be solved in a straightforward way either analytically, or numerically.

The basic problem is that since a typical void velocity profile in a BWR has an inflexion point, a simple polynomial representation has to be at least of three order, which has four unknown coefficients. However, the standard fixed instrumentation in a BWR has four LPRMs in one string, which yield only three transit times. Hence the problem is underdetermined.

The study of how this situation kan be handled started in Stage 2012, when the bubbly flow simulation model was already available. In order to be able to have a "proof-of-principle of the break frequency method, first we simply assumed having access to 6 detectors, such that the induced neutron noise was generated in 6 axial positions, from which one could derive a redundant system of equations for the coefficients of a third order polynomial. The justification of this study was based on the assumption that a similar experimental situation can be constructed by the use of TIP detectors, put into several axial positions in between the LPRMs, or outside of them. This line was followed up from Stage 2012 to 2014 ([17] - [19]).

In the conceptual study, using the 6 simulated detector signals, the reconstruction of the velocity profile was convincingly successful, as shown in Fig. 2.8. As an

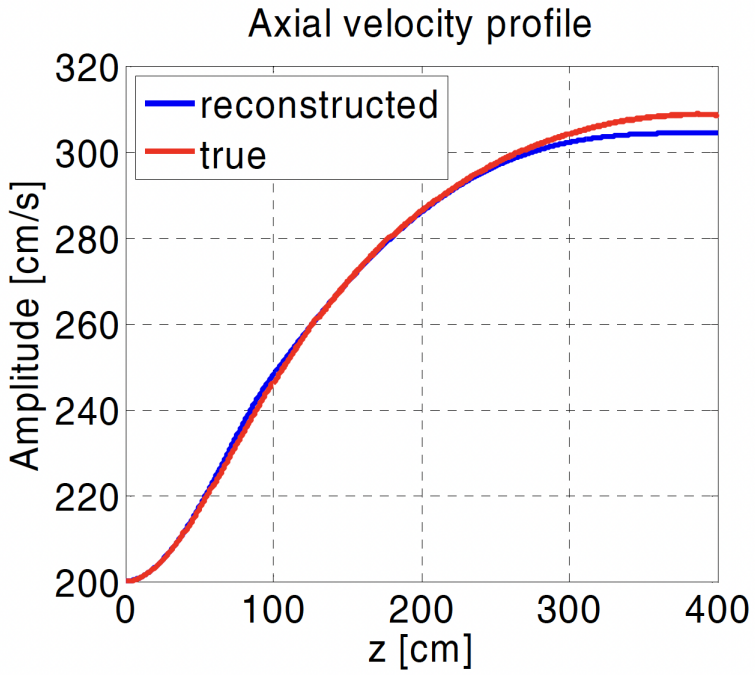

Figure 2.8: True axial velocity profile (the output from Monte Carlo model, red) and the reconstructed axial velocity profile (blue).

alternative method, instead of algebraic determination of expansion coefficients, an artificial neural network method was also tested to reconstruct the velocity profile, which was also successful as long as the problem was overdetermined.

In Stage 2012 also an experimental attempt was made to generate more than 3 transit times, by using a single TIP detector and performing measurements in 7 different axial positions (4 of these were at the same level as each of the four fixed in-core LPRM detectors. However, it turned out that the transit times derived from a combination of an LPRM detector and a TIP detector at a different axial height were largely incorrect, or simply could not be determined, due to lack of a linear dependence of the phase between the two detectors. The explanation was that the signal of the TIP detectors was filtered with a low-pass filter with a break frequency of 0.5 Hence from these measurements, it was not possible to obtain a fifth transit time. Repeated measurements in Stage 2013, with the low-pass filter removed, still showed the difficulty of obtaining reliable transit times between LPRM and TIP detector pairs, due to the different response time of the detectors and the difference in data acquisition. A final attempt was made in Stage 2014, where further improvements were effected in harmonising the data acquisition system between the LPRMs and the TIP detector. Since the results for the extra transit time were still not satisfactory, the method of using an extra tip detector for generating an extra transit time was abandoned.

The question of the determination of the void velocity was revived in Stage 2019, when we got some ideas on how the lack of a fourth transit time can be remedied. We put forward two suggestions. One was that there exist functions with an inflexion point that depend on only three parameters. Examples are the inverse trigonometric or sigmoid functions. Using such functions, it is sufficient to have access to three measured transit times. Another possibility is to use, in addition to the three transit times between the four LPRMs, the axial position of the onset of the boiling, to reconstruct a velocity profile of a third order polynomial. The onset point could be determined e.g. by the use of a TIP detector. Determining the onset of boiling is a very much simpler task than to generate a transit time between the TIP and an LPRM, as it does not require any synchronisation between the two. The onset of boiling could be determined either from the RMS of the TIP signal, or from the coherence between the TIP and the lowermost LPRM.

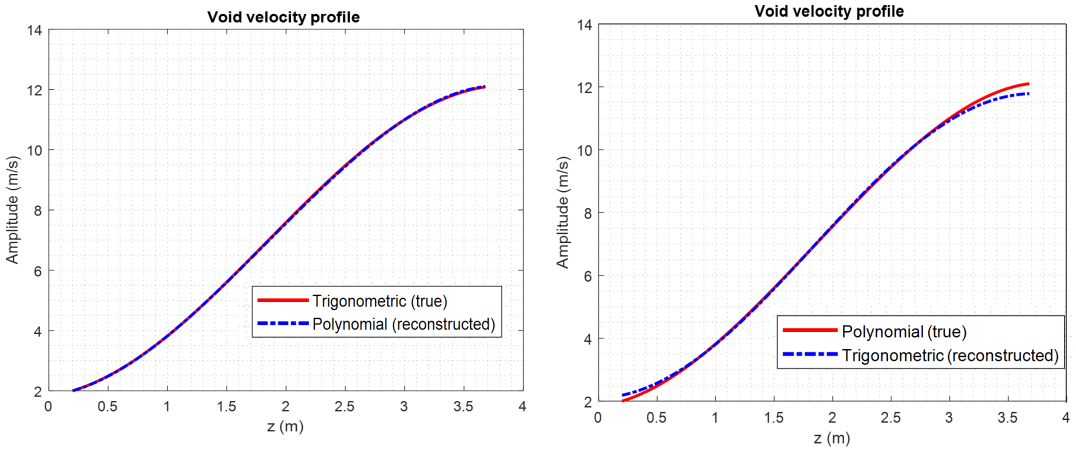

Figure 2.9: Reconstruction of two polynomial velocity profiles with incorrect values of the boiling onset point h in the reconstruction algorithm. The guessed value is $h = 0.33$ m in both cases. Left hand side figure: true value $h = 0.45$ m; right hand figure: true value is $h = 0.15$ m.

The feasibility of these two suggestions was investigated in Stages 2019 and 2020, with rather promising results ([23, 24, 44]. ThIt was found that use of a trigonometric profile was less efficient than that of a polynomial form, due to the smaller richness of the former what regards spatial variation. Hence the use of the polynomial form was found to be more effective. Although the polynomial form requires the knowledge of the onset point of boiling, this might be even guessed, due to the relatively short axial domain where the boiling can starts. We investigated the sensitivity of the method for the uncertainty in the knowledge of the onset point, by assuming an incorrect value of the boiling onset. As Fig 2.9 shows, the reconstructed void profile is rather insensitive to even large errors in the value of the onset point in the reconstruction algorith. This means that the method would work even without extra TIP measurement.

Despite the very promising results for the determination of the void velocity and hence the possibilities of detemining the local void fraction, this subject became closed, due to the phasing out of Ringhals-1 on 1 January 2020.

3. PWR RESEARCH (R2 - R4)

3.1 Determination of the axial elevation of control rods from the axial flux profile with ANNs

As mentioned in the Introduction, we heard about the interest of Ringhals in an alternative method to determine the axial position of partially inserted control rods in 1992, i.e. quite some time before the long-term project started, and even before the first joint work with the regional instability problem was started. Hence, when the long-term project started, this was one of the first subjects which we included, starting already in Stage 1, and was followed up in Stages 2 and 4.

The essence of the method we proposed was to use the information in the axial dependence of the flux in the close radial vicinity of the control rod - either in the fuel assembly housing the control rod cluster, or in a neighbouring assembly. The assumption is that the distortion of the axial dependence of the flux contains information on the position of the tip of the control rod. Fig. 3.1 gives an illustration. showing the undistorted (solid line) flux, as well as the flux measured in the centre of the fuel assembly holding the control rod (poing-dashed line) as well as in a neighbouring assembly (dashed line).

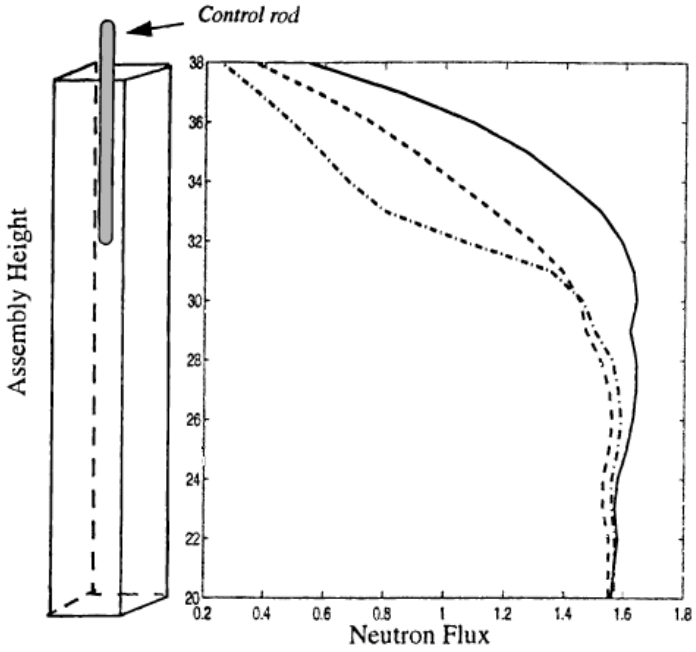

Figure 3.1: The neutron flux profile for a partially inserted control rod in the upper quarter part of the core both within the assembly (point-dashed line) and from a neighboring one (dashed line). For comparison, the flux profile for a withdrawn control rod is also included (solid line).

It is seen that indeed the axial flux shape is changed in the presence of the partially inserted rod, and that it carries information on the position of the control rod. However, this information content is very implicit, especially if the flux is measured in a neighbouring fuel assembly. No straightforward visual decision can be made on the position of the tip of the control rod. There is no parametric

algorithm, either analytical or numerical, which would take the flux shape as the input, and supply the control rod position as the output.

On the other hand, the reverse of this "inverse task", namely the direct task of calculating the axial flux shape for a given core loading and control rod position, is possible by in-core fuel management codes, with a good precision. This lends the possibility to use non-parametric methods, in particular artificial neural networks (ANNs). ANNs only need a large set of training samples, i.e. flux shapes with corresponding rod positions, for a large number of control rod positions. These can be calculated by solving the direct task, i.e. calculating the flux shape for a given control rod position. Using the flux shape - rod position pairs as a training set, the ANN can be trained to solve the inverse task, i.e. to determine the control rod position from the flux shape as input. A figure from the Swedish weekly popular science newpaper, Ny Teknik is used to illustrate the procedure (Fig. 3.2). (More on the article in Ny Teknik below).

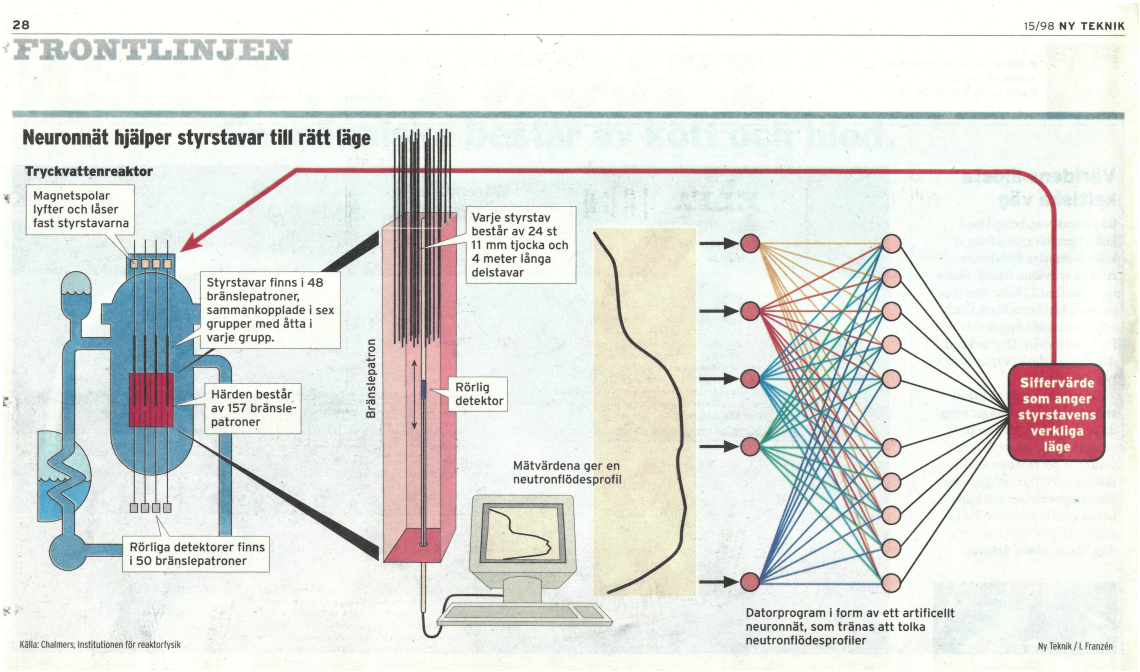

Figure 3.2: A schematic plot of the principle of the method.

The network selected for this study was a conventional three-layered feedforward network with backward error propagation. The network consists of an input layer, a hidden layer, and an output layer, as shown in Fig. 3.2). The input data, which in this case consist of axial neutron flux values, are first normalized such that they all lie between 0.1 and 0.9. They are then propagated in one direction (feed-forward) from input nodes via the hidden nodes to the output. The output layer is supposed to give the position of the control rod edge.

The flux profiles were calculated by using CASMO and SIMULATE, of which our Department had a university licence. Dara sets were generated for a number of cases, i.e. control rods in various core positions, and using the flux both within the assembly, as well as in a neighbouring assembly. For each case, the axial dependence of the flux was calculated for a large number of control rod positions, to yield a

training set of sufficient size.

The details of the calculations and the structure of the ANN, as well as the simulations and the training of the ANN are described in Refs [3, 4, 6, 45]. Different types of training were tested, such as assuming that the control rod can be inserted into the whole length to the core, or only into the upper quarter or the upper half of the core. The accuracy of the method was determined by running the trained network on input data which were not used in the training. The achieved accuracy depended on how much the rod was inserted (the deeper it was inserted, the better the accuracy), and whether the flux was measured inside the assembly or in the neighbouring assembly. As a general rule, the accuracy was found to be approximately 1 - 2 cm when the flux was measured inside the rodded fuel assembly, irrespective of whether the flux was measured within the rodded assmbly or in a neighbouring assembly. The accuracy only deteriorated to about 5-6 cm for peripheral core positions and in particular for very slightly inserted rods.

In the next step, we switched to using the detector reaction rates instead of the flux values, because in the practical applications it will be those which will be used, in contract to those of the flux. Since the university licence of SIMULATE did not contain this option, the calculations of the reaction rates were made by Ringhals.

Finally, the method was also tested in real measurements, where the flux could be measured with partially inserted control rods, when the control rod position was known. It was found that the same accuracy, a couple of centimetres, could be achieved whether the flux was measured within the assembly or in a neighbouring assembly. These results are reported in Ref. [45].

In the work described so far, the calculations of the flux values (or the reaction rates) were made at a given part of the cycle, in which the measurement was supposed to be made. Since the axial flux shape changes during the cycle, it was desirable to develop a method which could be used at an arbitrary time during the cycle. This meant that the dimensionality of the problem had to be increased, such that the burn-up became an extra parameter, and in addition the generation of flux or detector reaction rate had to be repeated at a number of burn-up values. This work was made outside the project, as a work of a consult, Albert Nagy, who did his MSc work in Chalmers. To this end, during Stage 4, the know-how and the codes were transferred to Ringhals.

Finally it may be worth mentioning that this project constituted one of the very first practical application of machine learning methods in nuclear engineering which was tested and verified in real measurements. This fact was observed by the weekly technical journal Ny Teknik, who published an extensive report on the method, also asserting its novelty and uniqueness. As a curiosity, we show below some excerpts from the article, as well as the summary on the cover page of the journal (Fig. 3.3).

1998 NUMMER 15 PRIS 24 KR

Ringhals blir säkrare

FRONTLINJEN: Med det centrala nervsystemet som förebild har Chalmersforskare hittat på en metod att mäta exakt i vilket läge styrstavarna befinner sig. Säkerheten i kärnkraftverken ökar och produktionsbortfallet minskar. Kraftbolag världen över är intresserade. Ringhals är först ut. **SIDAN 27**

FRONTLINJEN

Världens äldsta keltiska väg

Gen gör kaffeplantan koffeinfri

Han gör kärnkraften säkrare

Ringhals först med Imre Pázsits världsunika metod

Tell Andersson, bränsleansvarig på Ringhalsverket, får nu bättre möjligheter att kontrollera styrstavarna.

FOTOHANS BLOMBERG

Figure 3.3: Excerpts from the article published in Ny Teknik in number 15, 1998, on the implementation of the method in Ringhals.

3.2 Core-barrel vibration analysis

3.2.1 Introduction

Without doubt, this topic is the dominating one in the project, appearing essentially in all of the Stages. Core-barrel vibration analysis, or core barrel motion (CBM) surveillance with analysis of the ex-core neutron noise, has been performed at many PWR plants world-wide, being used for surveillance and trend analysis, already quite some time before the starting of the project (see e.g. the reviews [46] and [33]). CBM surveillance is performed by using the ex-core ionisation chambers, which are part of the standard instrumentation of all plants. As an example, Fig. 3.4 shows the arrangement of the 2 x 4 ex-core detectors at Ringhals 2, 3 and 4 with 4 detectors spaced at 90 degrees at two axial levels. Some plants, such as the older VVER-reactors, have three detectors in a horizontal plane, placed 120°apart. In a simplified way one can say that for small vibrations of the core barrel, such ex-core detectors act as displacement sensors of the radial movement/displacement of the core boundary towards the direction of the detector, by the modulation of the water thickness between the core boundary and the pressure vessel. This is the main principle of the CBM analysis with ex-core detectors, which hence does not include the solution of any dynamic space-time dependent diffusion or transport equations, only geometrical considerations.

The expression “core-barrel vibrations” or “core-barrel motion” is a collective designation for several different type of vibrations. The two dominating types are

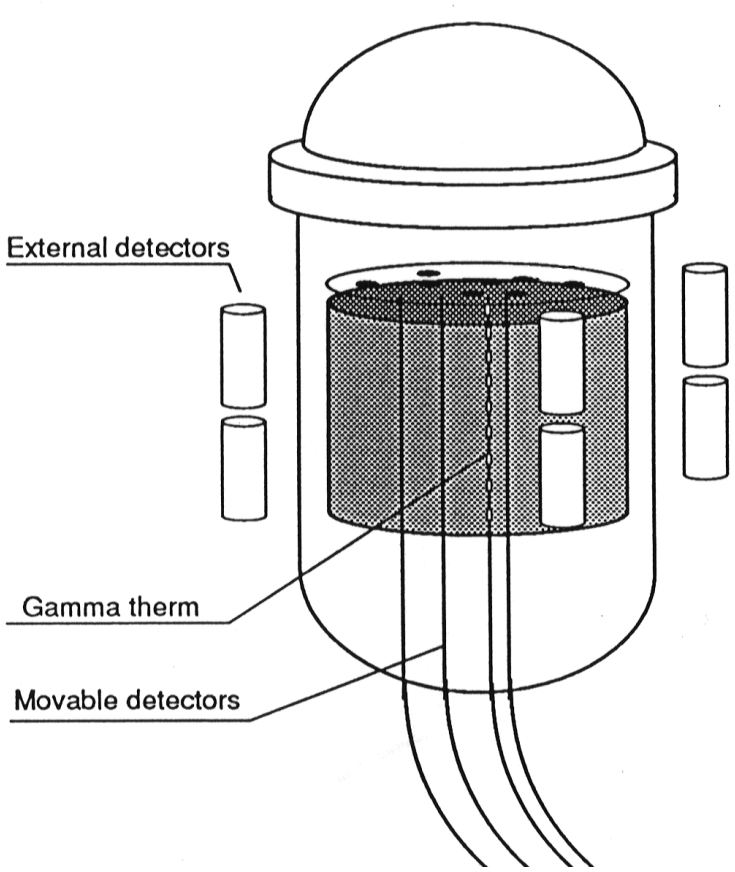

Figure 3.4: A schematic view of a Westinghouse-type PWR plant with ex-core detectors

the so-called beam mode and shell mode vibrations (see Fig. 3.5 for an illustration). The beam mode (also called pendulum mode) vibrations are a type of core-barrel movement where the shape of the core-barrel does not change, but the whole core-barrel executes a two-dimensional random walk in the horisontal plane, like a random pendulum. The reason for calling it "pendulum-type" is that the whole core-barrel acts as a pendulum, since it is hanging on flanges at the top, and the movement is like that of the pendulum; the largest amplitude is at the bottom, and the smallest (no movement) at the top. In a horisontal plane anywhere below the top, such as at the half height at the core, the movement is illustrated in the left hand side of Fig. 3.5. Although this illustration shows the beam mode vibrations as unidirctional, in

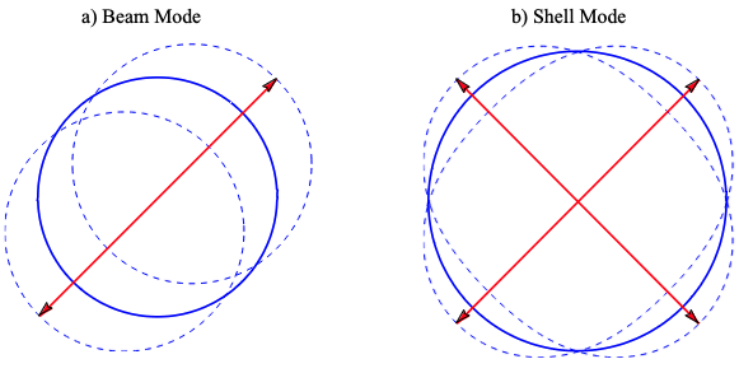

Figure 3.5: The two main vibrating modes of the core-barrel

reality the movemenf of the core-barrel, as described e.g. with the movement of its centre at the 2D plane, is a two-dimensional random motion.

In contrast, the shell mode vibrations constitute a type of motion where the centre of the core-barrel does not move, rather the shape of the outer boundary of the core is deformed periodially from circle to an ellipse, along the two main principal axes, which do not move. An illustration of this is seen in the right side of Fig. 3.5.

Apart from these two modes, as will be discussed later, the individual (uncorrelated) vibrations of the fuel assemblies lead to a noise which is related to the reactivity effect of the vibrations, and a new mode, called tilted mode vibrations, was also discovered during the collaboration. These two types have not been known in the international praxis before, the possibility of their existence was discovered during the project. These will be described in more detail in the forthcoming.

Throughout the project, we have made routine evaluation of the measurements taken by the eight ex-core detectors, and this is also how the project started. However, the evaluation methods have been constantly developed and updated all the time. We noted right at the beginning that the analysis methods available at the time had several shortcomings. Our first task was to eliminate the restrictions of the previous models. During the years, we have steadily improved and refined the analysis tools and techniques. By applying the increasingly more advanced and refined methods, and accumulating the experience with the analyses, we gained an increasing understanding and deeper insight of the vibrational characteristics and behaviour of the core barrel. Both the development and the results of the analysis will be described in the following subsections. Since the various aspects intertwine with each other, the subdivision of the topics might appear somewhat arbitrary and repetitive, but this is unavoidable. The subjects discussed constitute the following, somewhat arbitrary list:

- elaborating a more general analysis tool, by a) enhancing the separation of the beam and shell mode vibrations, and b) introducing a realistic description of random 2-D beam mode vibrations (the "$k - \alpha$" model)
- attempts to improve the surveillance of the shell mode vibrations by including in-core noise measurements
- developing a method of quantification of the beam mode vibrations with curve fitting; observation of a double peak at 8 Hz and the hypothesis about their origin)
- calculating the conversion factor between displacement and noise amplitude by core calculation methods; investigation of its evolution during the cycle and assessing the reactivity effect of individual fuel assembly vibrations as part of the explanation of the evolution of the 8 Hz peak during the cycle
- observing the evidence of tilted mode vibrations and development of a theoretical model for their analysis

- long-term trend analysis.

The presence of beam mode and shell-mode vibrations, at 8 Hz and 20 Hz, respectively, had long been known in Ringhals before the start of the project. Actually in the pre-project overview of the signal properties in Stage 0, we also checked the corresponding peaks in the ex-core detector APSDs, so we did not need to start with a basic classification of these two vibration peaks, only to concentrate on their qualitative and quantitative analysis.

3.2.2 Elaborating a more general analysis tool

At the beginning of the project, two methods were known in the literature for identification of the vibration modes. Both were implemented and used for the analysis of the current measurements. Both models assumed the presence of a global (reactivity) term plus certain types of core-barrel motion. The first one, SPEC-DEC, developed in Petten [47], could only identify unidirectional pendulum-type vibrations but no shell-mode vibrations. Whenever the algorithm identified a peak as pendular (beam-mode) vibration, it also determined the direction of the vibrations as well. The second algorithm, called VIBREAL, developed in Studsvik [48], could handle both beam mode and shell mode vibrations, and assumed that the beam mode vibrations consisted of a sum of an isotropic and a unidirectional vibration.

Both models were implemented by us and used in the analysis of the core-barrel vibrations already in Stage 1. However, we found several shortcomings of both methods. One of them was the lack of supplying quantitative information - most information was visual in form of spectra and plots. More important, the fact of accounting for only either isotropic or unidirectional vibrations, or a sum of these two, felt rather restrictive, since these are only special cases of real vibrations. Finally, even if the different vibration modes dominate at different frequencies, they have an influence of each other, and it is advisable to separate them. The earlier models achieved this by assuming statistical independence of the vibrations of the two modes. It felt that it would be useful to have a separation method that does not assume statistical independence.

In Stage 2, we developed and implemented a method for the last two problems. The first of the three problems, the quantitative representation of the results, will be taken up in Section 3.2.5, as it only concerns the beam mode vibrations.

The separation of the vibration modes which we suggested starts in the time domain, and is based on some symmetry properties of the beam and shell mode vibrations, which is reflected in the ex-core detector signals, and some further assumptions on the presence of a global (point kinetic) and uncorrelated background noise. Assuming that the 2-D random beam mode vibrations are described by the random functions $x(t)$ and $y(t)$ in the coordinate system connecting the diagonally opposite ex-core detectors, as shown in Fig. 3.6 (see also Fig. 3.5), one can assume that the normalised (by the static flux) signals $\delta\phi_i(t)$ of the detectors N_{4i}, $i = 1..4$,

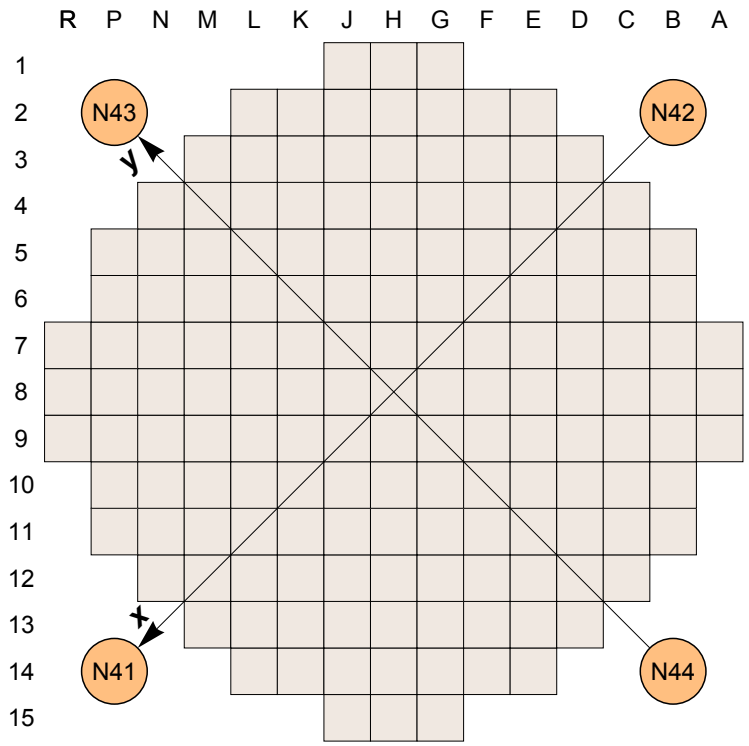

Figure 3.6: A horisontal cross section of the core, showing the positions of the ex-core detectors, and the co-ordinate system used in the model

can be written as

$$\begin{aligned}
\delta\phi_1(t) &= \delta r_1(t) + \delta P(t) + \mu\, x(t) + D(t) \\
\delta\phi_2(t) &= \delta r_2(t) + \delta P(t) - \mu\, x(t) + D(t) \\
\delta\phi_3(t) &= \delta r_3(t) + \delta P(t) + \mu\, y(t) - D(t) \\
\delta\phi_4(t) &= \delta r_4(t) + \delta P(t) - \mu\, y(t) + D(t)
\end{aligned} \tag{3.1}$$

Here, the $\delta r_i(t)$ stands for the uncorrelated background, $\delta P(t)$ is the reactivity term (its amplitude factor), $x(t)$ and $y(t)$ are the beam mode displacement components in the co-ordinate system shown in Fig. 3.6, μ is the scaling factor between the detector current and the core displacement corresponding to the beam mode, and $D(t)$ is the shell mode component. Assuming that from any combination of the signals the sum of δr_i, $i = 1 - 4$ is negligible compared to the sum of the other components, the reactivity, beam mode and shell mode components can be approximately extracted as follows [4, 49]:

$$\delta P(t) = \frac{1}{4}\sum_{i=1}^{4} \delta\phi_i(t), \tag{3.2}$$

$$\mu\, x(t) = \frac{1}{2}\big(\delta\phi_1(t) - (\delta\phi_2(t)\big), \tag{3.3}$$

$$\mu\, y(t) = \frac{1}{2}\big(\delta\phi_3(t) - (\delta\phi_4(t)\big), \tag{3.4}$$

and

$$D(t) = \frac{1}{4}\big(\delta\phi_1(t) + \delta\phi_2(t) - \delta\phi_3(t) - (\delta\phi_4(t)\big). \tag{3.5}$$

It is clear that the above separation of the vibration modes is only approximate, but at any rate the corresponding mode is enhanced compared to the others by this separation technique. Hence the analysis starts with the above separation technique in the time domain. After that, the analysis is continued with spectral methods (auto- and cross spectra) of the corresponding components. For the reactivity and the shell mode, this means simply to calculate the APSD of $\delta P(t)$ and $D(t)$, but for the beam mode, we have the two components $x(t)$ and $y(t)$, which yield the auto- and cross-spectra $APSD_x(\omega) \equiv S_{xx}(\omega)$, $APSD_y(\omega) \equiv S_{yy}(\omega)$ and $CPSD_{xy}(\omega) \equiv S_{xy}(\omega)$.

Describing the beam mode vibrations by the two components of the random motion gives a possibility to eliminate the restriction of the previous models to assume either isotropic or unidirectional vibrations. For this, we adopted a model, introduced by us earlier for the description of the random 2-D flow induced vibrations of control rods, the so-called "$k-\alpha$ "model [50]. According to that model, one can assume that the above three independent spectral quantities can be put in a form described by the three parameters $C(\omega)$, k and α as follows:

$$\begin{aligned} S_{xx}(\omega) &= |C(\omega)|^2 \,(1 + k\, \cos\, 2\alpha) \\ S_{yy}(\omega) &= |C(\omega)|^2 \,(1 - k\, \cos 2\alpha) \\ S_{xy}(\omega) &= |C(\omega)|^2 \, k \sin\, 2\alpha \end{aligned} \tag{3.6}$$

Here $|C(\omega)|^2$ is the generalised APSD of the amplitude of the beam mode vibrations, describing the severity of the vibrations, $k \leq 1$ is an anisotropy parameter, and α is the preferred direction of motion (when it is anisotropic). The case $k = 0$ corresponds to isotropic vibrations, and $k = 1$ to unidirectional vibrations along the direction α. The cases $0 < k < 1$ correspond to vibrations with equiprobability lines constituted by ellipses, with the main axis enclosing an angle α with the x-axis.

The $k-\alpha$ model is a generalisation and extended version of the previous models, in that it can account for any anisotropy of the beam mode vibrations, from isotropic to unidirectional, such that it describes a random 2-D walk. It has to be added that in reality, anisotropic vibrations with $k > 0.5$ are unlikely to occur. The suitability of the $k-\alpha$ model was confirmed in Stage 3 [5] by constructing the 2D probability distribution of the amplitudes for both the upper and lower detectors, which showed slightly elliptic forms with the direction of the main axis corresponding to the α derived from the $k-\alpha$ model, and also showing a larger amplitude for the lower detectors than for the upper ones, as expected for the pendulum type vibrations. The above model was implemented in our analysis tool and were used in all CBM analysis made in the continuation.

As an example of the separation (amplification) of the vibration modes and the reactivity component, obtained by the application of (3.2) - (3.6) is shown in Fig. 3.7. It is seen how the beam (pendulum) and shell modes are enhanced at their respective frequency band compared to each other. It is also seen that the reactivity component also has a peak around 8 Hz, which will be returned later on. The analysis of the beam mode and reactivity components will be made in later sections, first we treat the shell mode vibrations.

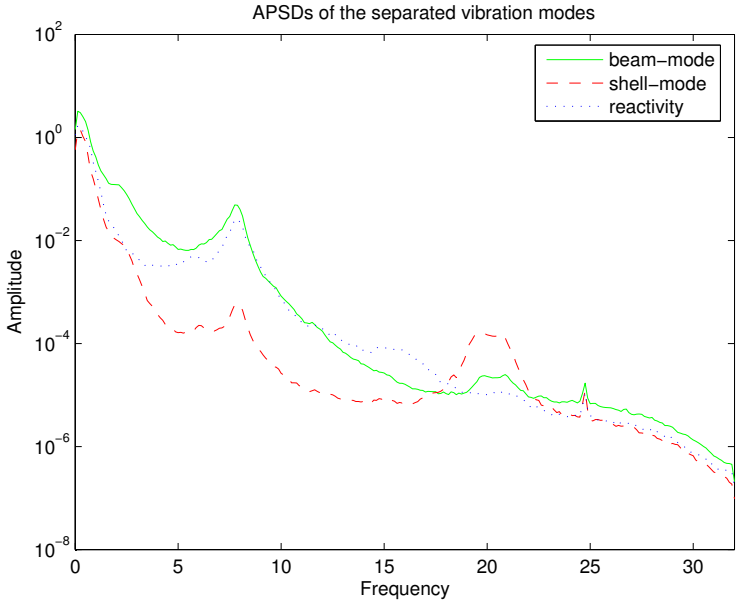

Figure 3.7: The APSDs of the three separated components

3.2.3 Diagnostics of shell-mode vibrations

The diagnostics of the shell mode vibration is much less straightforward than that of the beam mode. As it was touched upon earlier, and as it can easily be confirmed from Fig. 3.5 and Eqs (3.1) and (3.5), the geometrical arrangement of the ex-core detectors, with an equidistant angular spacing of 90° means that all four detectors carry exactly the same information, the signal designated by $D(t)$. This means that there is only one measured parameter, whereas there are two unknowns, the amplitude and the preferred direction of the shell mode vibrations, which can therefore not be extracted from the measurements. For example, a change in the measured detector signal amplitudes may equally indicate change of the vibration amplitude as well as change of the direction of the vibrations, and it is not possible to decide which is taking place. Finally, if the axes of the direction of the vibrations encloses 45° with the diagonal lines connecting the opposite detectors, the vibrations do not induce any ex-core neutron noise, thereby such vibrations cannot be detected by analysis of the ex-core signals. For all these reasons, although the magnitude of the shell-mode peak can always be determined from the measurements, unlike the beam mode amplitude, it is not suitable for a trend analysis either within the cycle or over several cycles.

For this reason we sought an alternative solution to improve the possibilities of the diagnostics of shell mode vibrations. The idea which we pursued was to investigate whether the shape changes of the core due to the shell mode vibrations would lead to a detectable in-core neutron noise, which could then also be utilised for the diagnostics of the shell mode vibrations, in addition to the information in the ex-core neutron detector signals. Even if the induced in-core neutron had the same azimuthal symmetry as the ex-core noise (which can be expected intuitively and which also turned out to be the case), in-core detectors can be selected at several positions in the horizontal cross section of the core. This would allow selecting posi-

tions which contain information which is independent of that of the ex-core signals and from each other, and hence it would make it possible to extract information on both the amplitude and preferred direction of the shell-mode vibrations.

Determination of the in-core noise induced by the shell mode vibrations was treated by modelling the temporal change of the shape of the core by the corresponding time- and azimuthally dependent change of the extrapolation lenght. Already in Stage 5 we elaborated the theory and it was shown, that the azimuthal dependence of the in-core noise is identical with that of the ex-core detectors [7]. Then, it was also shown that by choosing in-core detectors at suitable radial and azimuthal positions, both the (relative) amplitude, as well as the preferred direction of the shell mode vibrations can be unfolded. The optimum in-core detector positions were on radial lines enclosing 45° with the diagonal lines connecting the ex-core detectors. A plot of the radial dependence of the noise along a radial line, and the radial and azimuthal dependence of the in-core noise APSD are shown in Fig. 3.8.

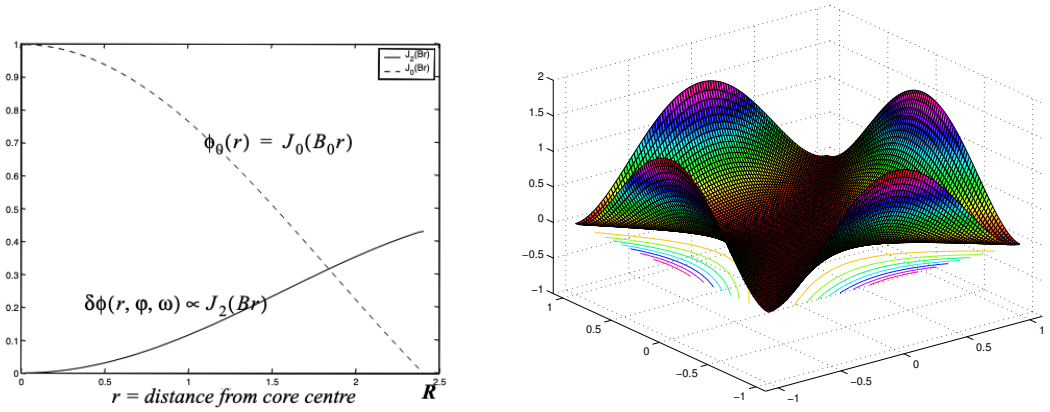

Figure 3.8: The radial dependence of the amplitude of the in-core noise (left figure) and the azimuthal and radial dependence of the APSDs of the in-core noise induced by shell-mode vibrations

In Stage 6 the method of extracting the direction of the axes of the shell mode vibrations was further refined. The method was tested on several cases when in-core and ex-core noise measurements were available. In about half of the cases we found results consistent with the model, and hence the direction of the vibrations could be estimated. In the other half, either we received results that were not consistent with the model, or the peak in the in-core signals at 20 Hz was too low to be useful. Further measurements were analysed in Stage 7, and in one case a definite statement on the direction of the vibrations could be made. Then the theoretical description was extended to a 1-D, two-group two-region model, which was suitable for the calculation of the local component of the noise at the core-reflector interface (Stages 8 and 9). Finally, in Stage 10 dedicated measurements were made by strategically chosen in-core detector positions.

The final conclusion from the various measurements was that despite their potential advantages, the use of in-core detectors in the diagnostics of shell mode vibrations did not bring the expected benefits. In most cases the contribution of

the shell mode vibrations to the in-core noise at 20 Hz was negligible. One possible reason for this is that in contrast to the model, which assumed detectors at fixed spatial positions, the detectors moved together with the vibrations, thereby significantly decreasing the noise in the detector. The model did not take into account the possible variations in core density due to the shape changes. Due to these difficulties, and to the fact that there were no indications that the shell mode vibrations would represent an operational concern, the diagnostics of the shell mode vibrations was discontinued after Stage 10.

3.2.4 Diagnostics of beam mode vibrations - long-term and short-term trends

The diagnostics of beam mode vibrations is conceptually much simpler than that of the shell mode. In contrast to the latter, the 90° spacing of the detectors is optimal for the diagnostics of the beam mode. As Eqs (3.3) and (3.4) show, the x and y components of the 2-D random movement can be enhanced and extracted from the four ex-core detector signals, and can be used e.g. for the construction of the amplitude probability distribution (APD) of the vibrations, which immediately gives an indication on the anisotropy and preferred direction of the vibrations. More interesting is the amplitude $|C(\omega)]^2$ of the vibrations, introduced in the so-called $k-\alpha$ model in (3.6). It is easily seen that this can be obtained from the auto-spectra of the x and y components as

$$APSD_{beam}(\omega) \equiv [C(\omega)|^2 = \frac{S_{xx}(\omega) + S_{yy}(\omega)}{2} \tag{3.7}$$

Although the spectra above are frequency dependent, the amplitude of the vibrations is described with the maximum value of the spectra at the peak. It is worth mentioning that not knowing the scaling factor μ of Eqs (3.3) and (3.4) between the amplitude of the vibrations to the induced change in the ex-core detector signals, the amplitude $APSD_{beam}$ contains an unknown scaling factor, and hence is not suitable to express the amplitude in length units. However, assuming that the scaling factor does not depend on core loading and the burn-up, only on the attenuation of the flux in the reflector, the amplitude can be used to compare measurements between cycles and within a cycle, and hence to follow up long-term and short-term trends.

Such a trend analysis for the 8 Hz peak of the beam mode vibrations was first performed in Stage 3 for a few measurements that were available from 1991, 93, 94 and 98, for some of the units. Only single measurements were available per cycle, at that time no multiple measurements were made in a single cycle. This investigation showed a slow, but definite increase of the amplitude of the beam mode vibrations over the period 1991-98. After this period, the attention was concentrated on the improvement of the diagnostics of the shell-mode vibrations, as described in Subsection 3.2.3. The interest in the beam mode vibrations was revived in the mid-00's, when some fatigue and wear in the lower core-barrel flange was noticed. To decrease the possible effect of vibration induced wear, the hold-down springs were replaced in Ringhals-3 during the refuelling in 2005. To follow-up the effect of the change of the hold-down springs, dedicated measurements were made in the spring of 2005 (before the change of the hold-down spring) and in the autumn of 2005 (after the change of the hold-down springs both in R3 and R4.

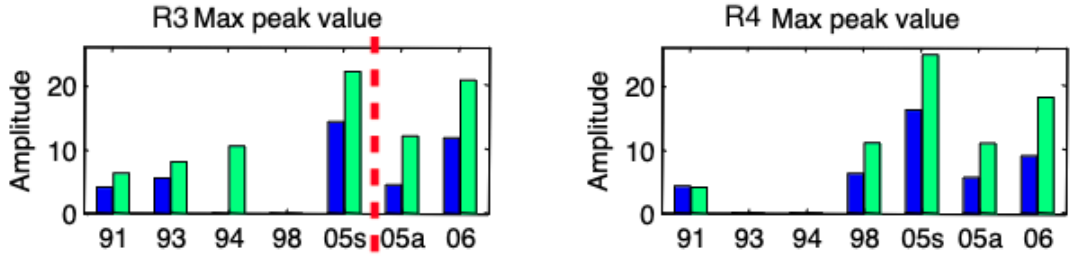

Figure 3.9: The evolution of the beam mode amplitude in R3 (left figure) and in R4 (right figure) during the years. The broken red line indicates the change of the hold-down springs in R3 after the refuelling in 2005. The date "05s" stands for spring 2005, and "05s" for autumn 2005. Results obtained in Stage 11 [13].

The results, shown in Fig. 3.9, partly show the long-term evolution and increase of the beam mode amplitude from 1991. More interestingly, they also show the change in the amplitudes both before and after the replacement of the hold-down spring in R3 in 2005 (the date is indicated by a broken red line in the Figure. As expected, the amplitude of the beam mode vibrations decreased significantly after the change of the hold-down spring, compared to its value before the replacement.

However, quite surprisingly, a similar decrease of the amplitude was observed in R4, in which no change of the hold-down springs took place. The explanation of these measurements lie in a fact that had went unnoticed to us before, since no multiple ex-core measurements within one cycle were analysed by us previously. Namely, after having started doing several measurements within one cycle, it became clear that the beam mode amplitudes in both R3 and R4 increase monotonically during the cycle, but after the refuelling they fall back to approximately the same low level as at the beginning of the previous cycle. Hence the decrease of the amplitude of the beam mode vibrations in R3 was not primarily due to the change of the hold-down spring, rather was just a manifestation of a periodically repeating pattern of the variation of the amplitudes during a cycle and between the cycles. Some slight general decrease of the vibration peaks could be seen when comparing the end-of-cycle measurements from the two cycler before and after the change of the hold-down spring, but this was much smaller than the change of the amplitude during one cycle.

The monotonic increase of the beam vibration peak during during a cycle has been also observed in other PWRs, hence it is not a curiosity of the Ringhals plants only. In principle, there may be two reasons for the increase of the beam mode peaks in neutron noise APSDs: either the amplitude of the vibrations is increasing, or the scaling factor between the mechanical displacements and induced neutron noise is changing due to burn-up. There is no consensus in the noise community about the reasons, although the majority assigns the increase of the peaks to the increase of the scaling factor. We have actually investigated this question by various means, which will be described in the following subsections. The investigations went on two lines. One was the quantification of the 8 Hz peak by an advanced curve fitting method and the resolution of the double peak around 8 Hz. The other was making reactor physics calculations of the evolution of the scaling factor during the cycle. This latter was also divided into two branches. Our calculations showed that the scaling factor between the movement of the core barrel as a whole and the induced ex-core noise did not change noticeably during the burn-up. Later, when we understood that

both collective motion of the fuel assemblies together with the core-barrel, as well as incoherent, flow induced vibrations of the individual fuel element take place and lead to two different peaks close to 8 Hz, we investigated the evolution of the scaling factor between the individual fuel assembly vibrations and the ex-core neutron noise. These will be described in the following.

3.2.5 Quantification of the peak amplitudes with curve fitting and the double peak at 8 Hz

One problem, or at least an inconvenience regarding the evaluation of the measurements and the application of the unfolding methods for the peak amplitude is that due to background noise and the presence of other noise sources, the vibration peaks appear on top of a broad-band background noise, which is not constant, but changes in frequency. In order to use the amplitude of the peaks, this background must be detached, i.e. subtracted from the vibration peak. In addition to the peak amplitude, for some applications other parameters of the peak, such as the peak frequency, and the width of the peak (full width ad half maximum, FWHM), are also of interest.

For a long time, the elimination of the background and deternination of these parameters was made by manual methods, interpolating intuitively the background over the frequency band of the peak. This step, often made by paper and pen on the printed copy of the spectra, is clearly subjective and is prone to lead to quantitative errors. It was therefore advisable to introduce an algorithmic method, which works on the numerical values of the spectrum, is objective, and yields quantitative data directly from the algorithm. The obvious way of elaborating such an algorithm is to assume an analytical form for the spectrum containing the peak, and determine the parameters of the peak by a curve fitting method.

As a first version, in Stage 11 we started with an assumed form of the autospectra (APSD) of the individual ex-core detector signals which corresponds to that of the displacement (vibrations) of a damped harmonic oscillator, driven by a random white noise. For one such single peak, assuming proportionality between the displacement (representing the core barrel on a line towards the ex-core detector) and the induced neutron noise, the frequency dependence of the neutron noise APSD has the form

$$APSDD_{\delta\phi}(f) = \frac{C^2}{(f^2 - f_0^2)^2 + 4\,D^2\,f_0^2\,f^2} \tag{3.8}$$

where C is proportional to the peak amplitude, f_0 is the eigenfrequency of the oscillator, and D is the damping constant. These are the parameters to be determined by fitting the functional form of (3.8) to the measured data.

Soon it turned out that a qualified assumption on the form of the peak is not sufficient for a good fit. This is because the real spectra used in the fitting procedure have a background (or other peaks) that extends both over and outside the peak. Hence, in order to get a better and more reliable fitting, two terms, one constant and one linear in frequency were added to the form (3.8) above to represent the effect of the background. This improved the fitting results somewhat, but was still not satisfactory, since the original spectra and the result of the fitting still deviated

from each other in a non-negligible way. In addition, it appeared that in the ex-core APSDs, sometimes two peaks appeared very close to each other in frequency around 8 Hz, so that they strongly overlapped. The fitting procedure above could separate only slightly overlapping peaks, but not the ones that overlapped heavily. There was a need for a method which was less sensitive to the exact form of the background, and which can separate peaks lying very close in frequency.

Such a method was found in the literature, developed and applied by Wood and Perez [51]. In their work, an ex-core detector APSD is assumed of the following form:

$$APSD(\omega) = \sum_{\lambda} \left\{ \frac{\mu_\lambda A_\lambda + (\omega - \nu_\lambda) B_\lambda}{\mu_\lambda^2 + (\omega - \nu_\lambda)^2} + \frac{\mu_\lambda A_\lambda - (\omega - \nu_\lambda) B_\lambda}{\mu_\lambda^2 + (\omega + \nu_\lambda)^2} \right\} \tag{3.9}$$

Here the values of the parameters to be determined by curve fitting have the following meaning:

λ is a running index, designating the serial number of the resonance peak;

A_λ is the pole strength of the λ^{th} peak

B_λ is the asymmetry or skewness factor of the λ^{th} peak

μ_λ is the damping coefficient of the λ^{th} peak

ν_λ is the damped frequency of vibration of the resonance.

The form (3.9) differs in many ways from the previous form (refeq:harmonic). Unlike the latter, it is not based on the model of a damped harmonic oscillator, it rather resembles to the Breit-Wigner formula of the energy dependence of nuclear resonances. However, for the fitting to the measured spectra, it proved to be completely superior. Apart from giving very accurate fittings, it has two huge advantages. One is that it can resolve double peaks lying very close to each other in frequency, even so close that they cannot be visually separated. The other is that it does not need to assume any background, only several peaks, even if one is only interested in one peak. This is because the tails of all the peaks that are part of the fitting constitute the background.

The above form was introduced in Stage 12, where only the part of the measured spectra up to 10 Hz was used for the fitting, since one was interested in the peak corresponding to the beam mode around 8 Hz. It was shown that the new fitting method could readily resolve the double peak around 8 Hz which was seen in many measurements, yielding one peak ("Mode 1") at around 6.8 Hz and another ("Mode 2") at 7.9 Hz. It was also found that the amplitudes of the two peaks behave differently during one cycle. The amplitude of Mode 1 is largely constant during the cycle, whereas the amplitude of Mode 2 increases. The results obtained in Stage 12 what regards the evolution of the amplitudes of these two components during the three measurements made in cycle 24 (fall 2006 - spring 2007) are shown in Fig. 3.10.

Based on various considerations (partly by comparison of the axial dependence of the in-core noise measurements, performed also in Stage 12, and partly by expe-

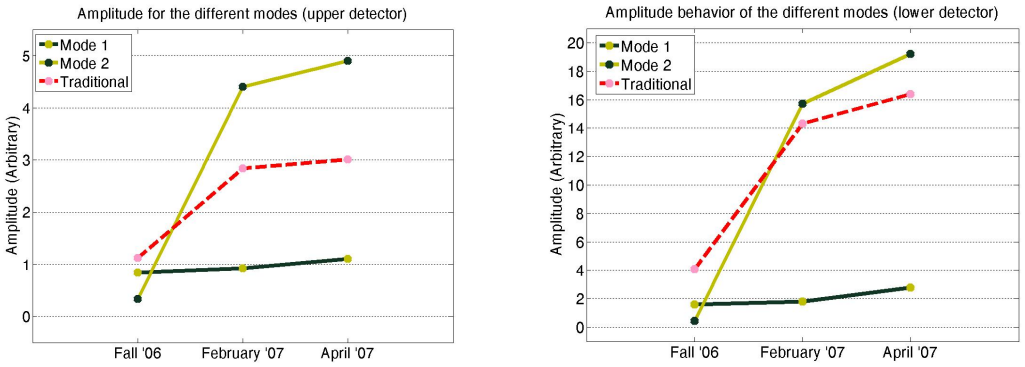

Figure 3.10: The evolution of the amplitude of the two vibration modes, one at approximately 6.8 Hz ("Mode 1") and one at 7.8 Hz ("Mode 2") for the three measurements in cycle 24 for the upper detectors (left figure) and the lower detectors (right figure). The result from the previous, "traditional" method with taking into account only one peak is also shown. The traditional method, assuming only one peak, yields results that are closer to the mode whose amplitude is higher.

rience with similar cases in the literature [52], we formulated the hypothesis that Mode 1 corresponds to the coherent movement of the fuel assemblies as one unit, following the core barrel motion, whereas Mode 2 corresponds to the individual, incoherent flow induced vibrations of the individual fuel assemblies. According to this hypothesis, the amplitude of the core-barrel vibrations does not increase during the cycle, whereas the peak corresponding to the fuel assembly vibrations does increase. This latter still can be due either to the increase of the vibration amplitudes, or to the increase of the scaling factor between the fuel assembly vibrations and the induced neutron noise during the cycle, due to fuel burn-up and changing boron content of the coolant. The question of the behaviour of the scaling factor for both Mode 1 and 2 was investigated during the collaboration, according to which the scaling factor of Mode 1 is constant, whereas that of Mode 2 will increase, although not universally (depending on the vibration properties. This is in agreement with findings reported in the literature [52], and will be elaborated more in Subsection 3.2.6.

What regards the development of the new fitting procedure, in Stage 13 we found that the fitting results improve (become more stable) if the fitting is performed up to 20 Hz. In that case more peaks (including the peak corresponding to the shell mode at 20 Hz are included, and the presence of more peaks improves the implicit modelling of the background. Indeed, an improvement of the fitting could be observed over the previous fitting results. The result of a fitting up to 20 Hz is shown in Fig. 3.11, displaying an excellent agreement between the measured and the fitted data, and the ability of the method to resolve the double peak around 8 Hz. In the continuation, this fitting procedure was applied in each stage, complemented with the inclusion of the so-called tilted mode, which will be described later (Subsection 3.2.7).

Concerning the evaluation of the double peak at 8 Hz, in Stages 12 and some of the consecutive Stages straight afterwards, the separation of the double peak around 8 Hz was made on the beam mode component APSD, Eq. (3.7). However, this APSD is made on signal combinations which assume the symmetry properties of the beam mode motion of the core barrel. The individual fuel assembly vibrations do not

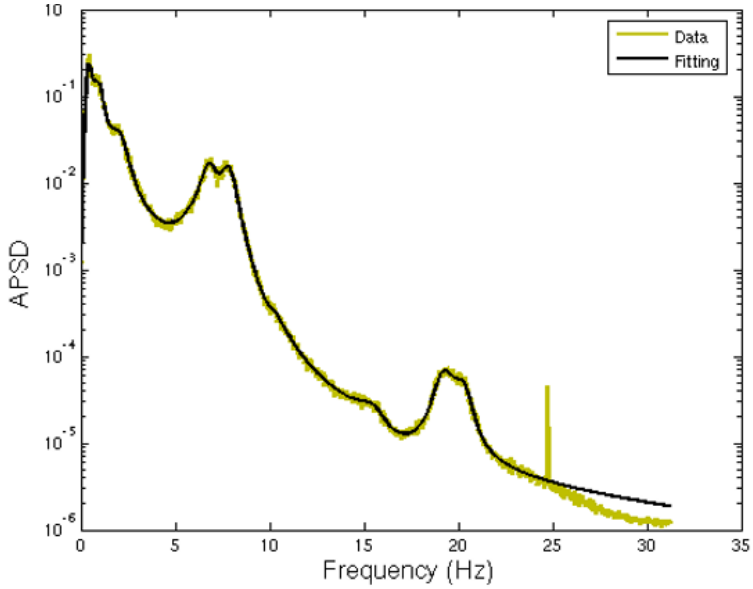

Figure 3.11: The results of a fitting with the new procedure and using data up to 20 Hz

obey this symmetry. In order to amplify the effect of the individual fuel assembly vibrations into one single indicator, we identified Mode 2 with the reactivity effect induced by the individual vibrations, Eq. (3.2), whose APSD is seen in Fig. 3.7. The validity of this assumption was investigated in Stage 2015 [20] by the use of the noise simulator CoreSim [53], developed at our Department. It was found that for realistic cases, the reactivity component of the ex-core noise represents well the total noise induced by individual fuel assembly vibrations. Hence in the continuation the peak corresponding to Mode 1 was identified from the beam mode spectra, and the peak of Mode 2 from the reactivity spectra. The applicability of this procedure was further confirmed by the fact that the frequency of Mode 1 was always lower than Mode 2, obtained this way.

The routine evaluation of the peaks around 7 and 8 Hz for Mode 1 and Mode 2 has been made based on the above principles throughout the collaboration. Some results will be shown in Subsection 3.2.8.

3.2.6 Calculation of the evolution of the conversion factor between the vibration modes and noise amplitude during the cycle

It is clear from the above that the knowledge of the behaviour of the scaling factor between core barrel and fuel assembly vibrations and the induced ex-core neutron noise would expedite significantly the evaluation of the ex-core measurements, and confirm or deny the possible hypotheses made. Hence from Stage 11 and onwards, this question was investigated through model calculations. At the beginning, following the dominating opinion in the noise community that the scaling factor between the beam mode vibrations and the ex-core noise increases with increasing burn-up and decreasing boron content of the coolant, this assumption was investigated. In Stage 11 we made a survey of the methods used to calculate the scaling factor in various models and approximations. It was investigated how the noise simulator, developed at the Department, can be used to estimate the scaling factor from the

gradient of the relationship between the detector current and the core boundary displacement. The noise simulator can take input data from SIMULATE, hence it is suitable for making calculations for actual Ringhals cores, including data from various stages of the cycle.

The simulator appeared to be suitable for calculating the scaling factor, although some development had to be made in order to be able to handle small (sub-millimeter) movements of the core boundary. Hence, in Stage 13 a thorough investigation of the dependence of the scaling factor on burnup and boron content was performed for a Ringhals-3 core. For better insight, three different studies were made: the first data set by accounting for both burnup and change of the boron content; the second data set accounted only for burnup, and the third only for the change in the boron concentration. Using data set #1 (the one corresponding to the real case), it was found that the scaling factor was slightly decreasing during the cycle. The analysis of data set #2 showed that the burnup alone leads to an increase of the scaling factor, and the analysis of data set #3 showed that the decrease of the boron concentration alone leads to a decrease of the scaling factor. In the total result the latter effect dominates, hence the overall decrease of the scaling factor during the cycle.

Thus we found that, contrary to the usual belief in the literature, the scaling factor of the beam mode core barrel vibrations does not increase during the cycle. This, on the other hand, is consistent with the hypothesis that the Mode 1 found in the Ringhals measurements, corresponds to the beam mode vibrations of the core barrel, and the fact that its amplitude does not increase during the cycle.

It remained to investigate how how the scaling factor between the individual fuel assembly vibrations and the ex-core neutron noise depends on burnup and boron content and to confirm or disprove a hypothesis raised by Sweeney et al. (1985) that scaling factor of fuel assembly vibrations increases during the cycle due to the effects of fuel burnup, the change of boron concentration, and the flux redistribution. This work was performed in Stage 2016 [21], and also reported in [54]. Numerical calculations were performed by modelling the vibrations of fuel assemblies at different locations in the core and calculating the induced neutron noise at three burnup steps. The APSD of the ex-core detector noise was evaluated with the assumption of vibrations either along a straight-line or along a random two-dimensional trajectory.

The results showed that the monotonic increase of the APSD does not occur for all fuel elements, vibration types and cross section perturbation models. Such an increase of the of APSD occurs predominantly for peripheral assemblies assuming 2-D random vibrations. However, assuming simultaneous vibrations of a number of fuel assemblies uniformly distributed over the core with random vibrations, the effect of the peripheral assemblies will dominate and hence the surmised monotonic increase of the amplitude of the ex-core neutron noise during the cycle can be confirmed. This result is in a good agreement with the hypothesis of Mode 2 being due to the individual fuel assembly vibrations, and with the fact that the increase of the amplitude of the Mode 2 peak is due to the increase of the associated scaling factor.

3.2.7 Evidence of tilting mode vibrations

For a long time, the CBM monitoring was restricted to the beam mode and shell mode vibrations. Apart from a difference in the amplitudes between the upper and lower detectors for the beam mode vibrations, both type of vibrations are essentially two-dimensional. Therefore, in all cases, only the four detectors at either the upper, or the lower axial level were analysed simultaneously.

However, around 2015, observations of wear at both the lower and upper core-barrel-support structures, i.e. the lower radial key and the reactor vessel alignment pins in the Ringhals PWRs indicated that vibration modes of the core barrel other than pendulum (beam mode) and shell mode are likely to occur. These type of movements, especially the beam mode alone, could not explain such a wear. The most straightforward and logical explanation of such signs of wear was to assume a tilting type of movement of the core barrel around a horizontal, diagonal pivot at the half height of the core (crossing through the centre of mass of the core). Such a movement, together with the indication of the symmetry relationships between the upper and lower, diagonally opposite ex-core detectors is shown in Fig. 3.12. The darkness of the detectors is meant to indicate the magnitude of the detector signal. illustration of the tilting mode.

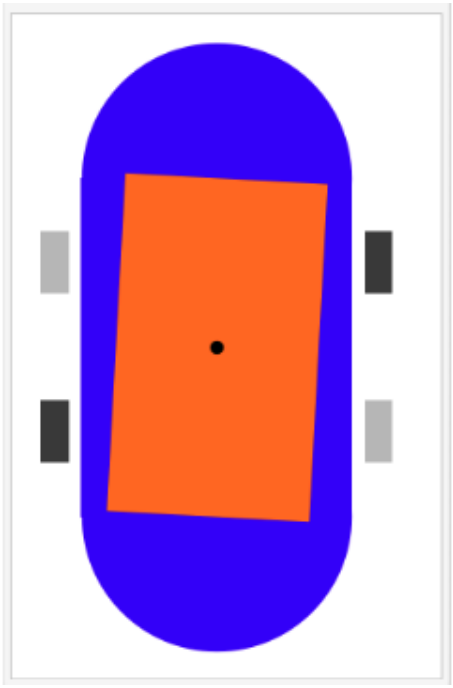

Figure 3.12: Illustration of the tilting mode vibration of the core barrel and the symmetries of the detector signals.

It is clear that analysing the four detector signals from one axial level, as it was made so far, this type of vibration cannot be distinguished from the beam mode vibrations, since the symmetries of the motion are the same for both types of CBM. The only way to separate the two by the different symmetry relationships is to take into account all 8 detector signals simultaneously, since there will be differences between the in-phase and out-of-phase relationships for the beam and the tilting mode for the detectors at different axial levels and radial positions. It

is easy to see that for instance the signals of the upper and lower detectors in the same radial position, such as N41U and N41L, will be in-phase for the beam mode, whereas they will be out-of phase for the tilting mode. Taking two axially displaced detectors at diagonally opposite radial positions, such as N41U and N42L, the situation is the opposite: such pairs are out-of-phase for the beam mode, but in-phase for the tilting mode. The conclusion is that by extending the procedure to all 8 detectors simultaneously, it is possible to develop mode separation methods such that in addition to the components considered so far (reactivity, beam, shell modes) also the tilting mode can be separated (enhance).

This can be made by an extension of the representation (3.1) to all 8 detectors. Such an extension has the form

$$\delta\phi_{N1U}(t) = \delta r_1(t) + \delta P(t) + D(t) + \mu\, x(t) - \lambda\, x(t) \tag{3.10}$$

$$\delta\phi_{N2U}(t) = \delta r_2(t) + \delta P(t) + D(t) - \mu\, x(t) + \lambda\, x(t) \tag{3.11}$$

$$\delta\phi_{N3U}(t) = \delta r_3(t) + \delta P(t) - D(t) + \mu\, y(t) - \lambda\, x(t) \tag{3.12}$$

$$\delta\phi_{N4U}(t) = \delta r_4(t) + \delta P(t) + D(t) - \mu\, y(t) + \lambda\, x(t) \tag{3.13}$$

$$\delta\phi_{N1L}(t) = \delta r_5(t) + \delta P(t) + D(t) + \mu\,(1+\alpha)\, x(t) + \lambda\, x(t) \tag{3.14}$$

$$\delta\phi_{N2L}(t) = \delta r_6(t) + \delta P(t) + D(t) - \mu\,(1+\alpha)\, x(t) - \lambda\, x(t) \tag{3.15}$$

$$\delta\phi_{N3L}(t) = \delta r_7(t) + \delta P(t) - D(t) + \mu\,(1+\alpha)\, y(t) + \lambda\, x(t) \tag{3.16}$$

$$\delta\phi_{N4L}(t) = \delta r_8(t) + \delta P(t) + D(t) - \mu\,(1+\alpha)\, y(t) - \lambda\, x(t) \tag{3.17}$$

Here, the $\lambda\, x(t)$ and $\lambda\, y(t)$ terms stand for the tilting mode component, and the factor $\alpha \ll 1$ accounts for the fact that the amplitude of the beam mode vibrations is larger at the lower level than at the higher level. All other notations are the same as in (3.1. The difference in the beam mode amplitudes at the two axial levels actually destroys the full symmetry, and makes the exact theoretical extraction of the tilting mode component impossible. One can obtain the expression for the x component of the tilting mode which is "contaminated" with the beam mode as follows:

$$\frac{\delta\phi_{N2U}(t) + \delta\phi_{N1L}(t)}{2} - \frac{\delta\phi_{N1U}(t) + \delta\phi_{N2L}(t)}{2} = \mu\,\alpha\, x(t) + 2\,\lambda\, x(t) \tag{3.18}$$

A similar expression can be written down for the y component. This shows that the tilting mode component cannot be fully extracted. However, the small value of α means that (3.18) (and its equivalent for the y component) give a good approximation of the tilting mode.

This type of signal separation was applied in enhancing the tilting mode. Since Stage 2018, the diagnostics of the tilting mode was added to that of the beam and reactivity modes,, and the evolution of the amplitude of the tilting mode was followed up.

3.2.8 Long-time trend analysis

Ever since the importance of performing a surveillance of the core barrel vibrations came up in the collaboration, it became interesting to follow up the evolution of

the amplitude of the vibrations. Due to the problem with quantifying the amplitude of the shell mode vibrations (see Subsection 3.2.3), the surveillance was concentrated on the beam mode. The significance of the surveillance of CBM due to the possibility of increased amplitude of vibrations appeared first during Stage 3, when we first performed a trend analysis for the few measurements available between 1991 and 1998 and noticed a slow, but steady increase of the amplitudes during this period (see Fig. 3.13). This problem was considered so important by Ringhals at the time, that the topic of Stage 3 was devoted solely to core barrel motion diagnostics, both method development and the results of the analysis.

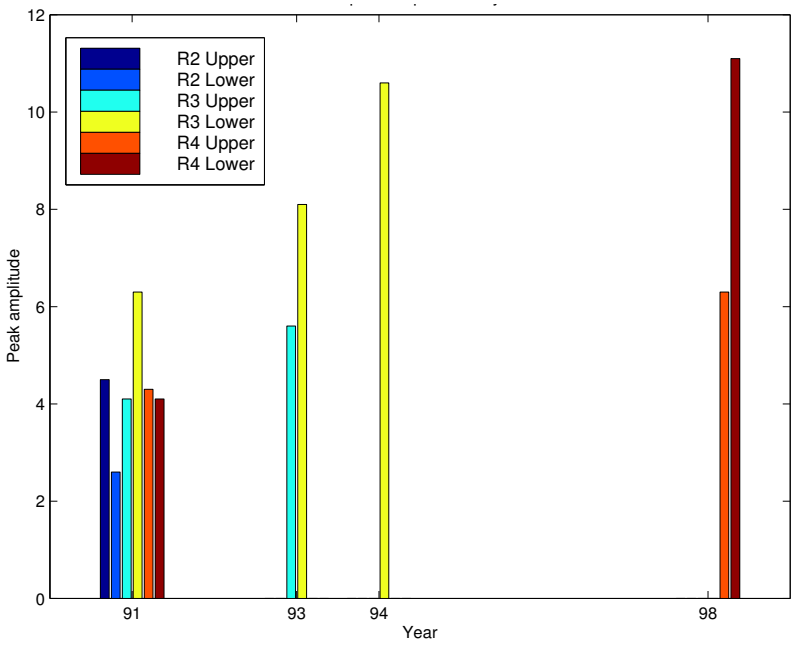

Figure 3.13: The peak amplitude of the beam mode vibrations in consistent arbitrary units for R2, R3 and R4 between 1991 and 1998.

As mentioned in Subsection 3.2.4 (shell mode vibrations), after Stage 3, for several years our attention was focused on the improvement of shell mode diagnostic methods. The interest turned back to the beam mode in connection of the change of the hold-down springs in R3 in 2005, when also the change of the beam mode amplitude within the cycle was realised (see Fig. 3.9). After that a very intensive surveillance program was started: measurements were made each fall and spring period for all three PWR units during 2006 - 2009. The analysis of the large amount of measurements was made by the consulting company Nuclear DatorFysik (NDF), and the evaluations were reported as NDF technical reports [55, 56, 57, 58, 59, 60, 61, 62]. An example of a three-year trend analysis, taken from [60], is shown in Fig. 3.14.

The surveillance program by Nucleus DatorFysik was performed by a routine usage of the existing methodology, without method development. Among others, the 8 Hz peak was not resolved into two modes, it was evaluated as one single peak, corresponding to the beam mode vibrations.The CBM surveillance got back to the Chalmers-Ringhals collaboration when the next stage of development program started with the new fitting program and the resolution of the 8 Hz peak into two

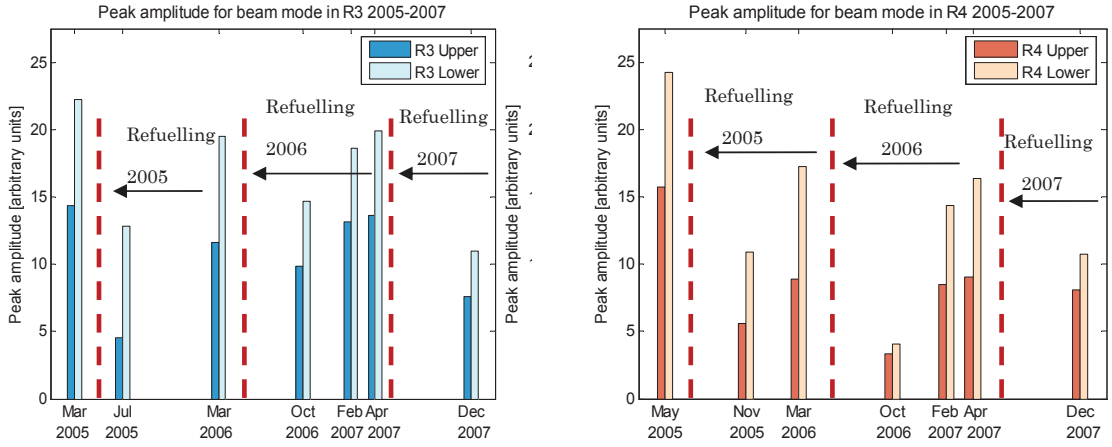

Figure 3.14: Evolution of the peak amplitude of the beam mode for some cycles in Ringhals 3 (left figure), and Ringhals 4 (right figure) between 2005 - 2007 [60].

modes. After that the CBM trend analysis was refined, and the evolution of both the core-barrel beam mode vibrations (Mode 1) and the fuel assembly vibrations (Mode 2) was included into the trend analysis.

When the analysis started with the new curve fitting method and the resolution of the 8 Hz peak into two, the results were understandably not compatible with the ones obtained by the old method, in which the 8 Hz peak was considered as a single resonance. Whereas the short-term evolution of the amplitudes of Mode 1 and Mode 2 within the cycle was evaluated every year, several years had to pass before a long-term trend analysis became meaningful. Actually the first long-term trend analysis, concerning the measurements made in R3, was reported in Stage 2019, covering the years 2018 - 21. Although only results for one unit are available, on the other hand the evolution of both the beam mode (Mode 1) and the reactivity mode (Mode 2, corresponding to fuel assembly vibrations) is followed up. Since then in each Stage the long-time trend analysis is performed cumulatively, i.e. reaching back to 2018. Therefore, we only display the latest trend analysis from Stage 2021, covering the five years 2018 - 2022, for both the beam mode (Fig. 3.15) and the reactivity mode (Fig. 3.16).

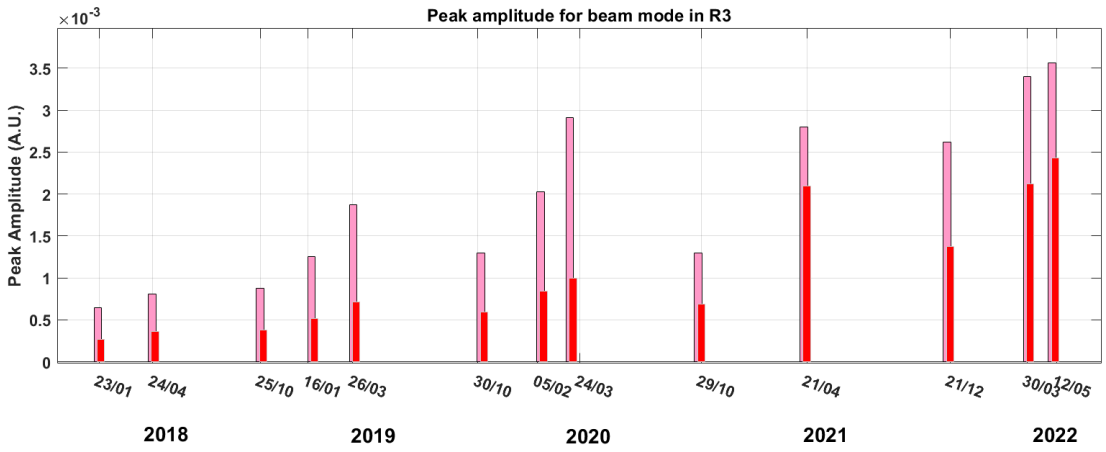

Figure 3.15: Five-year trend analysis of the amplitude of the beam mode (Mode 1). Red: upper detectors; pink: lower detectors.

The 5-year trend analysis of the beam mode vibrations in Fig. 3.15 shows partly a relatively fast increase of the amplitude within the cycle, and a slower, but definite long-term increase of the amplitude in the consecutive years. There is one small exception, namely between 2020 and 2021, the global increase is slightly reversed. One can also clearly see that the amplitude sensed by the lower detectors is larger than that of the upper detectors, as is expected from the beam mode.

The short term behaviour is in contrast to what we found in Stage 12 of having the amplitude essentially constant within the sample. It was noticed that the measurements in the past few years deviated from the behaviour postulated in the earlier hypothesis, both for the beam mode and the reactivity mode. The reasons for this deviation are not clear, but presumably can be ascribed to the several changes made to both R3 and R4, including the power uprate, upward flow conversion etc.

The long-term behaviour of the reactivity mode (Fig. 3.16) is similar to that of the beam mode. The difference between the upper and lower detectors is much smaller, and the increase within the cycle is larger than for the beam mode (which is consistent with the hypothesis about Mode 1 and Mode 2). The evolution of the reactivity component shows a somewhat larger local scatter, in particular from 2019 to 2021, there is a slight decrease of the amplitudes. The scatter may be due to several facts; partly, the fuel assembly properties may change after refuelling, and partly, that the fuel assembly vibrations are identified with their influence on the reactivity. However, according to the simulations we performed, the reactivity effect does not have a strict one-to-one relationship to the fuel assembly vibrations. Nevertheless, on the long run, a small overall increase of the amplitudes can be observed what regards the individual fuel assembly vibrations.

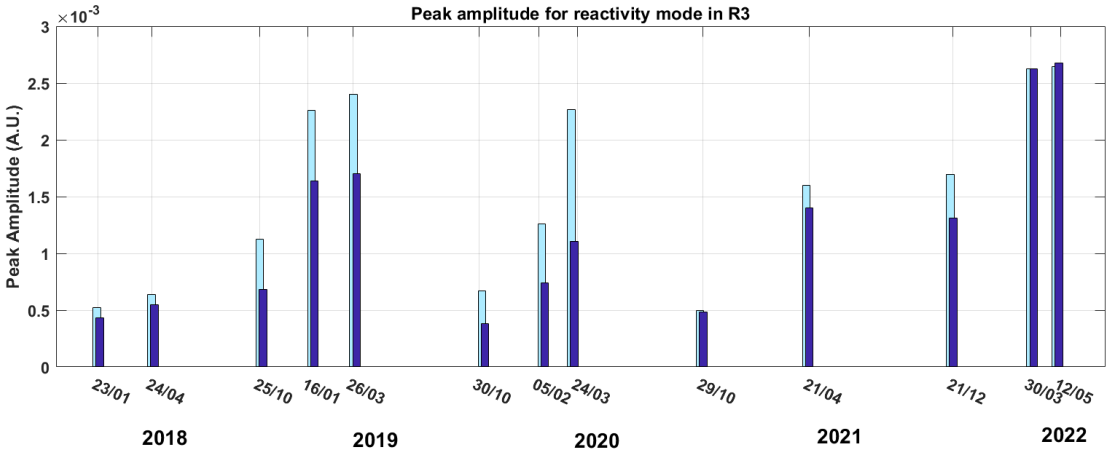

Figure 3.16: Five-year trend analysis of the amplitude of the reactivity mode (Mode 2). Dark blue: upper detectors; light blue: lower detectors.

3.3 Determination of the MTC by noise methods

Stage 4, 5 (with boron dilution), 7 (with gamma-thermometers) 8 (analysis of measurements), 10 (theoretical calculation of the MTC)

3.3.1 Introduction

The moderator temperature coefficient (MTC) of PWRs is defined as the reactivity variation due to a change of the inlet temperature of the coolant, divided by the average temperature change, and it must be correlated solely to the modification of the moderator properties. The MTC must be determined twice during each fuel cycle: at the Beginning Of Cycle (BOC) at Hot Zero-Power (HZP), and at near the End Of Cycle (EOC) at Hot Full Power (HFP). The objective of the measurement early in the cycle is to demonstrate that the MTC is negative (preventing from the consequences of a power increase), while the objective near the end of cycle is to show that it remains less negative than some prescribed limit (preventing from the consequences of a cooldown event).

There are a number of intrusive methods to determine the MTC, most notably the boron dilution method, among others. However, all these methods have very significant disadvantages. They take a long time, those at the EOC must be performed at reduced power and hence they are costly (due to loss of revenue), and they need to be corrected by calculations, to eliminate the secondary effects which are incurred by the change of the coolant temperature (such as the axial power shape, Doppler effects etc.) but are not included into the definition of the MTC. Therefore these methods are not purely experimental, rather they depend also on the accuracy of calculations.

We have actually tested the boron dilution method within the project related to the MTC problem. In Stage 5, we analysed a boron swap measurement, made in R4 in cycle 16, performed on 5 May 1999, and got some experience with the method.

The nuclear power industry has therefore been a long time looking for a method which is free of these limitations, i.e. it is non-intrusive, fast, and can supply the MTC without the need of complementing calculations. It was suggested that determining the MTC by noise methods, from the correlations between the in-core neutron noise and the temperature fluctuations of core exit thermocouples, would be suitable for that purpose. The method is non-intrusive, does not interfere with plant operation, it is fast, and in the frequency range 0.1 1 Hz, it is free from the feedback effects which would make the use of correction methods necessary. According to the above assumptions, assuming a simple point kinetic model, the MTC could then be obtained as

$$MTC_1 = \frac{1}{G_0(\omega)} \frac{CPSD_{\delta\phi/\phi_0,\delta T}(\omega)}{APSD_{\delta T}(\omega)} \tag{3.19}$$

where $G_0(\omega)$ is the well-known zero power transfer function. There are other, equivalent expressions, such as

$$MTC_2 = \frac{1}{G_0(\omega)} \frac{APSD_{\delta\phi/\phi_0}(\omega)}{CPSD_{\delta T,\delta\phi/\phi_0}(\omega)}, \tag{3.20}$$

or some combinations of the above, such as the arithmetic or harmonic mean. The idea behind the combinations is that the theoretical values (3.19) and (3.20) may be biased due to the fact that the coherence between the neutron and temperature noise is (much) less than unity, due to the presence of other noise sources that

induce neutron noise, and the combinations could serve as better estimators, if the two variants are biased into opposite directions.

However, it turned out that none of the above methods could supply acceptable estimates of the MTC. One problem was the generally low coherence between the temperature noise at the core exit and the in-core neutron noise, which decreased the reliability of the results significantly. The main fact is that all these methods served an MTC which was with a factor 2 - 5 smaller than the true one. Hence the noise method did not seem to be suitable for the absolute determination of the MTC by itself, only by the help of calibration methods, which required either reference measurements, or extensive calculations.

We took up the problem of determining the MTC from noise measurements relatively early, in Stage 4. Using noise measurements made in Ringhals-4 in cycle 15 in 1998, which included both core-exit thermocouple signals as well as in-core neutron detectors, the suitability of the estimators MTC_1 and MTC_2 were investigated. The MTC derived from the noise measurements was systematically lower with about a factor 2 than the nominal value of the MTC.

The dominating opinion in the noise community was that the reason for the failure of the noise method lie in the fact that it assumes point kinetic behaviour, whereas in reality the reactor may not behave in a point kinetic manner. However, all attempts aiming at arriving to better estimators than those given by (3.19) and (3.20), failed. The corrections obtained by using space-dependent neutron noise theory were marginal.

3.3.2 The principles of the solution of the problem

The breakthrough came when we realised that the reason of the failure of the noise method is not due to the deviation of the core response from point kinetics. Rather, the reason lies with the spatial character of the driving source of the neutron noise, i.e. the temperature fluctuations. In the traditional method, expressed by (3.19) or (3.20), it is assumed that the temperature fluctuations, measured by one single thermocouple, are characteristic for the whole core. This is equivalent to assume a spatially constant (although temporally random) temperature field in the core. However, this is not true in reality. The temperature fluctuations are not in phase with each other at the various radial positions (fuel channels), rather they are very loosely coupled. The radial correlation of temperature fluctuations decays fast in space, with a correlation length comparable to the size of the fuel channels. The temperature fluctuations in various radial point are often out of phase with each other, whereby the total reactivity effect will be much less than in the case when they fluctuate in-phase (infinite correlation length). It is clear that a much larger MTC is needed to generate a given neutron noise if the temperature fluctuations are weekly correlated (which is the case in reality) than in the case of coherent temperature fluctuations (which is assumed by the traditional method).

The whole problem then boils down to show that in the case of radially weekly correlated perturbations the MTC is indeed underestimated, and to find a method how in such a case the MTC can be unfolded. To this end we introduced the case of

spatially random perturbations which are characterised by a correlation length, and investigated its effect on the neutron noise [63]. Assuming that the local temperature fluctuations are proportional to the local change of the neutronic cross sections (in a one-group model to the absorption cross section), we introduced such a spatially random driving force by its temporal and spatial cross-correlation function as

$$CCF_{\delta\Sigma_a}(\boldsymbol{r},\boldsymbol{r'},\tau) = \delta(\tau)\,\sigma^2\,e^{-\frac{|\boldsymbol{r}-\boldsymbol{r'}|}{\ell}} \tag{3.21}$$

Here, ℓ is the correlation length and variance σ^2 stands for the strength of the perturbation, and it was assumed that the temporal fluctuations constitute a white noise (which is the usual assumption about temperature fluctuations in PWRs). Then the CPSD of the driving force is given as

$$CPSD_{\delta\Sigma_a}(\boldsymbol{r},\boldsymbol{r'},\omega) = \sigma^2\,e^{-\frac{|\boldsymbol{r}-\boldsymbol{r'}|}{\ell}} \tag{3.22}$$

Using this formula as the noise source in the noise equations, the induced neutron noise was calculated, for various values of the correlation length ℓ. It could be seen that the deviations from point kinetic behaviour were quite mild, even for quite small correlation lenghts. More important, from the model, the auto- and cross spectra of $\delta\phi/\phi_0$ and δT in the estimator MTC_1 of Eq.(3.19) could be calculated for different correlation lenghts. The one with $\ell = \infty$ corresponds to the traditional method; from the ratio of two MTCs, one with an infinite correlation length and another with a short one, the bias of the traditional MTC could be calculated. This way it was possible to prove that with with temperature fluctuations having a correlation length in the range of the fuel assembly size, the true MTC is underestimated by a factor 2 to 5.

If the spatial correlation length of the temperature fluctuations was known and constant, then such calculations could supply a calibration constant with which the result of the traditional method could be corrected. Since the correlation distance is not known, and moreover might change both during the cycle, between cyles, and even in one time instant spatially within the core, this method is not applicable. The obvious complete solution would be to have access to the temperature fluctuations throughout the core, or at least in a relatively large number of positions in a horizontal plane. Then, based on the first-order perturbation theory expression of the reactivity that case, it follows that the correct MTC can be obtained by the traditional noise estimators, if instead of the temperature measured in one single radial position, one uses the core averaged moderator temperature fluctuations in the form

$$\delta T_m^{ave}(t) = \frac{\int \delta T_m(\boldsymbol{r},t)\,\phi_0^2(\boldsymbol{r})\,\mathrm{d}\boldsymbol{r}}{\int \phi_0^2(\boldsymbol{r})} \tag{3.23}$$

3.3.3 Experimental verification with gamma-thermometers

The problem with the core averaged temperature fluctuations, Eq. (3.23), to be used in the "true estimator", is that it requires the availability of several thermocouples in a horizontal plane. Moreover, the application of (3.23) requires measurement

of in-core temperatures, in contrast to the core exit thermocouples, in order that the correct weighting can be made.

However, such a possibility arose in our collaboration by the fact that so-called gamma-thermometers were available in R2 in 12 radial positions. Because of the temperature time constants of the gamma-thermometers, these work as pure thermocouples in the frequency range 0.1 - 1 Hz, needed for the determination of the MTC. The ability of gamma-thermometers to measure the local temperature fluctuations in the required frequency range was investigated by us both theoretically and experimentally in Stage 5. We could even show that with cross-correlating the signals of gamma-thermometers within the same string, even the coolant flow velocity could be determined.

The access to the signals of the gamma thermometers gave us on the one hand the possibility to to check the assumption that the inlet (or in-core) temperature fluctuations are very loosely coupled with a short spatial correlation length, and on the other to test the suitability to use the expression (3.23) in the traditional MTC estimator to obtain the true MTC.

The left hand side of Fig. 3.17 shows the radial positions of the gamma-thermometer strings in R2 in 12 radial fuel assembly positions, with 9 gamma detectors in each string, as shown on the right hand side of the figure. In Stage 7 a particular measurement, performed in cycle 26, where also two movable in-core detectors were used in core positions L04 and H11, was evaluated. From the gamma thermometers, only the signals from axial level 7 (30% core height from the bottom of the core) were used.

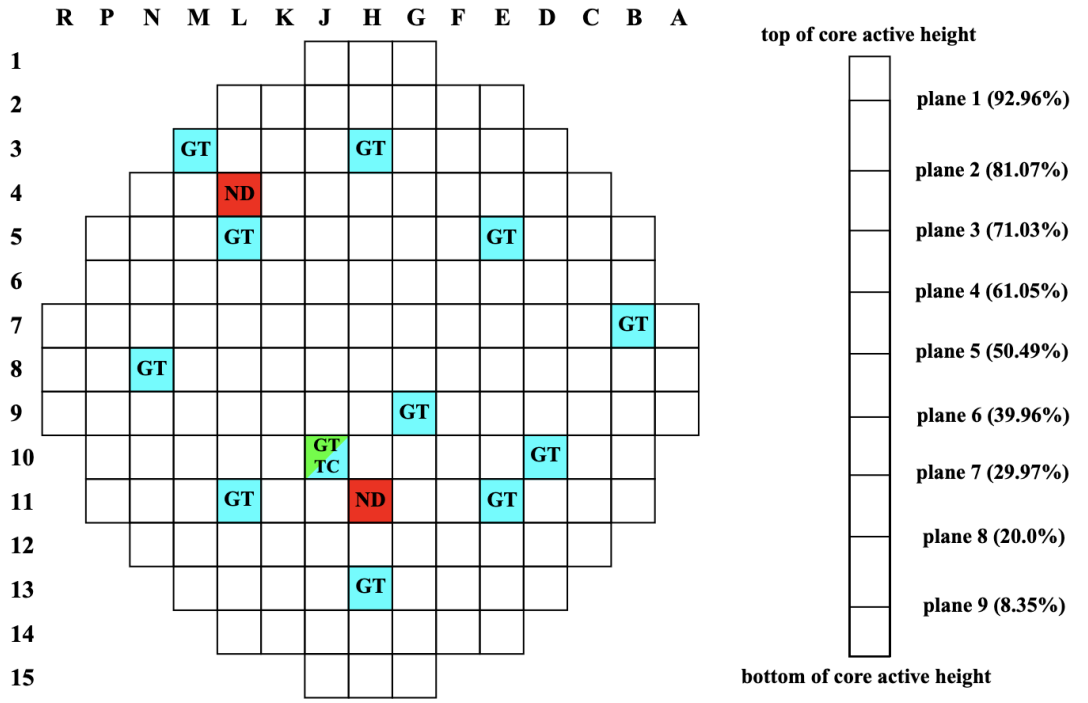

Figure 3.17: Position of the detectors for the noise measurement in Ringhals-2, cycle 26. Left hand side: the radial position of the gamma thermometers and two in-core neutron detectors. Right hand side the: axial positions of the gamma detectors in each fuel assembly).

The coherences between the 66 pairs of 12 gamma detectors at axial level 7 in the frequency range 0.1 - 1 Hz (where they act as thermocouples, measuring the coolant temperature fluctuations) are shown in Fig. 3.18, as a function of the distance between the pairs. It is seen that the coherences are very low, even for the closest pairs. This indicates that the correlation distance is very short, which explains the failure of the traditional noise estimator.

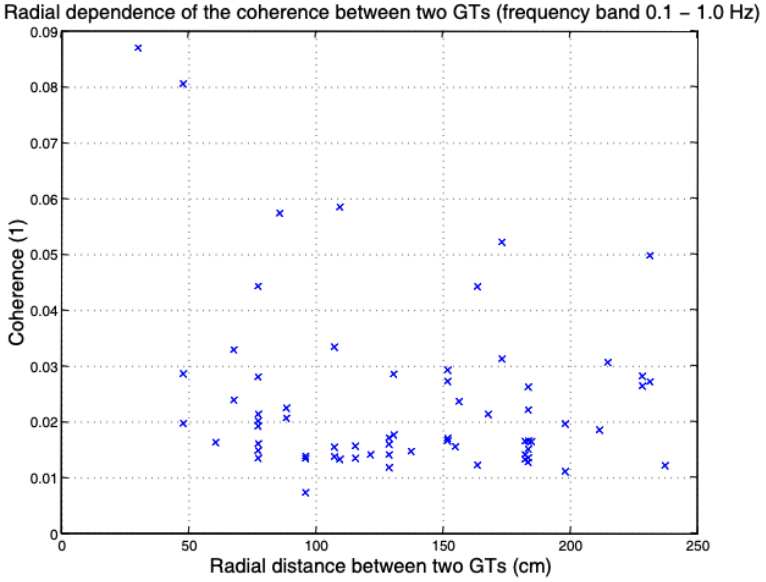

Figure 3.18: Dependence of the coherence between all GT pairs with their radial separation distance in the frequency range 0.1 - 1.0 Hz.

Having access to the temperature fluctuations in 12 radial positions, a good estimate of the weighted integral (3.23) can be calculated from the measurements of the temperature fluctuations as

$$\delta T_m^{ave}(t) \approx \frac{\sum_{i=1}^{12} \delta T_m(\boldsymbol{r_i}, t)\, \phi_0^2(\boldsymbol{r_i})}{\sum \phi_0^2(\boldsymbol{r_i})} \tag{3.24}$$

What regards the weighing factors $\phi_0^2(\boldsymbol{r_i})$, these could be calculated by SIMULATE, but it is more practical to use the static values of the gamma thermometers, which measure the static gamma flux. Assuming a proportionality between the gamma flux and the neutron flux, these can be used as weighting factors.

The average temperature fluctuations derived from the measurement were then used, together with the in-core neutron noise, to calculate the MTC. Although Eq. (3.19) indicates as if the estimated MTC was independent of the frequency, the right hand side of the equation indicates that this is not necessarily the case. Indeed the calculated MTC showed a marked dependence on frequency, with a maximum at about 0.5 Hz, It turned out that the best agreement with the true MTC, calculated by SIMULATE, was obtained to use this maximum. The results even depended on the block size of the FFT (Fast Fourier Transform) used in the calculation of the spectra. The results of the measurements are shown in Fig. 3.19.

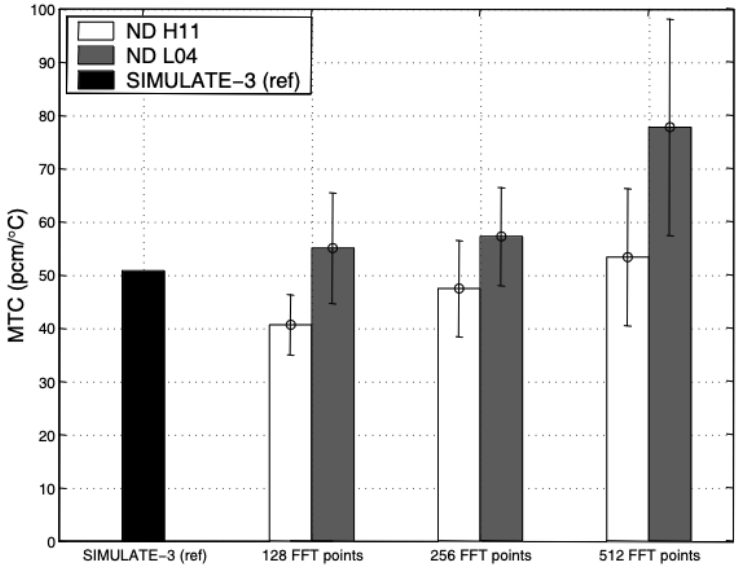

Figure 3.19: Comparison of the MTC noise evaluation of the MTC for the two in-core detectors and with different numbers of FFT points used., with the MTC calculated by SIMULATE.

The figure shows that the best results were obtained when using 128 or 256 frequency points and using the (somewhat peripheral) in-core detector L04, or when 512 FFT points were used together with the more central in-core detector H11.

Regarding the number of FFT points, the sampling rate is low (8 Hz), which would necessitate a long measurement time in order to have a sufficient number of blocks with high FFT number. However, the maximum duration of measurement time with the in-core detectors is 20 minutes, which did not make using a higher number of FFT points possible. Therefore, in Stage 8, further experiments were made partly by using an ex-core detector with 3 hours of measurement time, and partly by using 3 different in-core detectors in sequence, which gave 3 x 20 minutes measurement time. These two measurements made it possible to come up to 512 FFT points, which made the estimation of the MTC even more reliable.

Hence the feasibility of the correct estimation of the MTC by noise measurements, with the use of gamma thermometers, was demonstrated. We did some further theoretical work in Stage 10 to include possible feedback mechanisms into the theory which might lead to further improvements. However, this line of work was discontinued when the gamma thermometers were phased out in R2.

3.4 Thimble tube vibrations

This topics was taken up first in Stage 2018. For obvious reasons, the situation is very different from the BWR case, so we had to start the investigations from scratch. One very obvious difference is that there are no fix in-core detectors in the Ringhals PWRs, so dedicated measurements had to be made. Moreover, although a maximum of 5 movable in-core detectors can be introduced into the core simultaneously, these are all att different radial position, and there cannot be two detectors, axially displaced, in the same radial position.

We have started the analysis of the in-core signals with traditional spectral meth-

ods, which yield only very indirect information. During stage 2021, a continuous wavelet transform was used, but no wavelet coherence was calculated. The discrete wavelet based filtering method was first tested in the present stage, Stage 2022. The results will be reported in a separate report, hence they are not described here.

4. MISCELLANEOUS

In this section all the other topics will be very briefly listed with which we worked during the collaboration, and which have not been mentioned yet. The reasons why they are not mentioned in more detail are varied and many. In general, in contrast to the topics mentioned in the previous two sections, their significance for the purpose of the collaboration, or the impact of their possible application is lower than that of the former ones. Some of the topics listed in this chapter are also somewhat "exotic" or singular in the sense that they were treated only in one of the Stages. Also, unlike the subjects of the previous two sections, the overwhelming majority of these results was not published in international journals, only in internal reports, or not so seldom exclusively in the reports of the various Stages (projects) of the collaboration. At any rate, for each of the entries in the brief list below, information is given regarding in which Stage(s) the corresponding topics were described, so the interested reader can find more information in the corresponding reports.

4.1 Investigation of the ultra-low frequency oscillations in PWRs

The phenomenon to study is ultra-low frequency (< 0.01 Hz) oscillations in some of the signals in the core and the primary circuit, such as cold leg temperature, ex-core neutron detectors and core exit thermocouple signals. These oscillations lead to a general increase in the neutron noise amplitude level in R3 and R4, which leads to operational disturbances including certain alarms. The main goal of the study was to understand the root cause of these oscillations.

This subject came up already in Stage 1, where R3 data were analysed. The topics was also treated in Stages 13, 14, 2012, 2013 and 2014 with analysis of data from both R3 and R4.

The main tools of the analysis were partly usual FFT method (auto- and cross spectra as well as coherences), as well as Signal Transmission Path Analysis. With the latter, the cumulative noise source contribution ratio (CNSCR) between the signals can be determined, giving a percentage list of how much the fluctuation of a signal is due to the signal itself, of to the influence of some other signals which are included into the analysis. In the spectral analysis, flow velocity was estimated from the correlations between the ex-core detectors and the in-core thermocouples. An asymmetrical flow velocity distribution was found, and one possibility for the oscillations could be the spatial oscillation of the flow asymmetry, of which one case was reported in the literature. In the spectral analysis two transit times were found between the ex-core detectors and the in-core thermocouplse, which were explained by the fact that the ex-core detectors are affected by the flow both in the downcomer and in the upward flow in the core.

From the STPA methods one obtained indications that the probable driving force of the low frequency oscillations is the temperature fluctuations. However, neither the spectral, nor the STPA results were conclusive.

4.2 Determination of the response time and health test of gamma-thermometers

The objective of this work was to determine the time constants of the hot and cold junctions for several gamma thermometers, with an Auto-Regressive Moving Average (ARMA) modelling. This was a rather extensive work, including a large number of gamma thermometers and analysis methods, which was performed in Stage 6.

In Stage 9, a more extended analysis was performed, with the goal of checking the correct functioning of the gamma thermometers. This was initiated by requests from the Halden project, where indications were found regarding the deterioration of the gamma thermometer system (or in the data acquisition system). No definite conclusions about the health state of the detectors could be drawn, except that results of the flow velocity measurements differred from the previous ones. However, the study proved the integrity of the data acquisition system.

4.3 Estimation of water flow velocity with gamma-thermometers

The fact that the gamma thermometers are capable of measuring the coolant flow velocity in the frequency range of 0.1 - 1 Hz was already confirmed in Stage 5. However, after that the time constants of the gamma thermometers were determined in Stage 6, it was possible to give a better estimate of the flow velocity (the transit time) by accounting for the time constants of the gamma-thermometers. This was executed in Stage 7. The performance of the method is somewhat hampered by some deficiencies of the data collection system (the mean value of the signal should be removed before sampling).

4.4 Determination of subcritical reactivity through the source modulation technique

The question of measuring subcritical reactivity in power reactor cores during start-up has been always relevant. In Chalmers we were involved in several projects about reactivity measurements in accelerator driven systems (ADS). Some of the methods suggested for ADS were equally applicable for traditional power reactors during start-up. Such a method is the source modulation technique, in which the strength of the external source is modulated periodical. Due to the localised character of the source, deviations from point kinetics, and hence bias in the results could be expected. We have shown the somewhat surprising fact that when approaching criticality and the system behaves in a point kinetic way, the applicability of the method breaks down. This work was performed in Stage 10.

4.5 Axial dependence of the in-core noise for determining fuel vibration modes

The axial dependence of the in-core neutron noise in PWRs has been interesting for several reasons. One application is to classify the axial vibrating modes and corresponding eigenfrequencies of the fuel assemblies. Such a work was first performed in Stage 4. A number of peaks in the in-core APSDs and the corresponding

vibration modes were identified. A more extensive analysis was performed in Stage 12 and 13. In Stage 12, similarly to that in Stage 4, the peak amplitudes in the in-core noise APSDs were read out manually. In Stage 13, the new curve fitting method, originally developed for core barrel analysis, was used. The very extensive results of this work can be found in the above mentioned reports.

4.6 Basic study of the power reactor noise in non-multiplying systems

For obvious reasons, power reactor noise analysis is pursued in multiplying systems, which can be operated in the critical state. This gives the impression (and is tacitly accepted in the noise community) that power reactor noise, i.e. the neutron noise induced by the fluctuations of the cross sections, can only exist in multiplying systems. However, this is not the case, and the recognition and the proof of this fact has both a conceptual, as well as practical value, namely in the development of methods for determining the void fraction from neutron noise measurements. Therefore, in Stage 2015, we showed theoretically that perturbation of the cross sections leads to power reactor-type noise even in a non-multiplying system driven by an external source, and suggested an experiment which could prove it. In Stage 2016, in a collaboration with Swiss colleagues at EPFL and PSI, we performed the suggested experiments at the CARROUSEL facility. These consisted of using a water tank with a Pu-Be source as the source driven non-multiplying system, with air bubbles blown into the system as the perturbation of the cross sections. The experiments proved the correctness of the theoretical predictions.

4.7 Study of the possibility of using fission chambers in the current mode for zero power reactor measurements

This work has its origin in our work with nuclear safeguards, which lies outside the Ringhals-Chalmers collaboration. In safeguards, a non-intrusive method to identify and quantify unknown fissile material is based on pulse counting techniques, similarly to the Feynman- and Rossi-alpha methods of determining the subcritical reactivity. In the safeguards works, we realised the possibility that the pulse counting method can be replaced by current mode measurements, making it possible to extract the same statistical information from the continuous signals as from the discrete pulse counting methods. The advantage of the current mode measurements that the problems with the dead time can be avoided. It was logical to try to see whether it is possible to develop current-type measurement methods to be applied to the Feynman- and Rossi-alpha techniques. The rather involved theoretical work was reported in Staes 2016 and 2018. The experimental verification was made in the KUCA critical assembly of the Instituite of Intagrated Radiation and Nuclear Science (KURNS) of Kyoto University, in collaboration with researchers from the Budapest University of Technology and Economics (BME) and KURNS. The results, which were positive, were reported in Stages 2019 and 2020.

4.8 Investigation of baffle jetting

Investigations in this topics were initiated in Stage 2018. The problem was relevant to Ringhals-3 where, unlike in R2 and R4, the upflow conversion was not yet

made. The purpose was to investigate, through in-core noise measurements, the possibility of baffle jetting. It is known from international experience, that neutron noise measurements might be a tool to detect baffle jetting. In-core measurements should be made preferably at peripheral positions separated azimuthally. Such measurements were not available for us in Stage 2018. Another possibility is to utilize the fact that baffle jetting could lead to shell-mode vibrations and "core flowering" effects, both being detectable by ex-core detectors. The core flowering (azimuthally uniform expansion of the core radius) would lead to the same type of noise as the reactivity component, but at a frequency different from that of the fuel assembly vibrations at 7 Hz. For both vibration modes, a larger amplitude of the upper ex-core detectors could indicate that they are due to baffle jetting. In the evaluation of the ex-core measurements in Stage 2018, we found a reactivity term at around 15.5 Hz, and that the amplitude of both the reactivity and the shell mode at 20 Hz was larger in the upper detectors than in the lowers. This might indicate the presence of baffle jetting, but its position could not be given, due to the lack of in-core measurements. Similar results were obtained from the ex-core measurements in Stage 2019. Since the upflow conversion in R-3 was performed during refuelling in 2020, the work in this topics was discontinued.

4.9 Study of detection of subcooled boiling in PRWs

Subcooled boiling is expected to occur in the uppermost part of a PWR, and its monitoring and localisation (onset of boiling) is of interest. In Stage 2021, we investigated the possibility of determining the presence and onset of subcooled boiling using only one in-core detector. We extended a formerly elaborated model of bubbly flow, previously only used for void fraction determination through the local component of the neutron noise, to also include the reactivity effect of the boiling. We investigated two possible indicators: 1) the increase of the break frequency and the lower decay of the high-frequency tail of the APDS, and 2) the increase of the signal RMS (root mean square) value. To check the predictions of the model, one should have measurements with a movable detector at many axial points. Such a measurement was not available to us, only in-core measurements made at 7 axial elevations. These points were too scarcely spaced for the detection of subcooled boiling. In addition, the model did not take into account the effect of noise sources other than the subcooled boiling, which could further decrease the applicability of the method in practice.

4.10 Eigenvalue separation for BWR stability

The eigenvalue separation (ES) is defined as the difference between the inverses of the first higher order and the fundamental eigenvalue:

$$ES = \frac{1}{k_1} - \frac{1}{k_0} \geq 0 \tag{4.1}$$

In the literature, most of the work concerns how to calculate the ES for realistic cores. The objective of our study was to investigate how the dynamic properties of the system, in particular the properties of its neutron noise transfer function and the stability properties, depend on the ES. A relationship between the weak

neutronic coupling and the ES was quantitatively derived. The results serve to better understand under which circumstances the possibility of regional (out-of-phase) BWR instability can occur.

4.11 Conceptual study of a neutron flux gradient detector

In a current safeguards project, aiming at the detection missing/diverted fuel pins from a spent fuel assembly, we suggested the development of a neutron detector which is capable to measure the two-dimenional gradient of the neutron flux in the horizontal plane. In earlier work we have already pointed out the advantage of using, in addition to the scalar flux and its fluctuations, the scalar gradient and its fluctuation in noise diagnostics tasks. The performance of methods of locating localised perturbations is very much enhance by the us of such detectors. Therefore in Stage 2021, we performed, by Monte-Carlo simulations, the evaluation of the performance of such a hypothetical neutron flux gradient detector. The diameter of the detector, containing 4 small scintillators, is about 1 cm, such that it can be inserted into the guide tube of PWR fuel assemblies. The conceptual study proved the suitability of the detector to measure the 2-D flux gradient vector.

4.12 Water flow with measurement of N-16 activity

This subject has only been considered as a possible research item, but no concrete work was made. The discussion around it came up from the need of an alternative non-intrusive highly accurate measurement of the feedwater flow. In some foreign plants the fluctuations of the gamma field from the activated ^{16}N was used in a correlation flowmeter. Since our department pursued a project for water flow measurements with a pulsed neutron generator, we were interested in applying the experience from the project to the passive measurements. The project never took off.

5. PROJECT CONTRIBUTORS

5.1 Chalmers staff

Several present and past members of Chalmers nuclear engineering worked on the project, including PhD students and post-docs. Here a list of these persons is given in chronological order.

Ninos S. Garis
Ola Thomson (PhD student)
Joakim K-H. Karlsson (PhD student)
Lennart Norbert
Lasse Urholm
Christophe Demazière (PhD student)
Vasily Arzhanov (PhD student)
Carl Sunde (PhD student)
Johanna Wright (PhD student)
Petty Bernitt Cartemo (MSc student)
Victor Dykin (PhD student)
Lajos Nagy (Double degree PhD student, jointly with the Technical University of Budapest)
Moad Al-Dbissi (PhD student)
Paolo Vinai

5.2 External staff/visitors

In this category, the affiliation of the collaborators, and their position (if applicable) is specified corresponding to what they had during, or the beginning of their contribution. Several of them have changed affiliation or position/rank later.

Tim van der Hagen (TU Delft, the Netherlands)
Oszvald Glöckler (Ontario Hydro, Canada)
Emese Temesvári (Central Research Institute for Physics (KFKI), Budapest, Hungary)
Attila Rácz (KFKI, Budapest, Hungary)
Sándor Lipcsei (KFKI, Budapest, Hungary)
Cristina Montalvo (Technical University of Madrid (UPM), Spain)
Luis Alejandro ("Alex") Torres Delgado (Technical University of Madrid (UPM), Spain)
Tatiana Tambouratzis (University of Piraeus, Greece)
Henrik Nylén (Ringhals AB)
Hoai-Nam Tran (Duy Tan University, Ho Chi Minh City, Vietnam)
Mathieu Hursin (EPFL Lausanne/PSI, Switzerland)
Oskari Pakari (EPFL Lausanne/PSI, Switzerland)
Vincent Lamirand (EPFL Lausanne/PSI, Switzerland)

Olvera-Guerrero Omar Alejandro (Autonomus Metropolitan University, Mexico City, Mexico)
Yasunori Kitamura (Kyoto University Institute for Integrated Radiation and Nuclear Science (KURNS), Kumatori, Japan)
Máté Szieberth (Budapest University of Technology and Economics (BME), Budapest, Hungary)
Gergely Klujber ((BME, Budapest, Hungary)
Tsuyoshi Misawa (KURNS, Kumatori, Japan)

6. THESIS WORK

6.1 PhD theses

Joakim Karlsson
Development and application of reactor noise diagnostics
1977-07-17

Vasily Arzhanov
Power reactor noise studies and applications
2002-03-28

Christophe Demazière
Development of a Noise-Based Method for the Determination of the Moderator Temperature Coefficient of Reactivity (MTC) in Pressurized Water Reactors (PWRs)
2002-12-20
Winner of the Sigvard Eklund Prize for best PhD thesis, 2003

Carl Sunde
Noise Diagnostics of Stationary and Non-Stationary Reactor Processes
2007-04-27
Winner of the Sigvard Eklund Prize for best PhD thesis, 2007

Victor Dykin
Noise Applications in Light Water Reactors with Travelling Perturbations
2012-09-07
Winner of the Sigvard Eklund Prize for best PhD thesis, 2014

6.2 Licentiate theses

Ola Thomson
Noise analysis for two-phase flow measurements and reactor stability monitoring
Ola Thomson

Tell Andersson
On-Line Monitoring of Thermal Margins at Ringhals-2
1994-06-07

Joakim Karlsson
Investigations of Certain Problems in Reactor Noise Diagnostics
1997-06-09

Vasiliy Arzhanov
New Applications of Neutron Noise Theory in Power Reactor Physics
2000-05-26

Christophe Demazière
Development of a non-intrusive method for the determination of the moderator temperature coefficient

2000-12-21

Carl Sunde
Wavelet and spectral analysis of some selected problems in reactor diagnostics
2004-12-17

Johanna Wright
Development and investigation of reactivity measurement methods in subcritical cores
2005-05-30

Victor Dykin
The Effect of Different Perturbations on the Stability Analysis of Light Water Reactors
2010-09-17

7. PUBLICATIONS ARISING FROM THE PROJECT

7.1 Journal publications

1. van der Hagen T. H. J. J., Pázsit I. Thomson O. and Melkersson B. Methods for the determination of the in-phase and out-of-phase stability characteristics of a boiling water reactor. *Nuclear Technology* **107** No 2, 193 - 214. (1994)

2. Pázsit I. Determination of reactor stability in case of dual oscillations. *Ann. nucl. Energy* **22**, 377 - 387 (1995)

3. Garis N. S., Pázsit I. and Sahni D. C. Modelling of a vibrating reactor boundary and calculation of the induced neutron noise. *Ann. nucl. Energy* **23**, 1197 - 1208 (1996)

4. Thomson O., Garis N. S. and Pázsit I. Quantitative analysis of detector string impacting. *Nuclear Technology* **120**, 71 (1997)

5. Rácz A. and Pázsit I. Diagnostics of detector tube impacting with wavelet techniques. *Ann. nucl. Energy* **25**, 387-400 (1998)

6. Karlsson J. and Pázsit I. Noise decomposition in BWRs with applications to stability monitoring. *Nucl. Sci. Engng* **128**, 225 - 242 (1998)

7. Pázsit I., Karlsson J. and Garis N. S. Some developments in core-barrel vibration diagnostics. *Ann. nucl. Energy* **25**, 1079 - 1093 (1998)

8. Garis N. S., Pázsit I., Sandberg U. and Andersson T. Determination of PWR control rod position by core physics and neural network methods. *Nucl. Technology***123**, 278 - 295 (1998)

9. Pázsit I. Development of Core Diagnostic Methods and their Application at Swedish BWRs and PWRs. *J. Nucl. Sci. Technol.* **36**, 473 - 485 (1999)

10. Pázsit I., Garis N.S. and Lindén P. Application of neural networks in reactor diagnostics and monitoring. In the Springer Series **Studies in Fuzziness and Soft Computing**. Vol. **38**: *Fuzzy Systems and Soft Computing in Nuclear Engineering*, Ed. Ruan D., Physica-Verlag, Heidelberg, New York, pp 258 - 284 (1999) *(book Chapter)*

11. Pázsit I. and Arzhanov V., Linear reactor kinetics in systems with fluctuating boundaries. *Ann. nucl. Energy* **27**, 1385-1398 (2000)

12. Garis N. S., Karlsson J. K-H. and Pázsit I., Application of static fuel management codes for the calculation of neutron noise using the adiabatic approximation. *Kerntechnik* **65**, 227-235 (2000)

13. Demazière C. and Pázsit I. Theoretical investigation of the MTC noise estimate in 1-D homogeneous systems. *Ann. nucl. Energy* **29**, 75-100 (2002)

14. Arzhanov V. and Pázsit I. Detecting Impacting of BWR Instrument Tubes by Wavelet Analysis. **Power Plant Surveillance and Diagnostics** - *Modern Approaches and Advanced Applications*, Editors: Da Ruan and Paolo F. Fantoni, Springer, Physica Verlag XIV, pp 157 - 174 (2002) *(book chapter)*

15. Demazière C. and Pázsit I. On-line Determination of the MTC (Moderator Temperature Coefficient) by Neutron Noise and Gamma Thermometer Signals. **Power Plant Surveillance and Diagnostics** - *Modern Approaches and Advanced Applications*, Editors: Da Ruan and Paolo F. Fantoni, Springer, Physica Verlag XIV, pp 135 - 156 (2002) (book chapter)

16. Demazière C., Pázsit I., and Pór G., Evaluation of the boron dilution method for Moderator Temperature Coefficient measurements. *Nuclear Technology,* **140** (1), 147-163 (2002)

17. Andersson T., Demazière C., Nagy A., Sandberg U., Garis N. S., and Pázsit I., Development and application of core diagnostics and monitoring for the Ringhals PWRs. *Progress in Nuclear Energy*, **43** (1-4), 35-41 (2003)

18. Demazière C. and Pázsit I., Study of the MTC estimation by noise analysis in 2-D heterogeneous systems. *Progress in Nuclear Energy*, **43** (1-4), 313-319 (2003)

19. Demazière C., Pázsit I., Andersson T., Severinsson B., and Ranman T., Analysis of an MTC noise measurement performed in Ringhals-2 using gamma-thermometers and in-core neutron detectors. *Progress in Nuclear Energy*, **43** (1-4), 57-66 (2003)

20. Arzhanov V. and Pázsit I. Diagnostics of Core Barrel Vibrations by Ex-Core and In-Core Neutron Noise. *Prog. nucl. Energy* **43**, 151 - 158 (2003)

21. Demazière C. and Pázsit I. Investigation of the MTC noise estimate in 2-D heterogeneous systems. *Prog. nucl. Energy* **43**, 313 - 319 (2003)

22. Demazière C. and Pázsit I., Development of a method for measuring the MTC by noise analysis and its experimental verification in Ringhals-2. *Nuclear Science and Engineering*, **148** (1), 1-29 (2004)

23. Pázsit I. Diagnostics and surveillance methods in nuclear systems for real-time applications. *Int. J. for Real-Time Systems* **27**, 97-113 (2004)

24. Demaziére C. and Pázsit I. A phenomenological model for a strongly space-dependent decay ratio and its quantitative investigation. *Ann. nucl. Energy* **32**, 1305-1322 (2005)

25. Wright J. and Pázsit I. Neutron kinetics in subcritical source driven cores with applications to the source modulation method. *Ann. nucl. Energy* **33**, 149-158 (2006)

26. Sunde C., Demazière C., and Pázsit I., Calculation of the neutron noise induced by shell-mode core-barrel vibrations in a 1-D 2-group 2-region slab reactor model. *Nuclear Technology*, **154** (2), 129-141 (2006)

27. Demazière C., Analysis methods for the determination of possible unseated fuel assemblies in BWRs. *International Journal of Nuclear Energy Science and Technology*, **2** (3), 167-188 (2006)

28. Sunde C. and Pázsit I. Investigation of detector tube impacting in the Ringhals-1 BWR. *International Journal of Nuclear Energy Science and Technology*, Vol. 2 No 3, 189-208 (2006)

29. Sunde C. and Pázsit I. Wavelet techniques for the determination of the Decay Ratio in Boiling Water Reactors. *Kerntechnik* **71**, No 1-2, pp. 7 - 19 (2007)

30. Demazière C. and Pázsit I. Numerical tools applied to power reactor noise analysis. *Prog. nucl. Energy* **51**, 67 - 81 (2008)

31. Dykin V. and Pázsit I. Remark on the role of the driving force in BWR instability. *Ann. nucl. Energy* **36**, 1544 – 1552 (2009)

32. Pázsit I. and Dykin V. Investigation of the space-dependent noise induced by propagating perturbations. *Ann. nucl. Energy* **37**, Issue 10, 1329-1340 (2010)

33. Zylbersztejn F., Tran H. N., Pázsit I., Demazière C., and Nylén H., On the dependence of the noise amplitude on the correlation length of inlet temperature fluctuations in PWRs. *Annals of Nuclear Energy*, **57**, 134-141 (2013)

34. Dykin V. and Pázsit I. Simulation of in-core neutron noise for axial void profile reconstruction in Boiling Water Reactors. *Nucl. Technology* **183**, 354-366 (2013)

35. Dykin V., Jonsson A. and Pázsit I. Qualitative and quantitative investigation of the propagation noise in various reactor systems. *Prog. nucl. Energy* **70**, 98 - 111 (2014)

36. Tran H. N., Pázsit I. and Nylén H. Investigation of the ex-core noise induced by fuel assembly vibrations in Ringhals-3 PWR. *Ann. nucl. Energy* **80**, 434 - 446 (2015) (2014)

37. Pázsit I., Montalvo Martin C., Nylén H., Andersson T., Hernández-Solis A. and Bernitt Cartemo C., Developments in core-barrel motion monitoring and applications to the Ringhals PWRs. *Nucl. Sci.Engng* **182**, 213 - 227 (2016)

38. Pázsit I. and Dykin V. The role of the Eigenvalue Separation in reactor kinetics. *J. Nucl. Sci. Techn.* **55**, Issue 5, 484 – 495 (2018)

39. Kitamura Y., Pázsit I. and Misawa T. Determination of neutron decay constant by time-domain fluctuation analyses of neutron detector current signals. *Ann. nucl. Energy* **120**, 691 - 706 (2018)

40. Pázsit I., Dykin V., Konno H. and Kozlowski T. A possible application of Catastrophe Theory to Boiling Water Reactor instability. *Prog. nucl. Energy* **118**, 103054 (2020)

41. Hursin M., Pakari O., Perret G., Frajtag P., Lamirand V., Pázsit I., Dykin V., Por G., Ferroukhi H., and Pautz A. Measurement of the gas velocity in a water-air mixture in CROCUS by neutron noise technique. *Nucl. Technology* **206**, Issue 10, 1566 -1583 (2020)

42. Pázsit I, Torres L. A., Hursin M., Nylén, H. and Dykin V. Determining the axial void velocity profile in BWRs from in-core noise measurements. *Progress in Nuclear Energy* **138**, 103805 (2021)

43. Aldbissi M., Vinai P., Borella A., Rossa R. and Pázsit I., Conceptual design and initial evaluation of a neutron flux gradient detector. *Nucl. Inst. Meth.* **A 126**, 166030 (2022)

7.2 Conference papers/talks

1. J. Karlsson, I. Pázsit and N. S. Garis, Some Developments in Core Barrel Vibration Diagnostics, IMORN-27, The Informal Meeting on Reactor Noise, November 18 - 20 1997, Valencia, Spain

2. J. Karlsson and I. Pázsit, Noise Decomposition in BWRs with Application to Stability Monitoring, IMORN-27, The Informal Meeting on Reactor Noise, November 18 - 20 1997, Valencia, Spain

3. Demazière C. and Pázsit I., Theory of neutron noise induced by spatially randomly distributed noise sources. Proc. Int. Mtg. Advances in Reactor Physics and Mathematics and Computation into the Next Millennium (PHYSOR2000), Pittsburgh, Pennsylvania, USA, May 7-12, 2000, American Nuclear Society (2000)

4. Demazière C. and Pázsit I., Theoretical investigation of the MTC noise estimate in 1-D homogeneous systems. Proc. 28th Informal Mtg. Reactor Noise (IMORN-28), Athens, Greece, October 11-13, 2000, NCSR "Demokritos" (2000)

5. Por G. and Pázsit I. On Application of wavelets for filtering noise measurement. IMORN-28 conference, International Meeting On Reactor Noise, Athens, Greece, October 11-13, 2000

6. Arzhanov V. and Pázsit I. A Treatment of the Neutron Noise Induced by Vibrating Boundaries. IMORN-28 conference, International Meeting On Reactor Noise, Athens, Greece, October 11-13, 2000

7. Demazière C., Pázsit I., and Pór G., Estimation of the Moderator Temperature Coefficient (Analysis of an MTC measurement using boron dilution method). Proc. Int. Topl. Mtg. Nuclear Plant Instrumentation, Controls, and Human-Machine Interface Technologies (NPIC&HMIT 2000), Washington, DC, USA, November 13-16, 2000, American Nuclear Society (2000)

8. Demazière C. and Pázsit I. On-line Determination of the MTC (Moderator Temperature Coefficient) by Neutron Noise and Gamma Thermometer Signals.

Workshop on Power Plant Surveillance and Diagnostics, Halden, September 3-4, 2001

9. Arzhanov V. and Pázsit I. Detecting Impacting of BWR Instrument Tubes by Wavelet Analysis. Workshop on Power Plant Surveillance and Diagnostics, Halden, September 3-4, 2001

10. Andersson T., Demazière C., Nagy A., Sandberg U., Garis N. S., and Pázsit I., Development and application of core diagnostics and monitoring for the Ringhals PWRs. Proc. 8th Symposium on Nuclear Reactor Surveillance and Diagnostics (SMORN VIII), Gothenburg, Sweden, May 27-31, 2002, Chalmers University of Technology (2002) (proceedings published in a special issue of Progress in Nuclear Energy)

11. Demazière C. and Pázsit I., Study of the MTC estimation by noise analysis in 2-D heterogeneous systems. Proc. 8th Symposium on Nuclear Reactor Surveillance and Diagnostics (SMORN VIII), Gothenburg, Sweden, May 27-31, 2002, Chalmers University of Technology (2002) (proceedings published in a special issue of Progress in Nuclear Energy)

12. Demazière C., Pázsit I., Andersson T., Severinsson B., and Ranman T., Analysis of an MTC noise measurement performed in Ringhals-2 using gamma-thermometers and in-core neutron detectors. Proc. 8th Symposium on Nuclear Reactor Surveillance and Diagnostics (SMORN VIII), Gothenburg, Sweden, May 27-31, 2002, Chalmers University of Technology (2002) (proceedings published in a special issue of Progress in Nuclear Energy)

13. V. Arzhanov and I. Pázsit, Diagnostics of Core Barrel Vibrations by In-Core and Ex-Core Neutron Noise. SMORN-VIII, A Symposium on Nuclear Reactor Surveillance and Diagnostics, 27- May 2002, Göteborg, Sweden.

14. Demazière C. and Pázsit I., Development of a method for measuring the MTC by noise analysis and its experimental verification in Ringhals-2. Proc. Int. Mtg. New Frontiers of Nuclear Technology: Reactor Physics, Safety and High-Performance Computing (PHYSOR2002), Seoul, South-Korea, October 7-10, American Nuclear Society (2002) (proceedings published in a special issue of Nuclear Science and Engineering)

15. Arzhanov V. and Pázsit I. Theory and Application of the In-Core Neutron Noise induced by Fluctuating Core Boundaries. PHYSOR 2002, ANS Topical Meeting "International Conference on the New Frontiers of Nuclear Technology : Reactor Physics, Safety and High-Performance Computing", 7-10 October 2002, Seoul, Korea

16. Demazière C. and Pázsit I. A Phenomenological Model for the Explanation of a Strongly Space- Dependent Decay Ratio. ANS Topical Meeting "Nuclear Mathematical and Computational Sciences - A Century in Review - A Century Ahead", Gatlinburg, Tennessee, USA, April 7-10, 2003

17. Demazière C. and Pázsit I., Determination of the MTC by noise analysis methods. Proc. Annual Mtg. Nuclear Technology 2003 (JK2003), Berlin, Germany, May 20-22, 2003, European Nuclear Society (2003) (invited paper)

18. Sunde C. and Pázsit I. Investigation of Detector Tube Impacting in the BWR Ringhals 1. 29th International Mtg. Reactor Noise (IMORN-29), , 17-19 May 2004, Budapest, Hungary

19. Demazière C., Analysis methods for the determination of possible unseated fuel assemblies in BWRs. 29th International Mtg. Reactor Noise (IMORN-29), Budapest, Hungary, May 17-19, 2004.

20. Demazière C., Investigation of the frequency-dependence of the MTC noise estimator. Proc. Int. Mtg. Mathematics and Computation, Supercomputing, Reactor Physics and Nuclear and Biological Applications (M&C2005), Avignon, France, September 12-15, 2005, American Nuclear Society (2005)

21. Sunde C., Demazière C., and Pázsit I., Investigation of the neutron noise induced by shell-mode core-barrel vibrations in a reflected reactor. Proc. Int. Mtg. Mathematics and Computation, Supercomputing, Reactor Physics and Nuclear and Biological Applications (M&C2005), Avignon, France, September 12-15, 2005, American Nuclear Society (2005)

22. Demazière C., Investigation of the frequency-dependence of the MTC noise estimator. Int. Mtg. Mathematics and Computation, Supercomputing, Reactor Physics and Nuclear and Biological Applications (M&C2005), Avignon, France, September 12-15, 2005.

23. Demazière C., Pázsit I., and Wright J., Investigation of the validity of the point-kinetic approximation for subcritical heterogeneous systems in 2-group diffusion theory for measurement of the reactivity in ADS. Proc. Int. Conf. Nuclear Energy Systems for Future Generation and Global Sustainability (GLOBAL-2005), Tsukuba, Japan, October 9-13, 2005, Atomic Energy Society of Japan (2005)

24. Sunde C., Pázsit M and Pázsit I. Diagnostics of beam mode core-barrel vibrations in the PWRs Ringhals 2-4. PHYSOR 2006, American Nuclear Society's Topical Meeting on Reactor Physics 2006 September 10-14, Vancouver, BC, Canada

25. Demazière C. and Pázsit I. Numerical tools applied to power reactor noise analsys. 5th International Topical Meeting on Nuclear Plant Instrumentation Control and Human Machine Interface Technology (NPIC&HMIT 2006), November 12 - 16, 2006, Albuquerque, NM, USA.

26. Demazière C, Pázsit I and Sunde C. Noise Analysis in Support to Power Uprates. IAEA Technical Meeting on Power Uprate and Side Effect of Power Uprate in Nuclear Power Plants. 12 - 15 February 2007, Oskarshamn, Sweden

27. Dykin V. and Pázsit I. Investigation of the space-dependent noise induced by propagating density fluctuations. PHYSOR 2010 - Advances in Reactor Physics to Power the Nuclear Renaissance. Pittsburgh, Pennsylvania, USA, May 9-14, 2010

28. Pázsit I., Montalvo-Martín C., Hernandez-Solís A., Bernitt Cartemo P., Diagnostics of core barrel and fuel assembly vibrations in the Swedish Ringhals PWRs. 7th International Topical Meeting on Nuclear Plant Instrumentation, Control and Human Machine Interface Technology (NPIC&HMIT 2010), Las Vegas, Nevada, USA, 7 - 11 November 2010

29. Pázsit I. Surveillance and diagnostics based on noise analysis in Swedish nuclear power plants. LCES-2011, Low Carbon Earth Summit, Track 7-3, Dalian China, 18 - 26 October 2011

30. Montalvo-Martín C., Pázsit I. and Nylén H. Surveillance and diagnostics of the beam mode vibrations of the Ringhals PWRs. Int. Conf. on Advances in Reactor Physics – Linking Research, Industry, and Education (PHYSOR 2012), Knoxville, TN, USA, April 15-20, 2012, American Nuclear Society

31. Dykin V. and Pázsit I. Simulation of in-core neutron noise measurements for axial void profile reconstruction in boiling water reactors. Int. Conf. on Advances in Reactor Physics – Linking Research, Industry, and Education (PHYSOR 2012), Knoxville, TN, USA, April 15-20, 2012, American Nuclear Society

32. Demazière C., Investigation of the MTC noise estimation with a coupled neutronic/thermal-hydraulic dedicated model – "Closing the loop". Int. Conf. on Advances in Reactor Physics – Linking Research, Industry, and Education (PHYSOR 2012), Knoxville, TN, USA, April 15-20, 2012, American Nuclear Society

33. Dykin V. and Pázsit I. Simulation of in-core neutron noise for axial void profile reconstruction in Boiling Water Reactors. ANS Annual Meeting, Chicago, Illinois, 24-28 June 2012

34. Dykin V. and Pázsit I. Simulation of neutron noise induced by two-phase density fluctuations in a Boiling Water Reactor. Reactor Noise Knowledge Transfer Meeting, Prague, Czech, 16 – 19 October 2012

35. Dykin V. and Pázsit I. Neutron noise-based method to determine void fraction in a boiling water reactor. European Nuclear Conference ENC-12, 9 -12 December 2012, Manchester, United Kingdom

36. Pázsit I. and Dykin V. The role of the eigenvalue separation in reactor dynamics and neutron noise theory. PHYSOR 2014 - The Role of Reactor Physics toward a Sustainable Future. The Westin Miyako, Kyoto, Japan, September 28 - October 3, 2014

37. Pázsit I., Nylén H. and Montalvo Martín C. Refined method for surveillance and diagnostics of the core barrel vibrations of the Ringhals PWRs. PHYSOR 2014 - The Role of Reactor Physics toward a Sustainable Future. The Westin Miyako, Kyoto, Japan, September 28 - October 3, 2014

38. Pázsit I., Dykin V., Konno H. and Kozlowski T. The stability of boiling water reactors as a catastrophe phenomenon. ANS MC2015 - Joint International Conference on Mathematics and Computation (M&C), Supercomputing in Nuclear Applications (SNA) and the Monte Carlo (MC) Method. Nashville, Tennessee, 19–23 April 2015, on CD-ROM, American Nuclear Society, La-Grange Park, IL (2015)

39. Montalvo C., Pázsit I., Nylén H. and Dykin V. First evidence of the pivotal motion ("tilting mode") of the core barrel in the Ringhals-4 PWR. PHYSOR 2016 - Theory and Experiments in the 21st Century. Sun Valley Resort, Sun Valley, Idaho, USA, May 1 – 5, 2016

40. Hursin M. Pakari O., Perret G., Frajtag P., Lamirand V., Pázsit I., Dykin V., Por G., Ferroukhi H., and Pautz A. Measurement of the gas velocity in a water-air mixture in CROCUS by neutron noise technique. ANIMMA 2019, June 17-21, 2019 Portoroz, Slovenia

41. Hursin M., Pakari O., Perret G., Frajtag P., Lamirand V., Pázsit I., Dykin V., Por G., Nylén H. and Pautz A. Measurement of the gas velocity in a water-air mixture in CROCUS by neutron noise technique. M&C 2019, 25 – 29 August 2019, Marriott Portland Downtown Waterfront, Portland, OR, USA

42. Szieberth M., Nagy L., Klujber G., Kitamura Y., Misawa T., Barth I. and Pázsit I. Experimental demonstration of neutron fluctuation analysis based on the continuous signal of fission chambers: neutron multiplicity and reactor noise measurements. M&C 2021, The International Conference on Mathematics and Computational Methods Applied to Nuclear Science and Engineering. Raleigh, North Carolina, USA, 11 – 15 April 2021

43. Al-dbissi M., Vinai P., Borella A., Rossa R. and Pázsit I. Evaluation of the performance of a neutron gradient detector for partial defect testing in spent nuclear fuel assemblies. Paper 31, Proc. INMM 63rd Annual Meeting, 24 – 28 July 2022

8. ACKNOWLEDGEMENT

This one-year contract was performed by funding from Ringhals Vattenfall AB, contract No. 4501756928-062. Contact person from Ringhals was Dr. Henrik Nylén.

REFERENCES

[1] I. Pázsit (Ed.), "*Investigation of regional instability in Ringhals-1*," CTH-RF-100/RR-1, Chalmers University of Technology, Department of Reactor Physics, Göteborg, Sweden, December 1993.

[2] I. Pázsit, N. S. Garis, O. Thomson, and L. Norberg, "*Analys av brusmätningar genomförda under perioden 93-94 vid Ringhals-3 (In Swedish)*," Chalmers report CTH-RF-116/RR-2, Chalmers University of Technology, Department of Reactor Physics, Göteborg, Sweden, May 1996.

[3] I. Pázsit (Ed.), "*Final Report on the Research Project Ringhals Diagnostics and Monitoring, Stage 1*," CTH-RF-122/RR-3, Chalmers University of Technology, Göteborg, Sweden, September 1996.

[4] I. Pázsit, J. Karlsson, and N. Garis, "*Final Report on the Research Project Ringhals Diagnostics and Monitoring, Stage 2*," CTH-RF-132/RR-4, Chalmers University of Technology, Göteborg, Sweden, October 1997.

[5] J. K.-H. Karlsson and I. Pázsit, "*Final Report on the Research Project Ringhals Diagnostics and Monitoring, Stage 3: Analysis of core barrel vibrations in Ringhals 2, 3 and 4 for several fuel cycles*," CTH-RF-135/RR-5, Chalmers University of Technology, Göteborg, Sweden, October 1998.

[6] C. Demazière, V. Arzhanov, J. K.-H. Karlsson, and I. Pázsit, "*Final Report on the Research Project Ringhals Diagnostics and Monitoring, Stage 4*," CTH-RF-145/RR-6, Chalmers University of Technology, Göteborg, Sweden, September 1999.

[7] C. Demazière, V. Arzhanov, and I. Pázsit, "*Final Report on the Research Project Ringhals Diagnostics and Monitoring, Stage 5*," CTH-RF-156/RR-7, Chalmers University of Technology, Göteborg, Sweden, September 2000.

[8] C. Demazière, V. Arzhanov, and I. Pázsit, "*Final Report on the Research Project Ringhals Diagnostics and Monitoring, Stage 6*," CTH-RF-161/RR-8, Chalmers University of Technology, Göteborg, Sweden, October 2001.

[9] C. Demazière, V. Arzhanov, and I. Pázsit, "*Final Report on the Research Project Ringhals Diagnostics and Monitoring, Stage 7*," CTH-RF-167/RR-9, Chalmers University of Technology, Göteborg, Sweden, December 2002.

[10] C. Demazière, C. Sunde, V. Arzhanov, and I. Pázsit, "*Final Report on the Research Project Ringhals Diagnostics and Monitoring, Stage 8*," CTH-RF-177/RR-10, Chalmers University of Technology, Göteborg, Sweden, December 2003.

[11] C. Demazière, C. Sunde, and I. Pázsit, "*Final Report on the Research Project Ringhals Diagnostics and Monitoring, Stage 9*," CTH-RF-187/RR-11, Chalmers University of Technology, Göteborg, Sweden, January 2005.

[12] C. Sunde, J. Wright, C. Demazière, and I. Pázsit, "*Final Report on the Research Project Ringhals Diagnostics and Monitoring, Stage 10*," CTH-RF-194/RR-12, Chalmers University of Technology, Göteborg, Sweden, November 2005.

[13] C. Sunde, C. Demazière, and I. Pázsit, "*Final Report on the Research Project Ringhals Diagnostics and Monitoring, Stage 11*," CTH-NT-206/RR-13, Chalmers University of Technology, Göteborg, Sweden, February 2007.

[14] I. Pázsit, C. Demazière, C. Sunde, P. Bernitt, and A. Hernández-Solís, "*Final Report on the Research Project Ringhals Diagnostics and Monitoring, Stage 12*," CTH-NT-220/RR-14, Chalmers University of Technology, Göteborg, Sweden, August 2008.

[15] I. Pázsit, C. Montalvo Martín, V. Dykin, and T. Tambouratzis, "*Final Report on the Research Project Ringhals Diagnostics and Monitoring, Stage 13*," CTH-NT-230/RR-15, Chalmers University of Technology, Göteborg, Sweden, March 2010.

[16] I. Pázsit, C. Montalvo Martín, V. Dykin, and H. Nylén, "*Final Report on the Research Project Ringhals Diagnostics and Monitoring, Stage 14*," CTH-NT-253/RR-16, Chalmers University of Technology, Göteborg, Sweden, December 2011.

[17] V. Dykin, C. Montalvo Martín, H. Nylén, and I. Pázsit, "*Ringhals Diagnostics and Monitoring, Final Research Report 2012*," CTH-NT-269/RR-17, Chalmers University of Technology, Göteborg, Sweden, December 2012.

[18] V. Dykin, C. Montalvo Martín, H. Nylén, and I. Pázsit, "*Ringhals Diagnostics and Monitoring, Final Research Report 2013*," CTH-NT-286/RR-18, Chalmers University of Technology, Göteborg, Sweden, December 2013.

[19] V. Dykin, C. Montalvo Martín, H. Nylén, and I. Pázsit, "*Ringhals Diagnostics and Monitoring, Final Research Report 2012 - 2014*," CTH-NT-304/RR-19, Chalmers University of Technology, Göteborg, Sweden, December 2014.

[20] V. Dykin, C. Montalvo, N. Tran, H. Nylén, and I. Pázsit, "*Ringhals Diagnostics and Monitoring, Annual Research Report 2015*," CTH-NT-319/RR-20, Chalmers University of Technology, Göteborg, Sweden, December 2015.

[21] I. Pázsit, C. Montalvo, N. Tran, H. Nylén, and O. Olvera Guerrero, "*Ringhals Diagnostics and Monitoring, Annual Research Report 2016-17*," CTH-NT-333/RR-21, Chalmers University of Technology, Göteborg, Sweden, December 2017.

[22] I. Pázsit, L. A. Torres, C. Montalvo, Y. Kitamura, L. Nagy, and H. Nylén, "*Ringhals Diagnostics and Monitoring, Annual Research Report 2018-19*," CTH-NT-339/RR-22, Chalmers University of Technology, Göteborg, Sweden, June 2019.

[23] I. Pázsit, L. A. Torres, C. Montalvo, L. Nagy, M. Szieberth, G. Klujber, T. Misawa, Y. Kitamura, and H. Nylén, "*Ringhals Diagnostics and Monitoring, Annual Research Report 2019-20*," CTH-NT-342/RR-23, Chalmers University of Technology, Göteborg, Sweden, June 2020.

[24] I. Pázsit, L. A. Torres, C. Montalvo, L. Nagy, G. Klujber, M. Szieberth, T. Misawa, Y. Kitamura, V. Dykin, and H. Nylén, "*Ringhals Diagnostics and Monitoring, Annual Research Report 2020-21*," CTH-NT-344/RR-24, Chalmers University of Technology, Göteborg, Sweden, June 2021.

[25] I. Pázsit, L. A. Torres, C. Montalvo, , V. Dykin, A. dbissi M., V. P., and H. Nylén, "*Ringhals Diagnostics and Monitoring, Annual Research Report 2021-22*," CTH-NT-348/RR-25, Chalmers University of Technology, Göteborg, Sweden, June 2022.

[26] T. H. J. J. van der Hagen, I. Pázsit, O. Thomson, and B. Melkersson, "Methods for the determination of the in-phase and out-of-phase stability characteristics of a boiling water reactor," *Nuclear Technology*, vol. **107**, pp. 193–214, 1994.

[27] B. Melkersson, "*Slutrapport angående härdstabilitet för R1 efter mätningar RA90. (In Swedish)*," Ringhals report 339/91, 1991.

[28] I. Pázsit, "Determination of Reactor Stability in Case of Dual Oscillations," *Annals of Nuclear Energy*, vol. 22, no. 6, pp. 377–387, 1995.

[29] I. Pázsit, V. Dykin, H. Konno, and T. Kozlowski, "A possible application of catastrophe theory to boiling water reactor instability," *Progress in Nuclear Energy*, vol. 118, p. 103054, 2020.

[30] J. Karlsson and I. Pázsit, "Noise Decomposition in Boiling Water Reactors with Application to Stability Monitoring," *Nuclear Science and Engineering*, vol. 128, no. 3, pp. 225–242, 1998.

[31] J. K-H. Karlsson and I. Pázsit, "Localisation of a channel instability in the Forsmark-1 boiling water reactor," *Annals of Nuclear Energy*, vol. 26, no. 13, pp. 1183–1204, 1999.

[32] C. Demazière and I. Pázsit, "On the possibility of the space-dependence of the stability indicator (decay ratio) of a BWR," *Annals of Nuclear Energy*, vol. 32, no. 12, pp. 1305–1322, 2005.

[33] J. A. Thie, *Power Reactor Noise*. La Grange Park, Illinois, USA: American Nuclear Society, 1981.

[34] F. Åkerhielm, I. Pázsit, B.-G. Bergdahl, R. Oguma, S. Sandell, and J. Lorenzen, "*Noise measurements on a few selected LPRM-detectors (SPND and fission chambers) in Barsebäck 1*," Studsvik internal report NI-86/9, July 1986.

[35] I. Pázsit and O. Glöckler, "BWR Instrument Tube Vibrations - Interpretation of Measurements and Simulation," *Annals of Nuclear Energy*, vol. 21, no. 12, pp. 759–786, 1994.

[36] J. Thie. Personal communication, 1985.

[37] A. Rácz and I. Pázsit, "Diagnostics of detector tube impacting with wavelet techniques," *Annals of Nuclear Energy*, vol. 25, no. 6, pp. 387–400, 1998.

[38] D. Wach and G. Kosály, "Investigation of the joint effect of local and global driving sources in incore-neutron noise measurements," *Atomkernenergie*, vol. 23, pp. 244–250, 1974.

[39] G. Kosály, L. Maróti, and L. Meskó, "A simple space dependent theory of the neutron noise in a boiling water reactor," *Annals of Nuclear Energy*, vol. 2, no. 2, pp. 315–321, 1975.

[40] J. Loberg, M. Österlund, J. Blomgren, and K.-H. Bejmer, "Neutron detection–based void monitoring in boiling water reactors," *Nuclear Science and Engineering*, vol. 164, no. 1, pp. 69–79, 2010.

[41] I. Pázsit and O. Glöckler, "Cross-sectional identification of two-phase flow by correlation techniques," *Progress in Nuclear Energy*, vol. 15, pp. 661–669, 1985.

[42] V. Dykin and I. Pázsit, "Simulation of in-Core Neutron Noise Measurements for Axial Void Profile Reconstruction in Boiling Water Reactors," *Nuclear Technology*, vol. 183, no. 3, pp. 354–366, 2013.

[43] V. Dykin, "Using neutron noise to determine void fraction," *Nuclear Engineering International*, vol. 58, no. 709, pp. 16 – 17, 2013.

[44] I. Pázsit, L. A. Torres, M. Hursin, H. Nylén, V. Dykin, and C. Montalvo, "Development of a new method to determine the axial void velocity profile in BWRs from measurements of the in-core neutron noise," *Progress in Nuclear Energy*, vol. 138, p. 103805, 2021.

[45] N. S. Garis, I. Pázsit, U. Sandberg, and T. Andersson, "Determination of PWR control rod position by core physics and neural network methods," *Nuclear Technology*, vol. 123, no. 3, pp. 278–295, 1998.

[46] J. A. Thie, "Core motion monitoring," *Nucl. Technol.*, vol. 45, pp. 5–45, 1979.

[47] J. B. Dragt and E. Türkcan, "Borssele PWR noise: Measurements, analysis and interpretation," *Progress in Nuclear Energy*, vol. **1**, no. 2–4, pp. 293–307, 1977.

[48] F. Åkerhielm, R. Espefält, and J. Lorenzen, "Surveillance of vibrations in PWR," *Progress in Nuclear Energy*, vol. **9**, pp. 453–464, 1982.

[49] I. Pázsit, J. Karlsson, and N. S. Garis, "Some developments in core-barrel vibration diagnostics," *Annals of Nuclear Energy*, vol. 25, pp. 1079–1093, 1998.

[50] I. Pázsit and O. Glöckler, "On the Neutron Noise Diagnostics of Pressurized Water Reactor Control Rod Vibrations II. Stochastic Vibrations," *Nuclear Science and Engineering*, vol. **88**, pp. 77–87, 1984.

[51] D. Wood and R. Perez, "Modeling and Analysis of Neutron Noise from an Ex-Core Detector at a Pressurized Water Reactor," in *In: Proc. Int. Conf. SMORN-VI*, (Gatlinburg, Tennessee, USA), 1991.

[52] F. J. Sweeney, J. March-Leuba, and C. M. Smith, "Contribution of fuel vibrations to ex-core neutron noise during the first and second fuel cycles of the Sequoyah-1 pressurized water reactor," *Prog. Nucl. Energy*, vol. **15**, pp. 283–290, 1985.

[53] C. Demazière, "CORE SIM: A multi-purpose neutronic tool for research and education," *Annals of Nuclear Energy*, vol. 38, no. 12, pp. 2698–2718, 2011.

[54] H.-N. Tran, I. Pázsit, and H. Nylén, "Investigation of the ex-core noise induced by fuel assembly vibrations in the Ringhals-3 PWR," *Annals of Nuclear Energy*, vol. 80, pp. 434–446, 2015.

[55] M. Pázsit and I. Pázsit, "*Final report on the Analysis of Core Barrel Vibrations in Ringhals PWRs R2, R3 and R4 from the Measurements Made in Spring 2006*," Tech. Rep. NDF-01, Nucleus DatorFysik, Mölndal, Sweden, January 2007.

[56] M. Pázsit and I. Pázsit, "*Final report on the Analysis of Core Barrel Vibrations in Ringhals PWRs R2, R3 and R4 from the Measurements Made in Autumn 2006*," Tech. Rep. NDF-02, Nucleus DatorFysik, Mölndal, Sweden, February 2007.

[57] M. Pázsit and I. Pázsit, "*Analysis of the Coherences of Core Barrel Vibration Measurements in Ringhals 4 under 1991-2005*," Tech. Rep. NDF-03, Nucleus DatorFysik, Mölndal, Sweden, March 2007.

[58] M. Pázsit and I. Pázsit, "*Final report on the Analysis of Core Barrel Vibrations in Ringhals PWRs R2, R3 and R4 from the Measurements Made in February 2007*," Tech. Rep. NDF-04, Nucleus DatorFysik, Mölndal, Sweden, April 2007.

[59] M. Pázsit and I. Pázsit, "*Final report on the Analysis of Core Barrel Vibrations in Ringhals PWRs R2, R3 and R4 from the Measurements Made in April 2007*," Tech. Rep. NDF-05, Nucleus DatorFysik, Mölndal, Sweden, August 2007.

[60] I. Pázsit and M. Pázsit, "*Final Report on the Analysis of Core Barrel Vibrations in Ringhals PWRs R2, R3 and R4 from the Measurements Made in the Winter 2007/2008*," Tech. Rep. NDF-09, Nucleus DatorFysik, Mölndal, Sweden, March 2008.

[61] I. Pázsit, "*Review of core-barrel diagnostics with neutron noise analysis of ex-core detector signals in Ringhals 2-4 during 1991-2009*," Tech. Rep. NDF-11, Nucleus DatorFysik, Mölndal, Sweden, May 2009.

[62] I. Pázsit and M. Pázsit, "*Final Report on the Analysis of Core Barrel Vibrations in Ringhals PWR R4 from Measurements Made in February 2009*," Tech. Rep. NDF-12, Nucleus DatorFysik, Mölndal, Sweden, May 2009.

[63] C. Demazière and I. Pázsit, "Theoretical investigation of the MTC noise estimate in 1-D homogeneous systems," *Annals of Nuclear Energy*, vol. 29, no. 1, pp. 75–100, 2002.

APPENDIX

CHALMERS TEKNISKA HÖGSKOLA
Institutionen för reaktorfysik

CHALMERS UNIVERSITY OF TECHNOLOGY
Department of Reactor Physics

1994-09-19

Lars Fredlund
CRPT
Vattenfall AB
Ringhalsverket
430 22 VÄRÖBACKA

Tillgång av mätdata från Ringhals 3

Ett samarbetsprojekt mellan Ringhals och Reaktorfysik CTH i syfte att med brusanalys kunna identifiera härddriftparametrar har nyligen inletts. Handläggare från Er sida är Tell Andersson RBH och Anders Johansson RSTU.

Vid ett inledande möte vid Ringhals 94.08.23 diskuterades möjligheten för oss att få tillgång till vissa mätdata från en PWR. Av intresse skulle vara neutronflödessignaler samt processsignaler med nära anknytning till härden, t.ex. kalla benets temperatur och härdutloppstemperaturen. Det inledande syftet skulle vara att analysera de olika signaltypernas frekvensinnehåll samt eventuell korrelation dem emellan för att kunna göra en bedömning av signalernas användbarhet i tilltänkta applikationer.

Enligt uppgifter från Anders Johansson skulle tre mätningar gjorda mellan dec. 93 och apr. 94 vid Ringhals block 3 vara lämpliga för ändamålet. Mätningarna finns dokumenterade i mätrapporterna: 1421/93, 0211/94 och 0435/94. Er Johan Larsson är helt insatt i dessa mätningars innehåll.

Vad gäller frågor kring sekretess och säkerhet för eventuell data så har vi tidigare hanterat bl.a. mätdata från Ringhals block 1 vid forskningsuppdrag rörande härdstabiliteten i en BWR. Vi ser på dessa frågor med största allvar och tror att de kan lösas på ett för Er helt tillfredsställande sätt.

Med vänlig hälsning

Imre Pázsit
Inst för reaktorfysik
Chalmers tekniska högskola
412 96 Göteborg

Postadress
Postal address
S-412 96 Göteborg
SWEDEN

Gatuadress
Street address
Gibraltargatan 3

Telefon/Telephone
Nat 031-772 10 00
Int +46 31-772 10 00
Direkt/Direct
Nat 031-772 30 81
Int +46 31-772 30 81

Telex
2369 CHALBIB S

Telefax
Nat 031-772 30 79
Int +46 31-772 30 79

VATTENFALL
RINGHALS

1 (1)

Från	Hänvändelse till	Vårt datum 1994-09-15	Vår beteckning
		Er datum	Er beteckning
		Till: Lars Fredlund cRPT	
		Kopia till: Tell Andersson RBH Johan Larsson RPTF Anders Johansson RSTU	

Ärende

TILLGÅNG AV MÄTDATA FRÅN RINGHALS 3

Ett samarbetsprojekt mellan Ringhals och Reaktorfysik CTH med syfte att med brusanalys kunna identifiera härddriftparametrar har nyligen inletts. Handläggare från Er sida är Tell Andersson RBH och Anders Johansson RSTU.

Vid ett inledande möte på Ringhals 94.08.23 diskuterades möjligheten för oss att få tillgång till vissa mätdata från en PWR. Av intresse skulle vara neutronflödessignaler samt processignaler med nära anknytning till härden t.ex. kalla benets temperatur och härdutloppstemperaturen. Det inledande syftet skulle vara att analysera de olika signaltypernas frekvensinehåll samt eventuell korrelation dem emellan för att kunna göra en bedömning av signalernas användbarhet i tilltänkta applikationer.

Enligt uppgifter från Anders Johansson skulle tre mätningar gjorda mellan dec. 93 och apr. 94 på Ringhals block 3 vara lämpliga för ändamålet. Mätningarna finns dockumenterade i mätrapporterna : 1421/93, 0211/94 och 0435/94, Er Johan Larsson är helt insatt i dessa mätningars innehåll.

Vad det gäller frågor kring sekretess och säkerhet för eventuell data så har vi tidigare hanterat bl.a. mätdata från Ringhals block 1 vid forskningsuppdrag rörande härdstabiliteten i en BWR. Vi ser på dessa frågor med största allvar och tror att de kan lösas på ett för Er helt tillfredsställande sätt.

Imre Pázsit
kst för RF

Identitet
BREVXXXY.DOC (1:5) ADJO
F:\RSTU\ADJO
EL - INT.BREVDI

Sökord

CHALMERS UNIVERSITY OF TECHNOLOGY
SE 412 96 Gothenburg, Sweden
Phone: + 46 - (0)31 772 10 00
Web: www.chalmers.se